Faculteit wetenschappen
Chemie

Periodic mesoporous organosilicas: versatile materials hosting catalytic centers

Proefschrift voorgelegd tot het behalen van de graad van

Doctor in de wetenschappen

aan de Universiteit Antwerpen, te verdedigen door

Ward Huybrechts

Promotor: Prof. Dr. Pegie Cool

Antwerpen, 2018

Dankwoord

Vooreerst zou ik mijn ouders willen bedanken voor de mogelijkheden die ze me geboden hebben. Zonder hun steun zou ik deze mijlpaal niet gehaald hebben, bedankt! Ik kon ook steeds rekenen op de steun van mijn echtgenote, Rosanne, die altijd voor me klaarstaat. Zij heeft alle goede en minder goede momenten van dit doctoraat samen met mij meegemaakt.

Dat brengt me uiteraard bij mijn promotor, prof. Pegie Cool. Bedankt Pegie, om me de mogelijkheid te geven om na mijn master thesis aan een doctoraat te beginnen bij LADCA. In adem wil ik ook graag prof. Pascal Van Der Voort, prof. Joris Thybaut, prof. Dolores Esquivel, prof. Bert Maes, dr. Pieter Mampuys, dr. Jeroen Lauwaert, dr. Els De Canck bedanken voor de samenwerking tijdens dit interessant project dat vele wendingen gekend heeft. Hun feedback en ideeën waren steeds een grote hulp. Prof. Vera Meynen zou ik ook graag willen bedanken voor de waardevolle input en discussies, alsook om als hoofd van mijn doctoraatsjury te willen zetelen.

Uiteraard wil ik graag al mijn collega's van LADCA bedanken! De sfeer in de groep was steeds geweldig en dit maakte het des te aangenamer om gedurende meer dan vier jaar elke dag te gaan werken, bedankt iedereen!! Bij dezen zou ik ook mijn oud-bureau genoot Pieter willen bedanken, samen hebben we wat afgelachen. Ook Wesley zou ik uitvoerig willen bedanken, we begonnen samen aan onze bachelor in 2006, maar zeker tijdens de masteropleiding hebben we heel wat leuke momenten gehad! Later tijdens ons doctoraat kwamen we bij elkaar vaak opscheppen over de vooruitgang van ons onderzoek of misschien nog vaker klagen over dingen die niet liepen zoals ze moesten.

Special thanks to Qi, Stefano and Radu for all the hilarious moments, absurd discussions and fun during the extra-curricular activities.

Table of contents

List of abbreviations

CTAB/CTAC	Cetyltrimethylammonium bromide/chloride
OTAC	Octadecyltrimethylammonium chloride
FC4	Fluorocarbon surfactant
P123	Pluronic P123 poly(ethylene glycol)-poly(propylene glycol)-poly(ethylene glycol)
F127	Pluronic F127 poly(ethylene glycol)-poly(propylene glycol)-poly(ethylene glycol)
PEO-PLGA-PEO	Poly(ethylene oxide)-poly(lactic acid-*co*-glycolic acid)-poly(ethylene oxide)
Brij-30	Polyoxyethylene (4) lauryl ether
Brij-76	Polyoxyethylene (10) stearyl ether
$C_{n\text{-}s\text{-}n}$	Gemini surfactant
BTEB	1,4-bis(triethoxysilyl)benzene
SDA	Structure directing agent
HPLC	High performance liquid chromatography
TEOS	Tetraethoxyorthosilicate
Ee	Enantiomeric excess
XPS	X-ray photoelectron spectroscopy
SS NMR	Solid state nuclear magnetic resonance
(CP) MAS NMR	(Cross polarization) magic angle spinning nuclear magnetic resonance

BJH	Barret-Joyner-Halenda
DMF	*N,N'*-dimethylformamide
HPLC	High performance liquid chromatography
LC-MS	Liquid chromatography-mass spectrometry

Preface

Explaining the goal of this PhD to my friends and family was not simple. Of course, the fact that most of them were not scientifically schooled makes it even more difficult. Although *PMO* is an easy to remember abbreviation, the full name *Periodic Mesoporous Organosilica* made most people frown and lose interest immediately. However, even explaining it to other scientists, or chemists for that matter, could also be frustrating. Their first reaction often was: "*Oh, you're not working with zeolites?*". In hindsight, perhaps this is the reason that I only spent half a page on zeolites in **Chapter 1**. This chapter gives an overview of porous materials, focusing on hybrid materials in particular and their applications. Having tried to persuade the reader to switch his or her research to the world of PMOs, the following **Chapter 2** addresses our attempt in synthesizing a divinylbromobenzene bridged PMO. This chapter is divided in a first part where the synthesis of the precursor is discussed, and a second part comprising a strategy for brominating a benzene bridged PMO. However, the title of this PhD would not do itself justice if it weren't for chapters 3 and 4. **Chapter 3** describes the development of a novel aldol condensation catalyst based on a bifunctional PMO. This bifunctional PMO bears an L-serine group that is able to catalytically convert acetone and 4-nitrobenzaldehyde in an aqueous environment. This shows great potential for the use of these materials towards valorization of biomass-based resources and proves the symbiosis between the inorganic framework and the organic entity in PMOs. The last chapter in this thesis, **Chapter 4**, discusses the synthesis of benzene bridged PMO bearing an organic "superbase": a guanidine. This PMO was tested as a base catalyst for a carbon-carbon coupling reaction. This chapter also shows the impact of ordering of organic groups within the PMO on the modification degree.

Chapter 1

Porous materials – An overview

1.1 A brief history: from zeolites to mesoporosity

As discoveries go, the Swedish mineralogist Axel Fredrik Cronstedt could have never imagined the impact of his observations when he first encountered the mineral we now know as stilbite[1]. Using a blowpipe flame, he discovered that the material swelled when exposed to heat. He classified this mineral as a "zeolite", combining the Greek words, "zeo" and "lithos" meaning "to boil" and "a stone". Since then, these crystalline aluminosilicates have been widely investigated. Their three-dimensional structure consists of AlO_4 and SiO_4 tetrahedra and can be represented chemically by the structural formula:

$$M_{x/n}\,[(AlO_2)_x(SiO_2)_y] \cdot wH_2O$$

where n is the cation valence, w represents the water in the pores of the zeolite and x and y are the total number of tetrahedra per unit cell. These tetrahedra assemble into secondary building blocks, which build up the structural framework. Different frameworks then define different zeolitic types, irrespective of the composition[2].

However, it was only by the 1940's that numerous zeolites were commercialized by the (chemical) industry as a new class of materials and used for such applications as separation[3,4], purification[5,6] and later on as catalysts for cracking processes[7,8]. It was only then that the true potential of porous materials became clear and further research was spurred on by the growing market which was eager to apply these new materials.

Eventually, this gave rise to the discovery of the M41S materials by the researchers of Mobil[9], called Mobil Composition of Matter (MCM). Since the publication of this work in 1992, this article has been cited over 8500 times. Needless to say, this work was a breakthrough in the world of materials science. The importance of it lies in the fact that these new materials do not possess micropores (< 2 nm), but mesopores (2-50 nm). The latter property allows the entrance of larger molecules into the pores, resulting in a broader range of applications such as selective drug release[10–12], catalysis[13,14], etc. Moreover, a new templating mechanism was proposed: liquid crystal templating (LCT).

Surfactant molecules, used as structure directing agent (SDA), are allowed to form into micellar liquid crystals. The inorganic silica source (I), in this case tetraethyl orthosilicate (TEOS), can interact with the head group of the surfactant (S) in a variety of different ways, depending on the chemical environment[15]. Interactions, see Figure 1[16], can be electrostatic: S^+I^- (a), $S^+X^-I^+$ (b), S^-I^+ (d), $S^-M^+I^-$ (c) (with M and X being mediator ions); or through hydrogen bonding when nonionic surfactants are used: S^0I^0 (e), $S^0(XI)^0$ (f). An aging process allows the silica source to condense, forming siloxane bonds. Afterwards, removal of the template molecules can be performed through calcination or extraction, thus creating the actual pores.

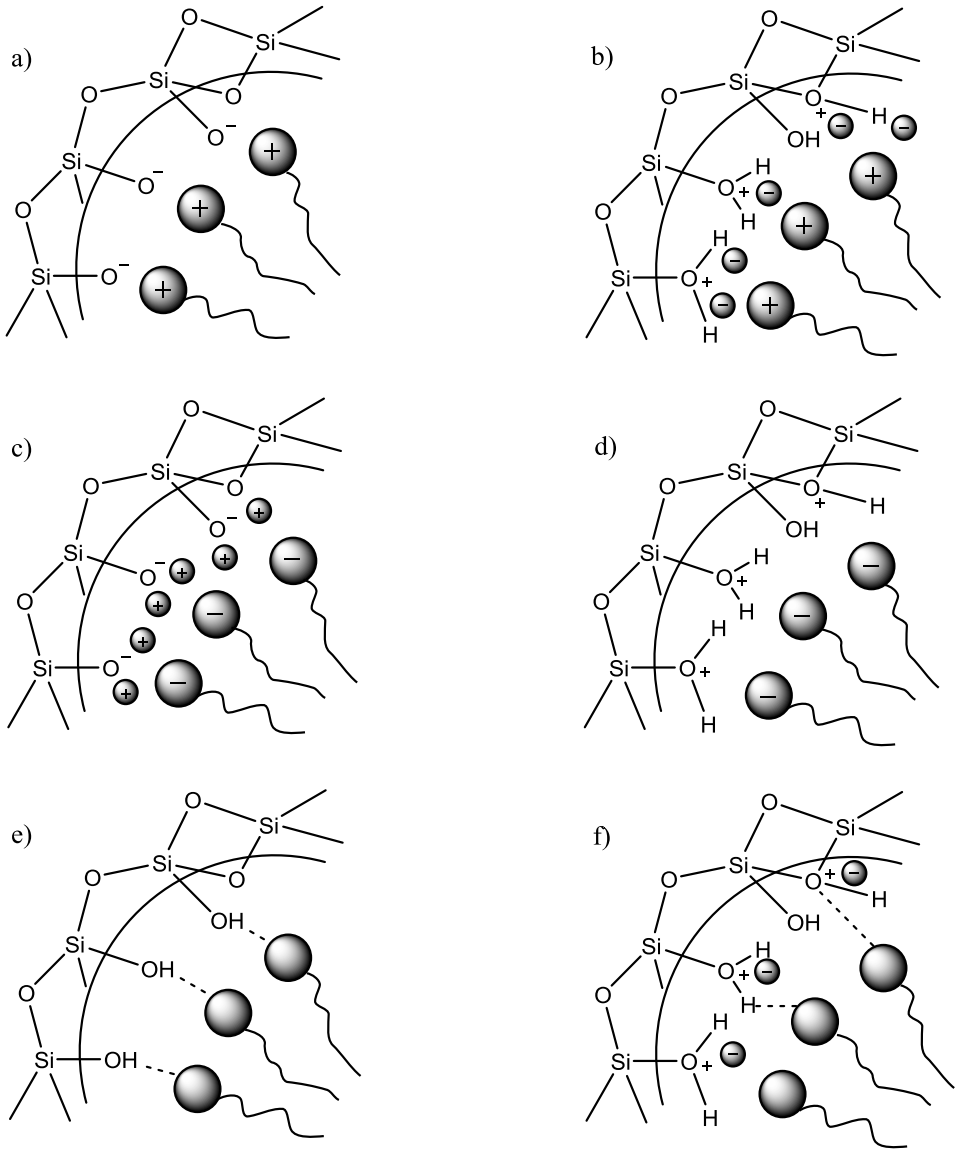

Figure 1. Interactions between inorganic precursor and surfactant.[16]

The use of previously mentioned nonionic surfactants, such as block copolymers led to a new breakthrough with the discovery of the Santa Barbara Amorphous (SBA) materials in 1998[17,18]. These materials have superior hydrothermal stability compared to the MCM type materials due to their thicker pore walls, moreover they contain micro- as well as mesopores. SBA-15, for example, can be prepared using a PEO-PPO-PEO triblock copolymer with different ratios of ethylene oxide (EO) and propylene oxide (PPO). The

PEO moieties are more hydrophilic than the PPO blocks, resulting in a stronger interaction between the former and the silica species while the PPO block is concentrated in a more hydrophobic cluster. Furthermore, the ordering properties of block copolymers are not only dependent on their composition but also on pH, temperature and solvent. Porosity characteristics of the desired material can therefore be controlled, being of pivotal importance from an application point-of-view.

1.2 Hybrid materials

Applications, however, often demand the presence of a certain functionality that acts as an active site. The use of porous materials for chromatographic purposes, for example, requires the perfect balance between hydrophilic and hydrophobic sites. Catalytically active materials, on the other hand, need the introduction of an active site because often these are not an inherent part of the material. One could therefore conclude that purely siliceous materials would not suffice. Inevitably, scientists looked at the vast opportunities that organic groups could offer. Combining the chemical diversity of the latter with the structural and (hydro)thermal stability of an inorganic framework provides an enormous potential, especially towards heterogeneous catalysis. Three different strategies have been developed in order to synthesize an inorganic-organic mesoporous silica material, which from now on will be called a *hybrid* material in this dissertation. These three approaches are known as: 1) a concerted condensation between a silica and an organosilane precursor (“co-condensation”), 2) post-synthesis modification of the pore surface of a purely siliceous material (“grafting”) and 3) integration of the organic moiety as a bridging unit in a silsesquioxane organosilica precursor, thus making it an inherent part of the pore wall and structure (“periodic mesoporous organosilica”).

1.2.1 Co-condensation

Four years after the discovery of the M41S family, the first ordered hybrid inorganic-organic mesoporous silica material was developed through co-condensation of siloxane and organosiloxane precursors[19].

Co-condensation combines a tetraalkoxysilane, such as TEOS, with a terminal trialkoxyorganosilane, represented by R-Si(OR')$_3$ in Figure 2, as a way to covalently bind an organic functionality on the pore walls. During this one-pot synthesis, the two precursors condense around the micellar template, allowing the organic functionality to be projected into the pores.

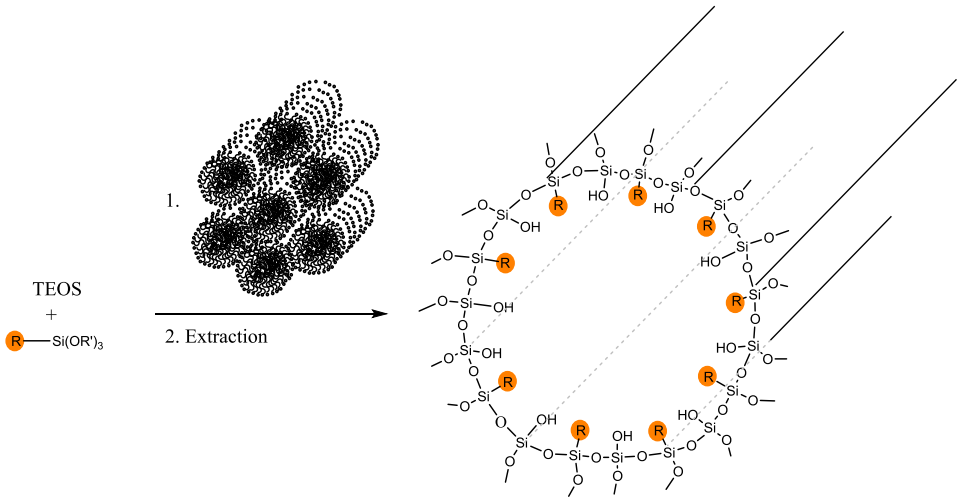

Figure 2. Schematic presentation of a co-condensation between TEOS and a non-specified trialkoxyorganosilane.

The advantage of this method is the homogeneously distributed organic groups, which are building-blocks of the material. Consequently, this means that there is no risk of pore blocking. However, there are some disadvantages as well: in order to retain mesoscopic order of the material, the total amount of the organic component must not exceed a certain mol %, depending on which organic functionality is used[16,19,20]. Related to this problem is the hydrolysis and condensation rate at which the silica- and organosilica precursor condense: in order to avoid homocondensation, leading to phase

separation and heterogeneously distributed components, the hydrolysis rate needs to be controlled before condensation around the template to take place[21,22].

1.2.2 Grafting

As opposed to co-condensation, grafting is a post-synthesis modification which occurs on the surface of the porous (silica) material, as can be seen in Figure 3. By reacting organosilanes, R-Si(OR')$_3$, with the silanol groups, one can incorporate different organic groups depending on the R group that is used. Another possibility, for example, is performing a chlorination of the silica surface with a subsequent Grignard reaction to functionalize the silica surface[23].

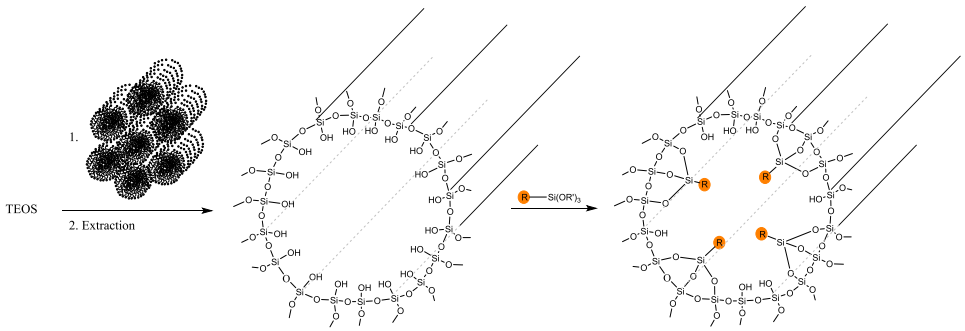

Figure 3. Example of a grafting procedure: post-synthetic attachment of an organosilane to the surface via siloxane bonds.

By covalently attaching the organic moiety on the already synthesized material, the mesostructure of the material is usually retained. However, a possible disadvantage is pore-blocking due to preferential binding of the organic groups at the pore entrance. This can then cause diffusion problems and leads to heterogeneously distributed organic components and finally total pore blocking.

1.2.3 Periodic Mesoporous Organosilicas (PMOs)

In 1999, three research groups working independently from one another synthesized the first periodic mesoporous organosilica (PMO) [24–26]. PMOs are organosilicon

materials based on silsesquioxane precursors which act as bridges and can therefore be built into the nanoporous framework with a uniform distribution, as represented in Figure 4. Essentially, the synthesis procedure is identical to the M41S or SBA type materials. A variety of surfactants can act as a template, Table 1 provides an overview of the most commonly used together with their chemical structure.

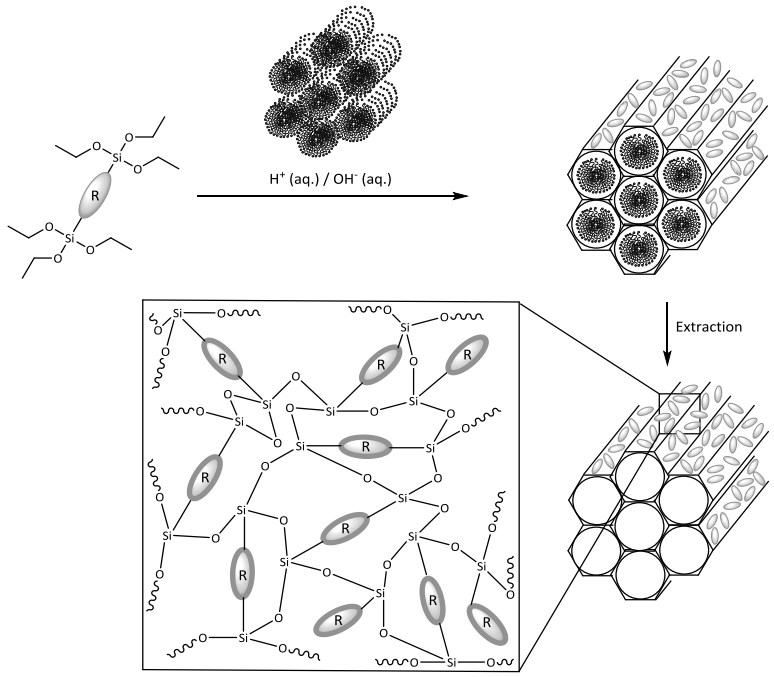

Figure 4. Schematic representation of a PMO synthesis. R = organic bridge

Table 1. Frequently used surfactants for PMO synthesis.

CTAB/CTAC[26–36]	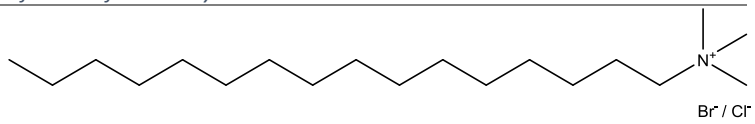
OTAC[37–41]	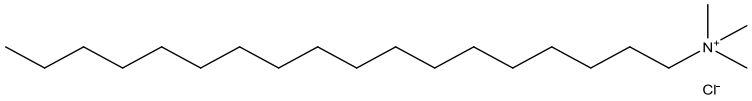
FC4[42–45]	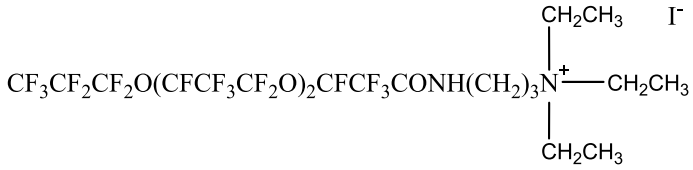
P123[46–58]	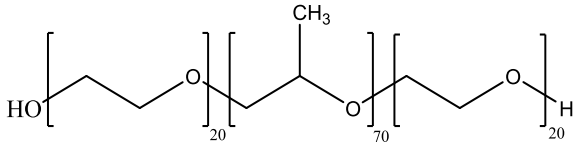
F127[31,42,57–64]	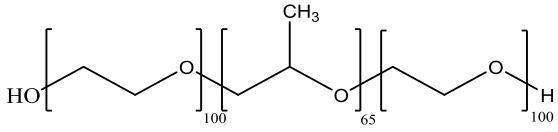
PEO-PLGA-PEO[42,54,65,66]	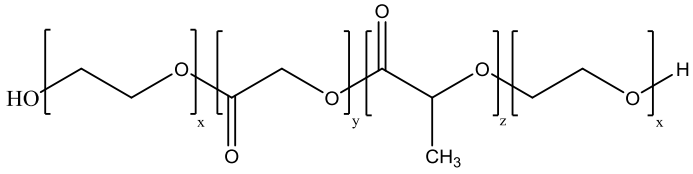
Brij-56[67–71]	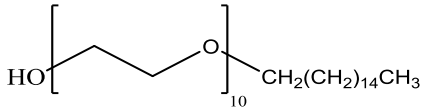
Brij-76[28,65,71–77]	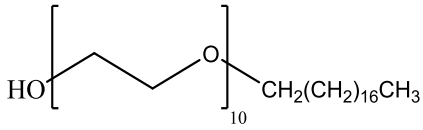

$C_{n\text{-}s\text{-}n}$[61,78,79]

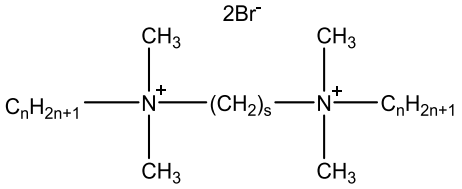

One can distinguish several different groups of surfactants. Firstly, the most frequently used are the alkyltrimethylammonium halides, such as CTAB/CTAC and OTAC. Under the appropriate synthesis conditions (concentration, pH, solvent, temperature), these surfactants can form micellar liquid crystals around which the organosilica precursor can condense.

This class of hybrid inorganic-organic materials possesses interesting properties brought forward by the symbiosis between the strength and high porosity of the inorganic framework, combined with the chemical functionality of the organic component. Contrary to pure silica materials, PMOs do not suffer the drawbacks of instability in harsh conditions and the lack of true active sites[28,80,81].

Smeulders et al. concluded that the hydrolization of the siloxane bonds leads to disintegration of the structure[81]. Consequently, water is the antagonist in this case thus making hydrophobic materials more stable. However, the hydrophobicity of the surface is not the only factor to be taken into consideration. The inner pore walls should also be of a hydrophobic nature in order to provide a higher chemical, mechanical and hydrothermal stability. This is where PMOs stand out compared to their purely siliceous analogues, due to the organic entities that are homogeneously present both on the surface as well as in the pore walls. Smeulders et al. observed that there is a direct correlation between the hydrophobicity of hybrid mesoporous silica materials and their stability[81]. As a result, the hydrothermal stability of PMOs are superior to the more conventional silica materials. Moreover, it was shown that applying a mechanical pressure of up to almost 1000 MPa only led to a less than 10% decrease in surface area for ethane bridged PMOs and about 30% for benzene bridged PMOs with the former retaining its pore diameter completely. In contrast, MCM and SBA materials lost 50% of

their surface area. Evidently, the difference between both PMOs lies in the hydrophobicity of the organic bridge. Hydrophobicity is however not the only reason for enhanced stability, it is its homogeneous distribution and strong anchoring throughout the entire material that makes PMOs so stable. As could be seen from Smeulders et al.'s chemical stability tests, comparing PMOs with hexamethyldisilazane (HDMS) grafted MCM after being stirred for 2 h in a 0.5 M NaOH solution. The latter material was established as the most hydrophobic one by immersion calorimetry, whilst not being the most chemically stable one. It was concluded that deterioration under these harsh conditions occurred very fast due to local defects in the hydrophobic layer. The HDMS grafted silica material was almost completely dissolved, while the PMOs only lost between 5-15% of their surface area.

A vast variety of organosilica precursors have already been used for synthesizing PMOs, an overview is provided in Figure 5. Although we now know that even complex organic structures can be utilized as bridging units in PMO synthesis, the first reports on PMOs described the use of organosilica precursors with simple organic bridges. Inagaki et al. used 1,2-bis(trimethoxysilyl)ethane **(2)** in combination with OTAC in a solution of NaOH[24]. This resulted in a S^+I^- interaction between surfactant and precursor. They performed the synthesis both with and without an aging step to obtain 2D hexagonally ordered rod like particles and 3D hexagonally ordered spherical particles, respectively. The obtained PMOs all possessed pores around 3 nm in diameter and their surface area varied between approximately 750 m^2/g and 1200 m^2/g. At about the same time, the research group of Stein et al. published an article describing the synthesis of PMOs with 1,2-bis(triethoxysilyl)ethane **(2)** and 1,2-bis(triethoxysilyl)ethylene **(3)**, using CTAB as surfactant[26]. This resulted in wormhole like channeled PMOs with a surface area of approximately 1200 m^2/g and a narrow pore size distribution between 2.2 nm and 2.4 nm. In contrast to Inagaki et al., Stein et al. performed the hydrolysis of the organosilica precursor in an acidic environment followed by condensation in basic environment. This means that the interaction between precursor and surfactant changed from a $S^+X^-I^+$ type to a S^+I^- type. Afterwards, he proved the accessibility of the ethylene groups by

performing a bromination reaction. The last founding father of PMOs, Ozin et al., published his findings in Nature in December 1999[25]. Using 1,2-bis(triethoxysilyl)ethylene **(3)** in combination with CTAB, they were able to synthesize a PMO with a periodic arrangement of channels in a hexagonal symmetry. Despite obtaining the lowest specific surface area of the three original publications, 637 m^2/g, they did obtain the largest pores with a diameter of almost 4 nm.

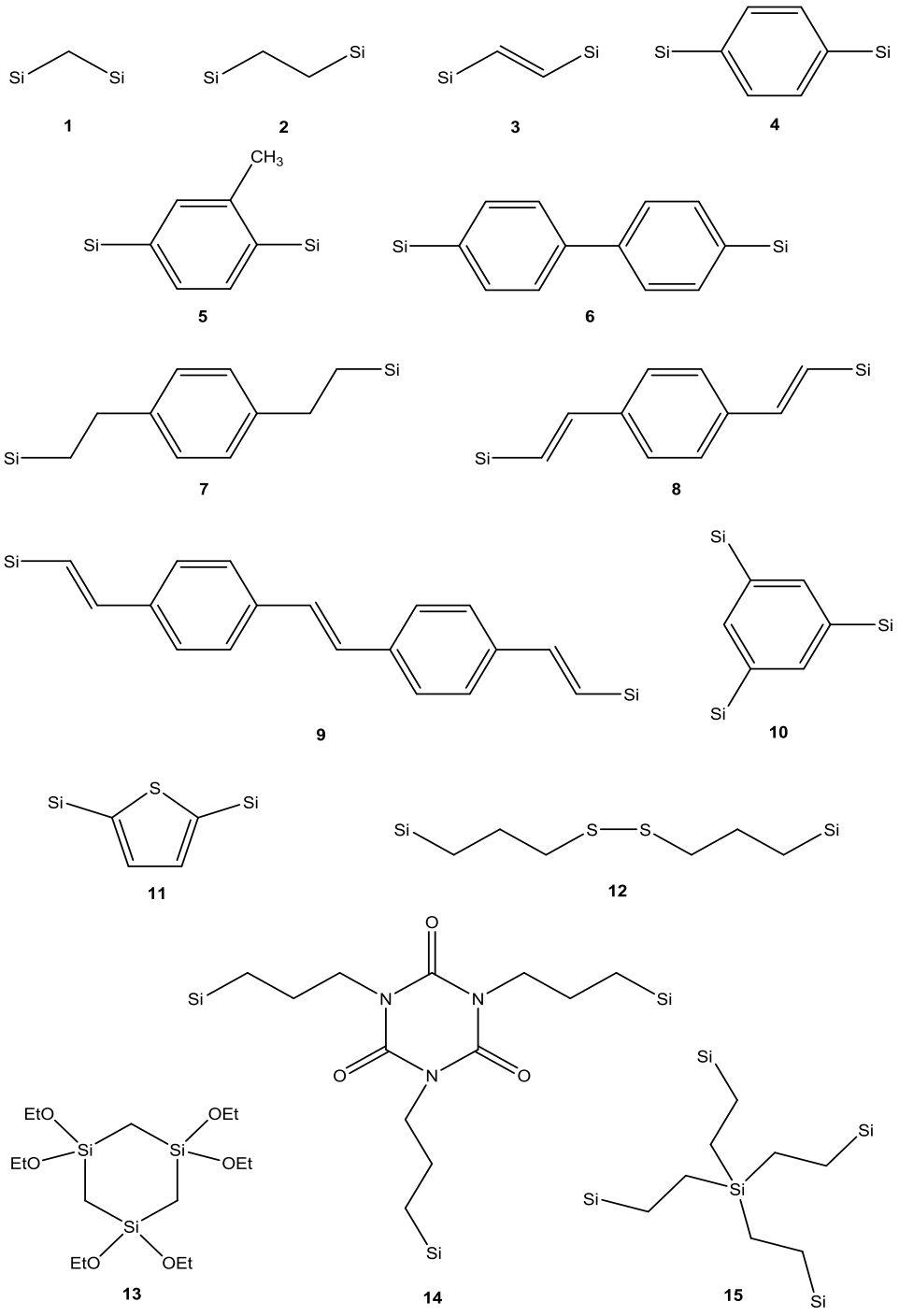

Figure 5. Limited overview of commonly used organosilica precursors in PMO synthesis. Terminal Si atoms: Si = Si(OR)$_3$ with R = CH$_3$ or CH$_2$CH$_3$.

Since then, periodic mesoporous organosilicas have attracted a lot of interest resulting in the development of various new precursors. In time, the rather simple short aliphatic organic bridges have evolved to more complex structures such as: aromatic rings, multiple (aromatic) ring structures, heterocycles and combinations of all the previous[32,38,40–42,50,51,53,65,73,81–99].

Inagaki et al. was the first to discover the remarkable effect of using aromatic bridging units in PMO synthesis[82]. When the right conditions were applied, an ordered PMO material could be obtained using 1,4-bis(triethoxysilyl)benzene (BTEB) **(4)** , as represented in Figure 6. More specifically, XRD and TEM analysis showed the existence of crystal-like pore walls throughout the PMO due to the π-π stacking of the bridging phenylene groups with a spacing of 7.6 Å along the channel direction. This molecular-scale periodicity, consisting of alternating hydrophilic silicate and hydrophobic benzene layers, presented new opportunities towards catalysis and structural orientation of guest molecules in the pores.

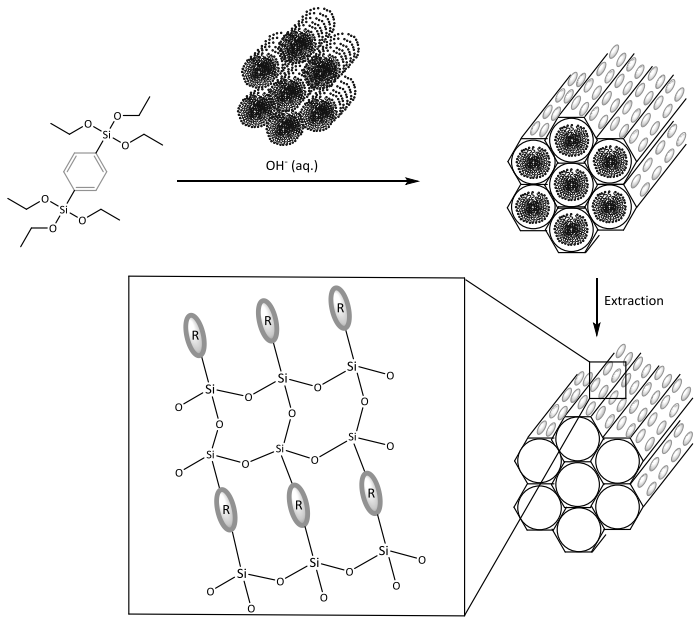

Figure 6. Schematic representation of the synthesis of BTEB PMO with crystalline-like pore walls. R = phenylene bridge

Later on, Inagaki et al. described molecular-scale periodicity in the pore walls of their PMO, similar to their previous article, using 4,4'bis(triethoxysilyl)biphenyl **(6)**[100]. Moreover, in 2005 Mokaya et al. showed that hybrid materials could also be prepared with a non-aromatic organosilica[101]. More specifically, using 1,2-bis(triethoxysilyl)ethylene **(3)** in combination with an aluminum source they obtained a structurally well-ordered material with crystal-like pore walls. Not much later Sayari et al. and Fröba et al. published their findings about the synthesis of PMO with crystal-like pore walls, without having to use the "traditional" rigid and planar precursors, such as ethylene or phenylene bridges[38,102]. By using 1,4-bis((triethoxysilyl)vinyl)benzene **(8)**, they were the first to make a PMO with these crystalline-like features with a bifunctional conjugated organic unit. Moreover, Fröba and co-workers also proved the accessibility of the vinylic bonds by post-synthetic bromination[38].

Bissilylated precursors are the most widely used organosilica source for PMO synthesis, although multi-silylated precursors have also been investigated. Especially Ozin's research group has booked significant progress in this field by describing the use of 1,3,5-tris(triethoxysilyl)benzene **(10)**, various dendrisilicas such as **(15)** and 1,3,5-tris(diethoxysila)cyclohexane **(13)**[95,96,98]. The latter material was considered to be a very interesting candidate for microelectronic applications. The PMO with three attachment points, based on **(10)** exhibited a high thermal stability. Zhang et al., on the other hand, were the first to be able to make a PMO solely based on the isocyanurate-containing silsesquioxane **(14)**[103]. The metal-chelating properties of this heterocycle offer interesting possibilities towards applications such as selective adsorption.

1.3 PMOs and their applications

By now, we are starting to get a pretty clear idea what PMO materials are capable of. Due to the vast number of organic entities that have been (or could potentially be) introduced as a bridging unit in PMOs, one could almost find a suitable PMO for every application. However, as mentioned before, specific requirements such as a certain

functional group (e.g. a thiol group for mercury adsorption) or chiral center (e.g. for asymmetric catalysis) can sometimes only be introduced in a post-synthetic way. Moreover, obtaining a very rigid PMO structure with hetero-atom containing precursors which are often long and flexible, is a difficult combination. Instead of attempting to develop a precursor that provides both rigidity and functionality, post-synthetic modification reactions can usually offer a more "simple" solution. This approach allows the preservation of the high ordering of the material. Post-synthetic modification can be performed in two different ways: as described in section Grafting1.2.2 via grafting of the silanol functionalities on the material's surface or via modification of the organic bridge. The disadvantages of the former method, summarized in section 1.2.2, combined with the superior chemical stability of a C-C bond compared to a much more easily hydrolysable Si-O-Si bond makes this way of post-synthetic modification inadequate for a great deal of applications. Describing all the modification reactions, inextricably linked to a specific application, so far performed on PMOs would therefore provide little added value to this dissertation. Hence, in the next section the most important applications will be discussed, including the (post-) synthetic pathway used to achieve the desired activity/property.

1.3.1 Chromatography and (selective) adsorption

The hydrophobic nature of PMOs makes them interesting candidates as a stationary phase in reversed phase chromatography. In 2004 both the group of Inagaki[104] and Fröba[105] described the synthesis of monodispersed spherical periodic mesoporous organosilica particles, based on the Stöber process[106], using respectively 1,4-bis(triethoxysilyl)benzene **(4)** or 1,2-bis(trimethoxysilyl)benzene. They concluded that mild basicity was required and employed ammonia instead of NaOH during the PMO synthesis, as well as small amounts of ethanol in order to obtain spherical shaped particles. These results led Fröba et al. to a follow-up paper in 2006, where they proved to be able to increase the size of the spherical benzene bridged PMO particles to dimensions similar to commercially available normal phase stationary phase Nucleosil

50-10, against which the PMO was tested[32]. The materials were both successfully tested in normal phase and reverse phase chromatography, due to the presence of both the organic bridging unit as well as silanol groups in the PMO. Moreover, the spherical PMO particles even demonstrated a higher separation efficiency than the commercial phase for mixtures of (poly)aromatic hydrocarbons.

Recently, Válcarel et al. reported the first use of phenylene bridged PMOs as a stationary phase for the solid phase extraction of pesticides from grape must[73]. Although this material proved effective in extracting pesticides prior to analysis by capillary electrophoresis with ultraviolet detection, it could only be reused twice without substantial changes in the analytical signals. On the other hand, limits of detection and quantification obtained were below the European Union's Maximum Residue Limits for the respective pesticides and the PMO was similar in sensitivity and selectivity compared to commercial sorbents.

Not much later, Van Der Voort's group used 1,3,5-tris(diethoxysila)cyclohexane **(13)** derivatives for successfully spray drying spherical PMO particles for the first time[107]. They then used this material as an ultra-stable packing for HPLC. Moreover, they proved the chemical and hydrothermal stability of the column by varying the pH between 1.75 and 13 and by raising the temperature to 150°C in 60% water. Furthermore, by functionalizing the organic bridge and therefore adjusting the affinity, they showed the enormous potential of PMO materials as a stationary phase in liquid chromatography.

PMOs are not only interesting candidates for chromatographic purposes, they have also been widely investigated as a means to immobilize harmful or toxic compounds by (selective) adsorption. An extensive review concerning this subject was published in 2010 by A. Walcarius and L. Mercier[108]. Besides the obvious advantages that mesoporous materials with a controllable PSD and high surface area can offer towards this application, PMOs provide even more benefits. One can not only choose between different organic bridges, it is even possible to combine multiple precursors or perform post-synthetic modifications in order to fine-tune the selectivity towards the adsorptive.

Harmful substances such as herbicides[109], heavy metals[71,110], CO_2[51,111] and toxic gases[37] have been successfully adsorbed through physisorption or chemisorption. However, not only harmful compounds have been investigated. Proteins, for example, can also be adsorbed on the surface of PMO materials. This makes applications such as biocatalysis possible through adsorption of enzymes[112,113]. Another interesting adsorbate with regard to future applications is H_2. Hydrogen storage in PMOs has been investigated and compared to inorganic silica materials[114]. One of the conclusions was that the pore volume was not of pivotal importance, but the presence of the benzene rings in the PMO structure. Therefore, in an article published in 2012, a study was performed to examine the effect of different organic groups on the H_2 adsorption properties of PMOs[115]. The authors came to the conclusion that PMOs with π electrons achieved a higher adsorption capacity towards hydrogen due to their more polarizable surface. In addition, they suggested that the molecular ordering of the organic groups has an influence as well. Consequently, Froudakis et al. examined the difference in hydrogen storage capacity between ordered and disordered phenylene bridged PMOs[84]. Their train of thought was that the possible increase in surface defects of the disordered materials might result in a higher adsorption capacity. However, the results did not support this argument as no clear difference was observed. Finally, a recent study on hydrogen and methane storage has shown that PMO materials synthesized with a combination of BTEB and TEOS, with a wider PSD and pore sizes close to the micro/mesopore border region led to an increased adsorbent-adsorbate interaction[116].

1.3.2 Low-κ dielectric material

Microelectronics are downscaling in size leading to increased performance and lower power consumption. This evolution continues at such a high pace that it even resulted in Moore's law, which predicts an ever increasing number of transistors (i.e. complexity) in dense integrated circuits. However, this thus implies that the distance between wires continues to shrink, therefore increasing parasitic capacitance and signal propagation delay. Lowering the signal delay by introducing low-κ dielectrics, which separate the

conducting parts from one another, is one of the main challenges in microelectronics research[117]. Moreover, it is not only important to introduce new materials with lower κ values than the traditional dielectric material, silicon dioxide, but also make sure that these materials are compatible with the damascene process. This process was developed when copper was introduced as the conductor instead of aluminum. By patterning the dielectric layer with trenches, the conducting copper can be laid in, followed by the removal of the overburden. The implementation of new dielectrics is often prevented because of incompatibility with the damascene process.

The potential of PMOs as a low-κ dielectric have been researched by various research groups. Firstly, the Si-C bond is less polarizable than the Si-O bond in SiO_2. Secondly, the air that is present in the pores makes the dielectric constant drop because the κ value of air is almost one which is the lowest value that can be obtained. Ozin and co-workers therefore developed a PMO thin film containing air pockets by an evaporation-induced self-assembly spin-coating procedure[36]. This leads to a thin film with a dielectric constant κ of 1.73, compared to 3.9 of SiO_2[118]. The group of Van Der Voort contributed to this field of research as well by creating films of PMO with an ultra-low κ value of 1.8, in addition to being hydrophobic and chemically stable in alkaline conditions[119]. Moreover, they developed a strategy to seal the mesopores in order to prevent the diffusion of metal ions from the wires[120,121].

1.3.3 Biological/-medical applications

Due to their unique properties, PMOs can be widely applied in biological/-medical applications. For example, they can assist in protein refolding by controlling the release of denaturated proteins into a refolding buffer[122]. Naturally, biomolecules can be permanently immobilized as well, with the aim of creating biocatalytic centers inside the pores of the material as will be discussed in section 1.3.5.2. Drug release however, is perhaps one of the most important biomedical applications of PMOs. By being able to construct a material which allows a controlled release of a certain drug, one can not

only effectively target specific cells to be attacked but severe side effects can be avoided. The driving forces behind the adsorption of biomolecules are electrostatic, hydrophobic and hydrogen-bonding[29]. These can be obtained by functionalizing the PMO surface with organic groups that interact with the guest molecules. Ha et al. have concluded that incorporating diurea sulfanilamide groups (Figure 7)in the walls of PMO materials can lead to high adsorption of the drugs captopril and 5-flurouracil[123]. These drugs can then be released in a controlled manner into a simulated body fluid. They achieved the same success by synthesizing an *N,N'*-diureylenepiperazine bridged PMO (Figure 7), proving that it is most likely the presence of hydrophilic ureylene moeieties that makes this material a good drug delivery system in these circumstances[124].

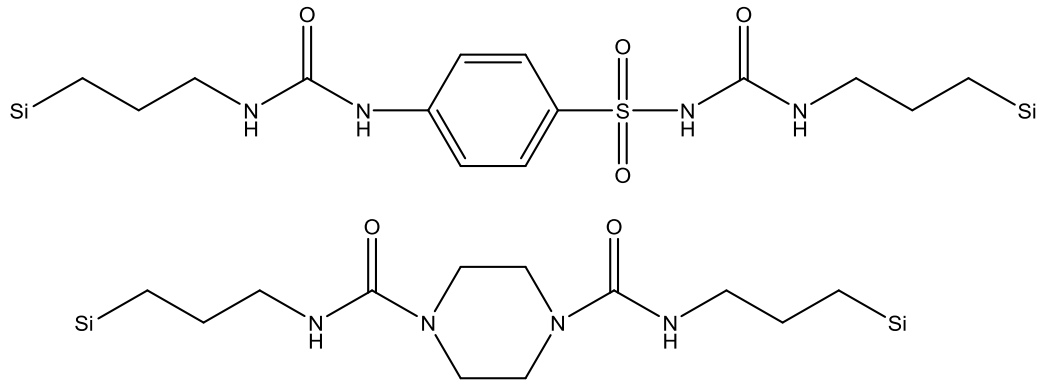

Figure 7. Diurea sulfanilamide (above) and N,N'-diureylenepiperazine (below) precursors. Terminal Si atoms: Si = $Si(OCH_2CH_3)_3$.

However, also the morphology and pore diameter are crucial parameters to be taken into account. The former characteristic was utilized in an ingenious way by Balkus et al., more specifically by developing a PMO with a wrinkled structure[125]. Increasing the surface area resulted in enhanced loading capacity of the anti-cancer drug paclitaxel. Their *in vitro* studies showed a slow and sustained drug release, due to the good hydrophobic interaction between the drug molecule and the benzene rings of the PMO. In 2013, the group of Ha synthesized a pyridine containing PMO as a carrier system for 5-fluorouracil[126]. The *in vitro* tests showed a good therapeutic effect with a controlled,

pH sensitive, release and enhanced cytotoxic effect towards cancer cells. Another very promising article was published three years ago by Shi et al., where hollow mesoporous organosilica nanoparticles were used as a transporting system for the chemotherapeutic agent doxorubicin[127]. By performing a coating reaction around SiO_2 nanoparticles, followed by etching the SiO_2 with HF, hollow mesoporous organosilica nanoparticles were obtained. Moreover, by using up to five different precursors during the coating process, they were able to incorporate multiple organic moieties, thus enhancing the adsorption capacity of guest molecules. In this case, the presence of phenylene and thioether groups led to both π-π supramolecular stacking and hydrophobic-hydrophobic- interactions between the framework and aromatic doxorubicin molecules. The drug was subsequently encapsulated into the hollow nanoparticles and tested *in vivo* to inhibit tumor growth and metastasis in tumor-bearing mice. Intracellullar glutathione is known to break disulfide bonds, thereby triggering the release of the loaded drug molecules[128]. Because the intracellullar concentration of glutathione (GSH) is much higher in cancer cells than in the corresponding healthy cells, this way of triggering the drug release is very effective. Recently, PMOs have also been investigated for smart cancer cell targeting by developing a PMO which is stably and selectively conjugated with a near-infrared fluorescence dye and the chemotherapeutic agent doxorubicin[129]. As discussed earlier, thioether groups and the tumor related molecule glutathione (GSH) were once more the driving force behind an efficient and effective drug release. In this work, however, both imaging and therapeutic capabilities are combined into a single nanoplatform resulting in a theranostic agent. By using near infrared imaging, the drug delivery could be efficiently monitored. Figure 8 shows the schematic approach towards the construction of the dye (Cy5.5) and drug loaded PMO and the release of the doxorubicin (DOX) molecule in a Her2 positive tumor cell[129].

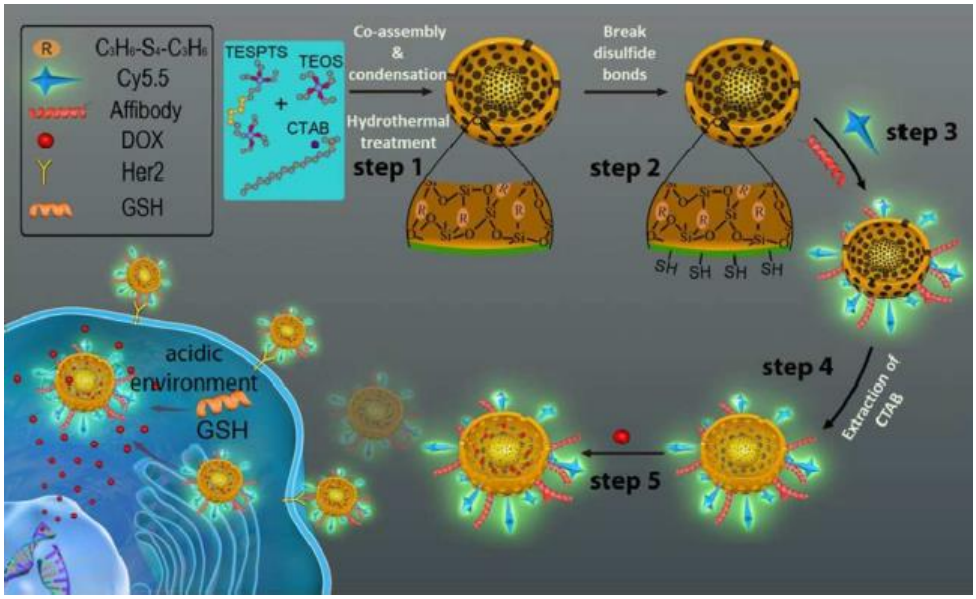

Figure 8. Schematic overview of the construction of doxorubicin (DOX) loaded PMO and release of the drug in a tumor cell.[129]

1.3.4 Photochemically active and light-harvesting PMOs

One of the first photochemically active hybrid materials was developed by Alvaro et al.[130]. They succeeded in incorporating *trans*-1,2-bis(4-pyridyl)ethylene (Figure 9) into the pore walls, which is photoresponsive. Upon irradiation with UV light, *cis/trans* isomerization takes place, leading to changing surface area and porosity. A few years later, they published a follow-up paper, stating the development of photoresponsive azobenzene-containing PMOs[131]. The innovative aspect of this work was the reversible porosity changes due to *cis/trans* isomerization that could be proven by adsorption experiments with gold nanoparticles. In comparison to Alvaro's group, Fröba and co-workers were able to construct PMOs with optical properties, solely built with organosilica precursors[41]. Furthermore, they realized an extension of the conjugated π-system to an 18 π-electron system, thus tuning the optical properties of the material. By introducing heteroatoms in the organic bridge, the PMO was able to absorb wavelengths up to 530 nm, i.e. visible light. Likewise, Inagaki's research group prepared a transparent and visible light absorptive acridone-bridged PMO (Figure 9), advocating

their light-harvesting antenna properties[132]. Four years later, in 2014, they reported the successful synthesis of visible light absorptive and hole transporting (p-type) 4,7-dithienyl-2,1,3-benzothiadiazole-bridged PMO (Figure 9) and the subsequent filling of the mesopores with an n-type material[133]. Constructing these p-n heterojunction structures, proved that these PMO films could function as an active layer for organic solar cells. Finally, very recently, Fröba et al. developed a biphenyl-bridged PMO in which they introduced two types of dye in the pore channels[134]. Light energy is absorbed by the organic bridges (donor) and is subsequently transferred to the acceptor chromophore dyes. This energy transfer can be performed in a very efficient way, up to 80% using two dyes. Depending on the acceptor used, the emission wavelength can then be tuned, demonstrating the exceptional light-harvesting properties of these hybrid materials.

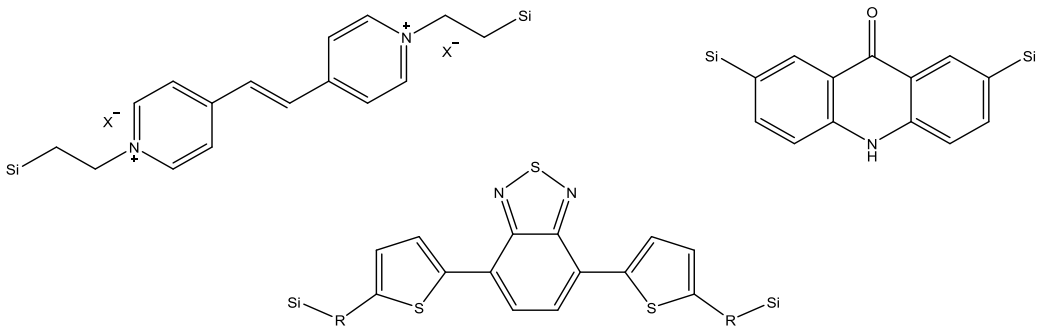

Figure 9. Photochemically active trans-1,2-bis(4-pyridyl)ethylene (top left), acridone (top right) and 4,7-dithienyl-2,1,3-benzothiadiazole based (bottom) precursors. Terminal Si atoms: Si = $Si(OR')_3$ with R' = CH_3 or CH_2CH_3 or $CH(CH_3)_2$.

Of course, light-harvesting alone is not the ultimate goal. It is a way to control the incident electromagnetic waves, light if you will, in such a way that it can be efficiently applied by an active site. PMOs with the acridone bridging unit, for example, were used by Inagaki et al. as light-harvesting antennae[135,136]. The excitation energy was then funneled to the reaction center where the photocatalytic activity could take place. The use of PMOs as catalysts is perhaps the most extensively studied application.

1.3.5 PMOs as heterogeneous catalysts

1.3.5.1 Metal (complex)-containing catalysis

Certain metals and their complexes are known to be excellent homogeneous catalysts. Therefore, heterogenization could make these catalysts more viable for industrial applications as well as offer a more environmentally friendly process. Direct incorporation of the metal complex in the PMO precursor allows an even distribution of the desired functionality throughout the entire framework. The successful preparation of vanadyl Schiff base containing PMOs (Figure 10) is an excellent example of this strategy[137]. The authors obtained a conversion between 71-86% for the catalytic cyanosilylation of different aldehydes. Only very recently, a PMO was synthesized with Fe(III) complexes built into the pore walls and tested as a catalyst in the oxidation reaction of benzene to phenol with H_2O_2[138]. After several cycles, the material showed no decrease in both conversion and selectivity.

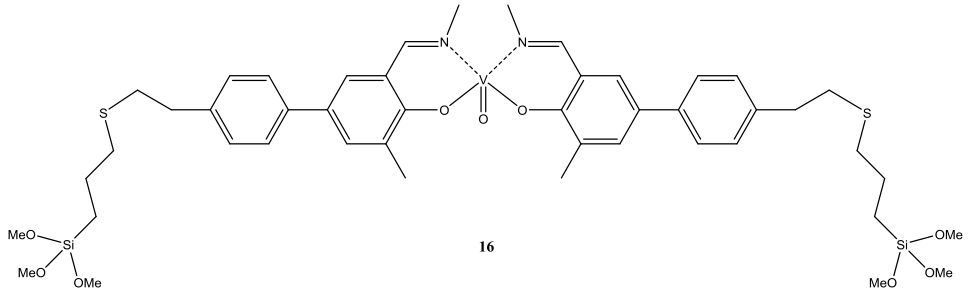

Figure 10. PMO precursor containing a vanadyl Schiff base complex.[137]

A different approach is the post-synthetic attachment of the metal (complex) to the bridging unit of the PMO. One can use an ionic liquid bridged PMO, such as bisimidazolium for example (Figure 11), followed by the introduction of copper(II) chloride[139]. Xu et al. synthesized this material and subsequently showed its high stability and catalytic activity towards the decomposition of cyclohexyl hydroperoxide.

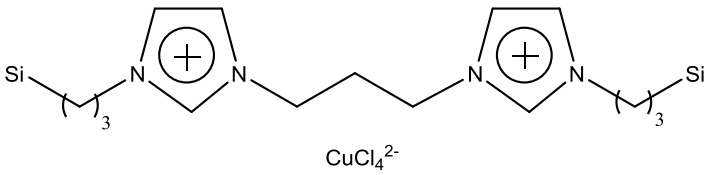

Figure 11. Cu(II) containing bisimidazolium ionic liquid bridged PMO.

Romero-Salguero and co-workers, on the other hand, realized the preparation of ethylene and phenylene bridged PMO impregnated with Pd nanoparticles[72]. These Pd-supported PMOs were active in the Suzuki cross-coupling reaction, leading to the formation of a new C-C bond, hence their importance in organic chemistry. Unfortunately, the catalysts deactivated upon reuse. Another relevant organic reaction such as the transition metal catalyzed direct C-H borylation of (hetero)arenes has also been the subject of PMO research[140]. Through heterogenization of the catalytically active iridium-bipyridine (Ir-BPy) complex, by using the bipyridine bridges in the PMO as ligands for iridium, Inagaki and Maegawa were able to use an inexpensive boron source for direct C-H borylation. Moreover, the catalytic performance lowered only slightly (88% to 69%) after different recycle steps. This post-synthetic metalation strategy was applied once more in their recent article[141]. Only now, the Ir-BPy-PMO was tested as a catalyst for the oxidation of water, and was found to exhibit superior activity when compared to other heterogeneous iridium catalysts prepared using different mesoporous supports. Although the structural order decreased after three reactions, the TOF only decreased after four reactions due to a loss in BET surface area. It was concluded that the densely packed bipyridine groups, leading to direct fixation of iridium complexes on the pore surface, were of pivotal importance for an efficient catalysis.

Very recently, Van Der Voort et al. were also able to prepare a PMO with oxidative catalytic properties[142]. A 100% monoallyl ring-type PMO (**(13)** with one allyl group attached to it) was constructed, followed by post-synthetic modification of the allyl group in order to obtain a bidentate ligand for a Ru(III)-complex. This Ru(III)-complex

containing PMO was then tested as a catalyst for the oxidation of cyclohexanol in water at 25°C.

1.3.5.2 Biocatalysis

Enzymes are nature's catalysts. After millions of years of evolution, these proteins are highly selective in their conversion of natural products. Needless to say, scientists have been attempting to exploit their catalytic activity by immobilizing enzymes on solid supports. Besides the well-known advantages of heterogenization, PMOs are also able to provide protection for these proteins by selectively allowing or denying certain molecules into their pore system. Thus, the high surface area, controllable porosity and built-in functionalities of PMOs can offer an ideal environment for enzymes to be anchored in.

Treatment of industrial waste water or degradation of dyes by horseradish peroxidase (HRP) is a fine example of the use of enzymes for industrial applications[143–145]. The first reports on the immobilization of HRP on PMOs were focused on the comparison between the stability and catalytic activity of said enzyme immobilized on the PMO surface and the free HRP[146]. The material was synthesized with a mixture of TEOS and organosilica precursor. The latter was either a urea- (-NH-CO-NH-) or carbamothioic acid (-NH-CO-S-) group bridged triethoxysilyl. More HRP could be adsorbed by increasing the N content in the material. A clear increase in stability and activity was observed compared to free HRP. Their follow-up paper in 2012 investigated the use of new PMO composites for the immobilization of HRP[147].

More recently, immobilization of the β-glucosidase enzyme on a bifunctional PMO was achieved[148]. By co-condensation of 1,2-bis(triethoxysilyl)ethane **(2)** and 3-aminopropyltriethoxysilane, a very high enzyme loading was obtained, while the catalytic activity was retained. Moreover, even after twenty cycles, the relative activity maintained higher than 75%.

An alternative approach to immobilization of enzymes is covalently binding it to the PMO surface. In 2010, an interesting article was published where the authors performed a co-condensation of 1,2-bis(triethoxysilyl)ethane **(2)** with up to 10% 3-(2,3-epoxypropoxy)propyltrimethoxysilane[149]. During the PMO synthesis, a fraction of the latter molecule experienced an epoxy ring opening reaction creating diol groups. The combination of the epoxy groups and the diol groups provided an efficient two-step covalent enzyme immobilization mechanism, resulting in a covalent bond between the PMO surface and the papain enzyme used in their work.

Finally, considerable research on the lipase enzyme has shown that this carboxylesterase can be applied in a variety of organic reactions due to their high versatility[150,151]. For this reason, a number of papers have been published discussing the immobilization of lipase on both mesoporous silica and organosilica materials[152,153]. Gao et al. succeeded in constructing a Pickering emulsion, an emulsion stabilized by solid particles, stabilized by lipase containing PMO as a biocatalyst for biodiesel production[154]. The test reaction used was the esterification of commercial oleic acid and ethanol. Compared to lipase as such and lipase adsorbed on the PMO surface, the Pickering emulsion stabilized by lipase containing PMO showed enhanced catalytic activity, stability and reusability.

Alternatively, lipases can not only be utilized in biocatalysis for biodiesel production, due to their chirality they allow for enantioselective synthesis as well[150]. This leads us to another field of research where PMOs have played a prominent role: asymmetric catalysis.

1.3.5.3 Asymmetric catalysis[155]

Asymmetric synthesis, or enantioselective synthesis, is of utmost importance in the pharmaceutical industry/research because different stereoisomers (enantiomers or diastereoisomers) can have a different biological activity. By incorporating chiral catalytic centers on a solid support such as a PMO, with all the benefits involved as

described earlier in this work, it is clear that this approach can lead to significant insights and applications for the chemical community. In 2015, a very comprehensive review has been published comprising the most recent advances that have been made towards the introduction of chirality into organosilica materials[155]. One can follow three different methods in order to obtain chirality in PMOs: chiral building blocks; chiral post-synthetic modification of an achiral structure; chiral transfer by a chiral dopant[156]. The first method evidently leads to materials with the highest amount of functionalities. Van Der Voort et al. have summarized the chiral precursors used in the synthesis of 100% pure PMOs in their 2013 review, as can be seen in Figure 12[157].

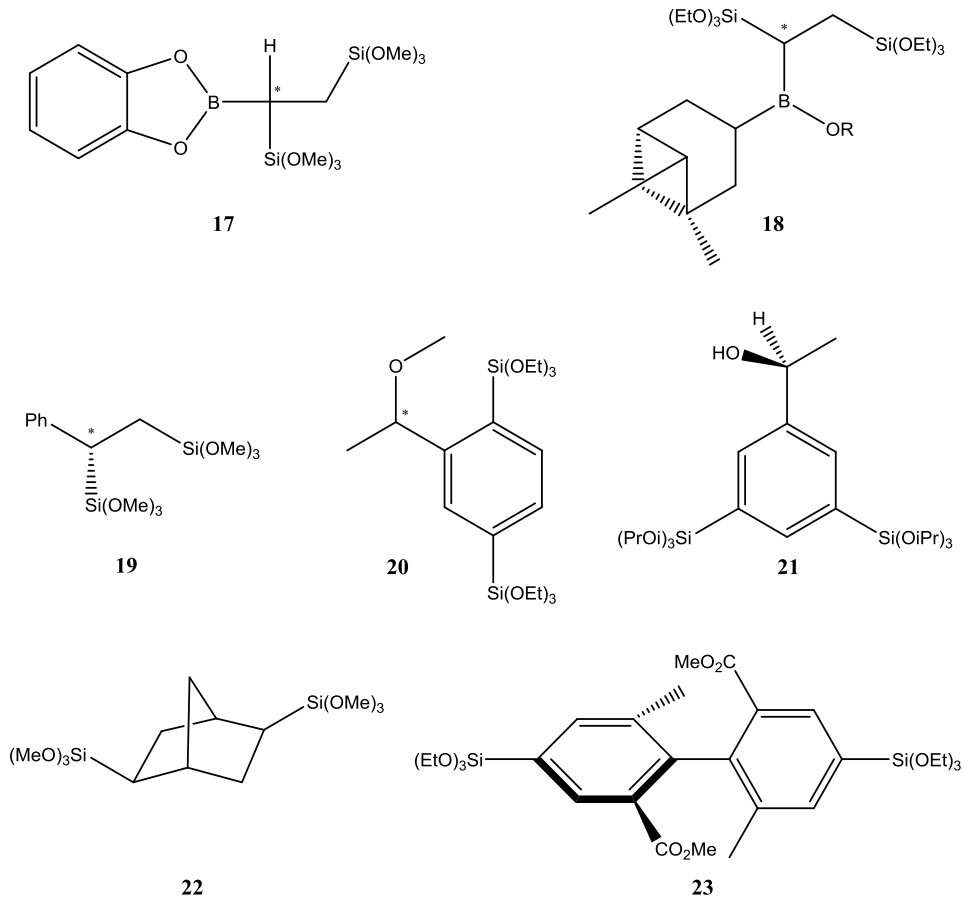

Figure 12. Chiral precursors used in the synthesis of 100% pure PMOs.[157]

The group of Polarz is one of the leading research teams when it comes to chiral PMO structures. They were the first to successfully produce a PMO using an undiluted chiral organosilica source, more specifically by utilizing precursor **(17)**[158]. They did, however, not prove the chirality of the PMO itself. This proof was provided for the first time by Inagaki et al. in 2008, by destroying their PMO based on precursor **(19)** in order to elute the organic groups from the material[159]. Shortly after this publication, the group of Fröba successfully synthesized a chiral benzylic ether-bridged PMO using precursor **(20)**[160]. In contrast to the destructive method used by Inagaki, they devised a non-destructive way in order to determine the chirality of the final PMO material by measuring the optical activity of the solid material.

Polarz et al. also constructed a PMO with **(21)**[161]**.** Afterwards, they treated the material with Me_2AlCl, replacing the chiral alcohol group with the Lewis acid Al^{III}. The catalytic activity was then tested for the asymmetric carbonyl ene reaction between trichloroethanal and α-methylstyrene. They concluded that by modifying the free surface silanol groups with bulky isopropyl groups, the rotational freedom of the Al-O contact formed between the Lewis acid Al^{III} center and the C=O of trichloroethanal was strongly hindered. This implied that the position of the prochiral center was fixed with regard to the asymmetric carbon of the organosilica surface, resulting in higher ee (up to 80%). Moreover, they observed an increase in ee value with decreasing pore size. One can thus conclude that confinement effects in nanoporous materials and the presence of secondary surface groups are of pivotal importance when performing enantioselective catalysis.

PMOs with larger groups were also successfully synthesized, however the presence of a more rigid co-precursor was necessary. Often, these large precursors act as a ligand for transition metals, which form the active catalytic center (as discussed earlier on with **(16)**). One of the most important molecules used in asymmetric transition-metal catalysis is 2,2'-bis(diphenylphosphino)-1,1'-binaphtyl (BINAP)[155,162]. The alcohol derivative, 1,1'-bi-2-naphtol (BINOL) (Figure 13), is readily available in both

enantiomeric forms and consequently has received a lot of attention for its use in PMO synthesis[155,163,164]. Garcia et al. were able to introduce this compound, hence making a chiral PMO, and tested its catalytic activity in the Ti-promoted asymmetric oxidation of methyl phenyl sulfide[163]. Yang et al., on the other hand, achieved catalytic activity in the asymmetric addition of diethylzinc to benzaldehyde with a slightly different BINOL based PMO material[165].

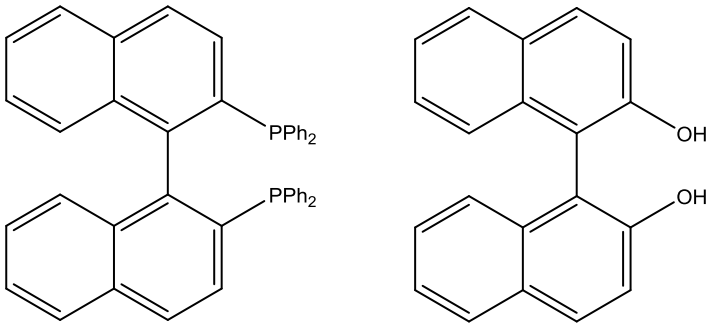

Figure 13. Chemical structures of 2,2'-bis(diphenylphosphino)-1,1'-binaphtyl (BINAP) and 1,1'-Bi-2-naphtol (BINOL)

The same authors were also successful in the synthesis of BINAP PMO, where the BINAP groups acted as ligands with a Ru-complex[166]. The asymmetric hydrogenation of β-keto esters catalyzed by this material reached a conversion of 99% and an enantiomeric excess as high as 92-99%.

1.3.5.4 Acid, base and bifunctional PMOs

Brønsted acid containing PMOs have been more intensively researched than their base counterpart. Moreover, sulfonic acids are by far the most widely used acid functionalities in acid PMO catalysis. Often, thiol functionalities are first introduced in the material, followed by their oxidation giving rise to the desired sulfonic acid group[56,167,168]. Another option is the oxidative cleavage of disulfide bonds in the pore walls[169]. Thirdly, one can functionalize the pore walls immediately with sulfonic acid functionalities by utilizing chlorosulfonic acid[74] or alternatively through direct sulfonation using H_2SO_4[170]. Sulfonated PMOs are proven catalysts in, for example,

etherification[171], esterification[74,167–169,172], condensation[170] and transesterification reactions[56]. The latter reaction is exceedingly important in the conversion of vegetable oils with methanol into biodiesel. It can be concluded that the balance between the hydrophilicity and hydrophobicity of the surface combined with the pore size of the mesochannels plays a vital role in the catalytic activity of PMOs[56,157,172].

As mentioned earlier, base catalysis by PMOs is not as frequently performed as acid catalysis. Nonetheless, several very interesting publications have appeared over the last ten years concerning this topic. Generally, amine groups act as the catalytic site for, for example, Knoevenagel condensations[173–176] and Henry reactions[175–177]. More complex structures such as melamine or urea bridged PMOs have been found to catalyze the coupling of epoxides with CO_2[52,178] as a carbon capture and utilization strategy and phenyl thiazolium modified PMOs as benzoin condensation catalyst[179].

As the name suggests, bifunctional PMOs are hybrid materials that do not contain only one functionality, but in which two distinct functionalities are present. This can be achieved by post-synthetic modifications, by co-condensation of two different precursors, or by combining both techniques. Nevertheless, it is clear that this is not a simple procedure. Either, one has to take into account the different hydrolysis and condensation rates of the different precursors, or one has to post-synthetically introduce two (antagonistic) functionalities without them interacting with one another. On the other hand, the introduction of two catalytically active sites in one material can lead to a catalytic conversion and selectivity that cannot be obtained by single-site catalysts. Some very inspiring work has already been performed in this field of research[93,180–185].

An interesting reaction which can potentially benefit from a bifunctional acid-base PMO is the aldol condensation. This carbon-carbon coupling reaction is extensively used in the pharmaceutical industry[186], in the field of flavor and fragrance chemistry[187], as well as in the biodiesel production[188–191]. Nowadays, aldol condensations are commonly catalyzed by strong homogeneous Brønsted bases such as NaOH[186,192–194]. In 2015

however, the group of J. Thybaut suggested that amines with neighboring primary alcohol groups, especially on the β-carbon, which are anchored on silica supports, would be optimal aldol condensation catalysts[195]. The amine acts as a base, while the alcohol group creates a promoting effect resulting from the hydrogen bonding between the latter and the carbonyl moiety of the reactant[193,196–198]. Interestingly, when Van Der Voort et al. functionalized ethylene bridged PMO with cysteine and cysteamine, they concluded that the silanol groups had a stronger promoting effect than the carboxylic acid group[55].

1.4 Aim of this work

The aim of this PhD is firstly: to develop structurally stable, leaching free, ordered porous heterogeneous catalysts for the aldol condensation. We will do so by post-synthetic modification of periodic mesoporous organosilicas to bifunctional stable catalysts. Secondly: to investigate the potential of aniline bridged PMO towards further post-synthetic modification with functional groups which are of interest for catalytic evaluation.

To achieve these goals, the following aspects were investigated:

1. The development of stable functionalized PMOs by starting with aniline bridged PMO, which can be made in a reproducible way[174], and establishing a post-synthetic strategy to convert the amine group with bromine. On the other hand, following Fröba's recipe[199], we attempted to reproduce and enhance the synthesis of 2,5-bis((*E*)-2-(triethoxysilyl)vinyl)aniline (BTEVA) bridged PMO. Combining the two in the end, should lead us to the development of divinylbromobenzene bridged PMO, susceptible for modification by a variety of different organic reactions. (Chapter 2)
2. The synthesis of L-serine modified benzene bridged PMO, bearing an amine with an alcohol function on the β-carbon, with the aim of producing a material

that is catalytically active in the aldol condensation of acetone and 4-nitrobenzaldehyde. (Chapter 3)

3. In light of using PMOs as base catalysts, we investigated the ability to post-synthetically modify benzene bridged PMO with *N,N'*-diisopropylcarbodiimide (DIC), in order to obtain a hybrid mesoporous material functionalized with an organic "superbase" group: a guanidine. Preliminary catalytic tests were performed on the Henry reaction of nitromethane and benzaldehyde. (Chapter 4)

1.5 References

1. van Bekkum, H., Flannigan, E. M., Jacobs, P. A. & Jansen, J. C. in *Introduction to zeolite science and practice* (2001).
2. Baerlocher, C., McCusker, L. & Olson, D. *Atlas of zeolite framework types*. (Elsevier, 2007). doi:10.1016/B978-044453064-6/50287-5
3. Urey, H. C. & Taylor, T. I. Fractionation of the Lithium and Potassium Isotopes by Chemical Exchange with Zeolites. **429,** 429–438 (1938).
4. Barrer, R. M. Fractionation of mixtures of hydrocarbons. (1942).
5. Tschirner, F. Purification of water by zeolites. (1935).
6. Dolbear, C. E., Wiseman, P. & Wiseman, K. P. Method of sweetening petroleum distillates. (1940).
7. Weisz, P. B. Upgrading of naphthas. (1963).
8. Hopkins, P. Cracking activity of some synthetic zeolites and the nature of the active sites. *J. Catal.* **12,** 325–334 (1968).
9. Beck, J. S., Vartuli, J.C., Roth, W.J., Leonowicz, M.E., Kresge, C.T., Schmitt, K.D., Chu, C.T-W., Olson, D.H., SHeppard, E.W., McCullen, S.B., Higgins, J.B., Schlenker, J.L., A New Family of Mesoporous Molecular Sieves Prepared with Liquid Crystal Templates. *J. Am. Chem. Soc.* 10834–10843 (1992). doi:10.1021/ja00053a020
10. Wang, S. Ordered mesoporous materials for drug delivery. *Microporous Mesoporous Mater.* **117,** 1–9 (2009).
11. Sánchez-Sánchez, Á., Suárez-García, F., Martínez-Alonso, a. & Tascón, J. M. D. pH-responsive ordered mesoporous carbons for controlled ibuprofen release. *Carbon N. Y.* **94,** 152–159 (2015).
12. Freitas, L. B. D. O., Bravo, I. J. G., Macedo, W. A. D. A. & de Sousa, E. M. B. Mesoporous silica materials functionalized with folic acid: preparation, characterization and release profile study with methotrexate. *J. Sol-Gel Sci. Technol.* (2015). doi:10.1007/s10971-015-3844-8
13. Shiju, N. R., Alberts, A. H., Khalid, S., Brown, D. R. & Rothenberg, G. Mesoporous silica with site-isolated amine and phosphotungstic acid groups: a solid catalyst with tunable antagonistic functions for one-pot tandem reactions. *Angew. Chem. Int. ed.* **50,** 9615–9 (2011).
14. Shang, F., Sun, J., Wu, S., Yang, Y., Kan, Q., Guan, J., Direct synthesis of acid-base bifunctional mesoporous MCM-41 silica and its catalytic reactivity in Deacetalization-Knoevenagel reactions. *Microporous Mesoporous Mater.* **134,** 44–50 (2010).
15. Huo, Q., Margolese, D.I., Ciesla, U., Feng, P., Gier, T.E., Sieger, P., Leon, R., Petroff, P.M., Schüth, F., Stucky, G.D., Generalized synthesis of periodic surfactant/inorganic composite materials. *Nature* **368,** 317–321 (1994).
16. Hoffmann, F., Cornelius, M., Morell, J. & Fröba, M. Silica-based mesoporous organic-inorganic hybrid materials. *Angew. Chem. Int. Ed. Engl.* **45,** 3216–3251 (2006).
17. Zhao, D., Huo, Q., Feng, J., Chmelka, B. F. & Stucky, G. D. Nonionic Triblock and Star Diblock Copolymer and Oligomeric Surfactant Syntheses of Highly Ordered, Hydrothermally Stable, Mesoporous Silica Structures. *J. Am. Chem. Soc.* **120,** 6024–6036 (1998).
18. Zhao, D., Feng, J., Huo, Q., Melosh, N., Fredrickson, G.H., Chmelka, B.F., Stucky, G.D., Triblock Copolymer Syntheses of Mesoporous Silica with Periodic 50 to 300 Angstrom Pores. *Science (80-.).* **279,** 548–552 (1998).

19. Burkett, S. L., Sims, S. D. & Mann, S. Synthesis of hybrid inorganic-organic mesoporous silica by co-condensation of siloxane and organosiloxane precursors. *Chem. Commun.* 1367 (1996). doi:10.1039/cc9960001367
20. Hall, S. R., Fowler, C. E., Lebeau, B. & Mann, S. Template-directed synthesis of bi-functionalized organo-MCM-41 and phenyl-MCM-48 silica mesophases. *Chem. Commun.* 201–202 (1999).
21. Lim, M. H., Blanford, C. F. & Stein, A. Synthesis of Ordered Microporous Silicates with Organosulfur Surface Groups and Their Applications as Solid Acid Catalysts. *Chem. Mater.* **10,** 467–470 (1998).
22. Van der Voort, P., Vercaemst, C., Schaubroeck, D. & Verpoort, F. Ordered mesoporous materials at the beginning of the third millennium: new strategies to create hybrid and non-siliceous variants. *Phys. Chem. Chem. Phys.* **10,** 347–360 (2008).
23. Price, P. M., Clark, J. H. & Macquarrie, D. J. Modified silicas for clean technology. *J. Chem. Soc., Dalt. Trans* 101–110 (2000).
24. Inagaki, S., Guan, S., Fukushima, Y. & Ohsuna, T. Novel Mesoporous Materials with a Uniform Distribution of Organic Groups and Inorganic Oxide in Their Frameworks. *J. Am. Chem. Soc.* 9611–9614 (1999).
25. Asefa, T., MacLachlan, M. J., Coombs, N. & Ozin, G. A. Periodic mesoporous organosilicas with organic groups inside the channel walls. *Nature* **402,** 867–871 (1999).
26. Melde, B. J., Holland, B. T., Blanford, C. F. & Stein, a. Mesoporous sieves with unified hybrid inorganic/organic frameworks. *Chem. Mater.* **11,** 3302–3308 (1999).
27. Park, S. S., Moorthy, M. S. & Ha, C.-S. Periodic mesoporous organosilica (PMO) for catalytic applications. *Korean J. Chem. Eng.* **31,** 1707–1719 (2014).
28. Goethals, F., Meeus, B., Verberckmoes, A., Van der Voort, P. & Van Driessche, I. Hydrophobic high quality ring PMOs with an extremely high stability. *J. Mater. Chem.* **20,** 1709–1716 (2010).
29. Esquivel, D., Van der Voort, P. & Romero-salguero, F. J. Designing advanced functional periodic mesoporous organosilicas for biomedical applications. *AIMS Mater. Sci.* **1,** 70–86 (2014).
30. Zhu, G., Yang, Q., Jiang, D., Yang, J., Zhang, L., Li, Y., Li, C., Synthesis of bifunctionalized mesoporous organosilica spheres for high-performance liquid chromatography. *J. Chromatogr. A* **1103,** 257–264 (2006).
31. Li, Y., Keilbach, A., Kienle, M., Goto, Y., Inagaki, S., Knochel, P., Bein, T., Hierarchically structured biphenylene-bridged periodic mesoporous organosilica. *J. Mater. Chem.* **21,** 17338 (2011).
32. Rebbin, V., Schmidt, R. & Fröba, M. Spherical particles of phenylene-bridged periodic mesoporous organosilica for high-performance liquid chromatography. *Angew. Chemie - Int. Ed.* **45,** 5210–5214 (2006).
33. Asefa, T., Kruk, M., MacLachlan, M.J., Coombs, N., Grondey, H., Jaroniec, M., Ozin, G.A., Novel bifunctional periodic mesoporous organosilicas, BPMOs: Synthesis, characterization, properties and in-situ selective hydroboration - Alcoholysis reactions of functional groups. *J. Am. Chem. Soc.* **123,** 8520–8530 (2001).
34. Shi, J. Y., Wang, C.A., Li, Z.J., Wang, Q., Zhang, Y., Wang, W., Heterogeneous organocatalysis at work: Functionalization of hollow periodic mesoporous organosilica spheres with MacMillan catalyst. *Chem. - A Eur. J.* **17,** 6206–6213 (2011).
35. Zhang, Y., Jin, Y., Dai, P., Yu, H., Yu, D., Ke, Y., Liang, X., Phenylene-bridged hybrid silica spheres for high performance liquid chromatography. *Anal. Methods* **1,** 123–127 (2009).

36. Seino, M., Wang, W., Lofgreen, J.E., Puzzo, D.P., Manabe, T., Ozin, G.A., Low-k periodic mesoporous organosilica with air walls: POSS-PMO. *J. Am. Chem. Soc.* **133,** 18082–18085 (2011).
37. Martens, S., Ortmann, R., Brieler, F.J., Pasel, C., Lee, Y.J., Bathen, D., Fröba, M., Periodic Mesoporous Organosilicas as Adsorbents of Toxic Trace Gases out of the Ambient Air. *Zeitschrift für Anorg. und Allg. Chemie* **640,** 632–640 (2014).
38. Cornelius, M., Hoffmann, F. & Fröba, M. Periodic mesoporous organosilicas with a bifunctional conjugated organic unit and crystal-like pore walls. *Chem. Mater.* **17,** 6674–6678 (2005).
39. Beretta, M., Morell, J., Sozzani, P. & Fröba, M. Towards peptide formation inside the channels of a new divinylaniline-bridged periodic mesoporous organosilica. *Chem. Commun. (Camb).* **46,** 2495–2497 (2010).
40. Esquivel, D., Jiménez-Sanchidrián, C. & Romero-Salguero, F. J. Comparison of the thermal and hydrothermal stabilities of ethylene, ethylidene, phenylene and biphenylene bridged periodic mesoporous organosilicas. *Mater. Lett.* **65,** 1460–1462 (2011).
41. Cornelius, M., Hoffmann, F., Ufer, B., Behrens, P. & Fröba, M. Systematic extension of the length of the organic conjugated π-system of mesoporous silica-based organic–inorganic hybrid materials. *J. Mater. Chem.* **18,** 2587 (2008).
42. Cho, E. B., Kim, D. & Jaroniec, M. Preparation of mesoporous benzene-silica nanoparticles. *Microporous Mesoporous Mater.* **120,** 252–256 (2009).
43. Djojoputro, H., Zhou, X.F., Qiao, S.Z., Wang, L.Z., Yu, C.Z., Lu, G.Q., Periodic mesoporous organosilica hollow spheres with tunable wall thickness. *J. Am. Chem. Soc.* **128,** 6320–6321 (2006).
44. Lin, C. X. (Cynthia), Yuan, P., Yu, C. Z., Qiao, S. Z. & Lu, G. Q. (Max). Cooperative self-assembly of silica-based mesostructures templated by cationic fluorocarbon/hydrocarbon mixed-surfactants. *Microporous Mesoporous Mater.* **126,** 253–261 (2009).
45. Han, Y. & Ying, J. Y. Generalized fluorocarbon-surfactant-mediated synthesis of nanoparticles with various mesoporous structures. *Angew. Chemie - Int. Ed.* **44,** 288–292 (2004).
46. Li, C., Yang, J., Shi, X., Liu, J. & Yang, Q. Synthesis of SBA-15 type mesoporous organosilicas with diethylenebenzene in the framework and post-synthetic framework modification. *Microporous Mesoporous Mater.* **98,** 220–226 (2007).
47. Vercaemst, C., Ide, M., Allaert, B., Ledoux, N., Verpoort, F., Van Der Voort, P., Ultra-fast hydrothermal synthesis of diastereoselective pure ethenylene-bridged periodic mesoporous organosilicas. *Chem. Commun.* 2261–2263 (2007). doi:10.1039/b705412b
48. Cho, E.-B. & Kim, D. Multifunctional periodic mesoporous organosilicas prepared with block copolymer: Composition effect on morphology. *Microporous Mesoporous Mater.* **113,** 530–537 (2008).
49. Esquivel, D., van den Berg, O., Romero-Salguero, F. J., Du Prez, F. & Van der Voort, P. 100% thiol-functionalized ethylene PMOs prepared by 'thiol acid-ene' chemistry. *Chem. Commun. (Camb).* **49,** 2344–6 (2013).
50. Mandal, M. & Kruk, M. Versatile approach to synthesis of 2-D hexagonal ultra-large-pore periodic mesoporous organosilicas. *J. Mater. Chem.* **20,** 7506 (2010).
51. Sim, K., Lee, N., Kim, J., Cho, E-B., Gunathilake, C., Jaroniec, M., CO2 adsorption on amine-functionalized periodic mesoporous benzenesilicas. *ACS Appl. Mater. Interfaces* **7,** 6792–6802 (2015).

52. Prasetyanto, E. A., Ansari, M. B., Min, B.-H. & Park, S.-E. Melamine tri-silsesquioxane bridged periodic mesoporous organosilica as an efficient metal-free catalyst for CO2 activation. *Catal. Today* **158,** 252–257 (2010).
53. Morell, J., Güngerich, M., Wolter, G., Jiao, J., Hunger, M., Klar, P.J., Fröba, M., Synthesis and characterization of highly ordered bifunctional aromatic periodic mesoporous organosilicas with different pore sizes. *J. Mater. Chem.* **16,** 2809 (2006).
54. Xia, H.-S., Zhou, C.-H. (Clayton), Tong, D. S. & Lin, C. X. Synthesis chemistry and application development of periodic mesoporous organosilicas. *J. Porous Mater.* **17,** 225–252 (2010).
55. Ouwehand, J., Lauwaert, J., Esquivel, D., Hendrickx, K., Van Speybroeck, V., Thybaut, J.W., Van Der Voort, P., Facile Synthesis of Cooperative Acid-Base Catalysts by Clicking Cysteine and Cysteamine on an Ethylene-Bridged Periodic Mesoporous Organosilica. *Eur. J. Inorg. Chem.* (2016). doi:10.1002/ejic.201501179
56. Karimi, B., Mirzaei, H. M. & Mobaraki, A. Periodic mesoporous organosilica functionalized sulfonic acids as highly efficient and recyclable catalysts in biodiesel production. *Catal. Sci. Technol.* **2,** 828 (2012).
57. Gehring, J., Schleheck, D., Trepka, B. & Polarz, S. Mesoporous Organosilica Nanoparticles Containing Superacid and Click Functionalities Leading to Cooperativity in Biocidal Coatings. *ACS Appl. Mater. Interfaces* **7,** 1021–1029 (2015).
58. Mandal, M. & Kruk, M. Ethylene-bridged Periodic Mesoporous Organosilicas with Large Spherical Pores Templated by PEO-PPO-PEO Surfactant Micelles Swollen by Ethylbenzene. *Zeitschrift für Anorg. und Allg. Chemie* **640,** 624–631 (2014).
59. Luka, M. & Polarz, S. Wiring functional groups in mesoporous organosilica materials. *J. Mater. Chem. C* **3,** 2195–2203 (2015).
60. Zhou, X., Qiao, S., Hao, N., Wang, X., Yu, C., Wang, L., Zhao, D., Lu, G.Q., Synthesis of Ordered Cubic Periodic Mesoporous Organosilicas with Ultra-Large Pores. *Chem. Mater.* **19,** 1870–1876 (2007).
61. Hao, T. T., Shi, J.Y., Zhuang, T.Y., Wang, W.D., Li, F.C., Wang, W., Mesostructure-controlled synthesis of chiral norbornane-bridged periodic mesoporous organosilicas. *RSC Adv.* **2,** 2010 (2012).
62. Ide, M., El-Roz, M., De Canck, E., Vicente, A., Plankaert, T., Bogaerts, T., Van Driesche, I., Lynen, F., Van Speybroeck, V., Thybault-Starzyk, F., Van Der Voort, P., Quantification of silanol sites for the most common mesoporous ordered silicas and organosilicas: total versus accessible silanols. *Phys. Chem. Chem. Phys.* **15,** 642–50 (2013).
63. Cho, E.-B., Kim, D., Górka, J. & Jaroniec, M. Three-dimensional cubic (Im3m) periodic mesoporous organosilicas with benzene- and thiophene-bridging groups. *J. Mater. Chem.* **19,** 2076 (2009).
64. Hu, Y., Qian, K., Yuan, P., Wang, Y. & Yu, C. Synthesis of large-pore periodic mesoporous organosilica. *Mater. Lett.* **65,** 21–23 (2011).
65. Cho, E.-B., Kim, D. & Jaroniec, M. Bifunctional periodic mesoporous organosilicas with thiophene and isocyanurate bridging groups. *Langmuir* **25,** 13258–13263 (2009).
66. Cho, E.-B., Han, O. H., Kim, S., Kim, D. & Jaroniec, M. Multifunctional periodic mesoporous organosilicas with bridging groups formed via dynamic covalent chemistry. *Chem. Commun. (Camb).* **46,** 4568–4570 (2010).
67. Kapoor, M. P., Setoyama, N., Yang, Q., Ohashi, M. & Inagaki, S. Oligomeric polymer surfactant driven self-assembly of phenylene-bridged mesoporous materials and their physicochemical properties. *Langmuir* **21,** 443–449 (2005).

68. Kapoor, M. P., Kasama, Y., Yanagi, M., Yokoyama, T., Inagaki, S., Shimada, T., Nanbu, H.n Lekh, R.J., Cubic phenylene bridged mesoporous hybrids from allylorganosilane precursors and their applications in Friedel–Crafts acylation reaction. *Microporous Mesoporous Mater.* **101,** 231–239 (2007).
69. Keilbach, A., Döblinger, M., Köhn, R., Amenitsch, H. & Bein, T. Periodic mesoporous organosilica in confined environments. *Chem. - A Eur. J.* **15,** 6645–6650 (2009).
70. Hamoudi, S. & Kaliaguine, S. Periodic mesoporous organosilica from micellar oligomer template solution. *Chem. Commun.* 2118–2119 (2002). doi:10.1039/b207134g
71. Nakai, K., Oumi, Y., Horie, H., Sano, T. & Yoshitake, H. Bromine addition and successive amine substitution of mesoporous ethylenesilica: Reaction, characterizations and arsenate adsorption. *Microporous Mesoporous Mater.* **100,** 328–339 (2007).
72. Corral, J., Lopez, M.I., Esquivel, D., Mora, M., Jimenez-Sanchidrian, C., Romero-Salguero, F.J., Preparation of Palladium-Supported Periodic Mesoporous Organosilicas and their Use as Catalysts in the Suzuki Cross-Coupling Reaction. *Materials (Basel).* **6,** 1554–1565 (2013).
73. Carpio, A., Esquivel, D., Arce, L., Romero-Salgero, F.J., Van Der Voort, P., Jimenez-Sanchidrian, C., Valcarcel, M., Evaluation of phenylene-bridged periodic mesoporous organosilica as a stationary phase for solid phase extraction. *J. Chromatogr. A* **1370,** 25–32 (2014).
74. Esquivel, D., Jiménez-Sanchidrián, C. & Romero-Salguero, F. J. Thermal behaviour, sulfonation and catalytic activity of phenylene-bridged periodic mesoporous organosilicas. *J. Mater. Chem.* **21,** 724 (2011).
75. Dickson, S. E. & Crudden, C. M. Transformable periodic mesoporous organosilica materials. *Chem. Commun. (Camb).* **46,** 2100–2102 (2010).
76. Hunks, W. J. & Ozin, G. a. Periodic mesoporous phenylenesilicas with ether or sulfide hinge groups--a new class of PMOs with ligand channels. *Chem. Commun. (Camb).* 2426–7 (2004). doi:10.1039/b410397a
77. Sayari, A. & Yang, Y. Nonionic oligomeric polymer directed synthesis of highly ordered large pore periodic mesoporous organosilica. *Chem. Commun.* 2582–2583 (2002). doi:10.1039/b208512g
78. Lee, H. I., Pak, C., Yi, S.H., Shon, J.K., Kim, S.S., So, B.G., Chang, H., Yie, J.E., Kwon, Y-U., Kim, J.M., Systematic phase control of periodic mesoporous organosilicas using Gemini surfactants. *J. Mater. Chem.* **15,** 4711–4717 (2005).
79. Hyung, I. L., Ji, M. K. & Stucky, G. D. Periodic mesoporous organosilica with a hexagonally pillared lamellar structure. *J. Am. Chem. Soc.* **131,** 14249–14251 (2009).
80. Cassiers, K., Linssen, T., Mathieu, M., Benjelloun, M., Schrijnemakers, K., Van Der Voort, P., Cool, P., Vansant, E.F., A Detailed Study of Thermal, Hydrothermal , and Mechanical Stabilities of a Wide Range of Surfactant Assembled Mesoporous Silicas. *Chem. Mater.* 2317–2324 (2002). doi:10.1021/cm0112892
81. Smeulders, G., Meynen, V., Silvestre-Albero, A., Houthoofd, K., Mertens, M., Silvestre-Albero, J., Martens, J.A., Cool, P., The impact of framework organic functional groups on the hydrophobicity and overall stability of mesoporous silica materials. *Mater. Chem. Phys.* **132,** 1077–1088 (2012).
82. Inagaki, S., Guan, S., Ohsuna, T. & Terasaki, O. An ordered mesoporous organosilica hybrid material with a crystal-like wall structure. *Nature* **416,** 304–307 (2002).
83. Smeulders, G., Meynen, V., Van Baelen, G., Mertens, M., Lebedev, O.I., Van tendeloo, G., Maes, B.U.W., Cool, P., Rapid microwave-assisted synthesis of benzene bridged periodic

mesoporous organosilicas. *J. Mater. Chem.* **19,** 3042 (2009).
84. Kalantzopoulos, G. N., Enotiadis, A., Maccalini, E., Antoniou, M., Dimos, K., Policicchio, A., Klontzas, E., Tylianakis, E., Binas, V., Trikalitis, P.N., Agostino, R.G., Gournis, D., Froudakis, G.E., Hydrogen storage in ordered and disordered phenylene-bridged mesoporous organosilicas. *Int. J. Hydrogen Energy* **39,** 2104–2114 (2014).
85. Rác, B., Hegyes, P., Forgo, P. & Molnár, Á. Sulfonic acid-functionalized phenylene-bridged periodic mesoporous organosilicas as catalyst materials. *Appl. Catal. A Gen.* **299,** 193–201 (2006).
86. Bispo, C., Ferreira, P., Trouve, A., Batonneau-Gener, I., Liu, F., Jerome, F., Bion, N., Role of acidity and hydrophobicity in the remarkable catalytic activity in water of sulfonic acid-functionalized phenyl-PMO materials. *Catal. Today* **218–219,** 85–92 (2013).
87. Esquivel, D., Jiménez-Sanchidrián, C. & Romero-Salguero, F. J. Thermal behaviour, sulfonation and catalytic activity of phenylene-bridged periodic mesoporous organosilicas. *J. Mater. Chem.* **21,** 724 (2011).
88. Lourenço, M. a O., Siegel, R., Mafra, L. & Ferreira, P. Microwave assisted N-alkylation of amine functionalized crystal-like mesoporous phenylene-silica. *Dalt. Trans.* **42,** 5631–5634 (2013).
89. Temtsin, G., Asefa, T., Bittner, S. & Ozin, G. A. Aromatic PMOs: tolyl, xylyl and dimethoxyphenyl groups integrated within the channel walls of hexagonal mesoporous silicas. *J. Mater. Chem.* **11,** 3202–3206 (2001).
90. Lourenço, M. a. O., Mayoral, A., Díaz, I., Silva, A. R. & Ferreira, P. Amino-modified periodic mesoporous biphenylene-silica. *Microporous Mesoporous Mater.* **217,** 167–172 (2015).
91. Hunks, W. J. & Ozin, G. A. Challenges and advances in the chemistry of periodic mesoporous organosilicas (PMOs). *J. Mater. Chem.* **15,** 3716 (2005).
92. Bracco, S., Beretta, M., Cattaneo, A., Comotti, A., Falqui, A., Zhao, K., Rogers, C., Sozzani, P., Dipolar Rotors Orderly Aligned in Mesoporous Fluorinated Organosilica Architectures. *Angew. Chemie Int. Ed.* n/a-n/a (2015). doi:10.1002/anie.201412412
93. Alauzun, J., Mehdi, A., Reyé, C. & Corriu, R. J. P. Mesoporous materials with an acidic framework and basic pores. A successful cohabitation. *J. Am. Chem. Soc.* **128,** 8718–8719 (2006).
94. Olkhovyk, O., Pikus, S. & Jaroniec, M. Bifunctional periodic mesoporous organosilica with large heterocyclic bridging groups and mercaptopropyl ligands. *J. Mater. Chem.* **15,** 1517 (2005).
95. Landskron, K., Hatton, B. D., Perovic, D. D. & Ozin, G. A. Periodic Mesoporous Organosilicas Containing Interconnected [Si (CH 2)] 3 Rings. *Science (80-.).* **302,** 266–269 (2003).
96. Landskron, K. & Ozin, G. a. Periodic mesoporous dendrisilicas. *Science* **306,** 1529–1532 (2004).
97. Burleigh, M. C. *et al.* A New Family of Copolymers: Multifunctional Periodic Mesoporous Organosilicas. *Communications* **16,** 3–5 (2004).
98. Kuroki, M., Asefa, T., Whitnal, W., Kruk, M., Yoshina-Ishii, C., Jaroniec, M., Ozin, G.A., Synthesis and properties of 1,3,5-benzene periodic mesoporous organosilica (PMO): Novel aromatic PMO with three point attachments and unique thermal transformations. *J. Am. Chem. Soc.* **124,** 13886–13895 (2002).
99. Yoshina-Ishii, C., Asefa, T., Coombs, N., MacLachlan, M. J. & Ozin, G. A. Periodic mesoporous organosilicas, PMOs: fusion of organic and inorganic chemistry 'inside' the channel walls of hexagonal mesoporous silica. *Chem. Commun.* 2539–2540 (1999).

doi:10.1039/a908252b

100. Kapoor, M. P., Yang, Q. & Inagaki, S. Self-assembly of biphenylene-bridged hybrid mesoporous solid with molecular-scale periodicity in the pore walls. *J. Am. Chem. Soc.* **124,** 15176–15177 (2002).
101. Xia, Y., Wang, W. & Mokaya, R. Bifunctional hybrid mesoporous organoaluminosilicates with molecularly ordered ethylene groups. *J. Am. Chem. Soc.* **127,** 790–798 (2005).
102. Sayari, A. & Wang, W. Molecularly Ordered Organosilicates Prepared with and without Surfactants. *J. Am. Chem. Soc.* **127,** 12194–12195 (2005).
103. Zhang, W. H., Zhang, X., Hua, Z., Harish, P., Schroeder, F., Hermes, S., Cadenbach, T., Shi, J., Fischer, R.A., Synthesis, bifunctionalization, and application of isocyanurate-based periodic mesoporous organosilicas. *Chem. Mater.* **19,** 2663–2670 (2007).
104. Kapoor, M. P. & Inagaki, S. Synthesis of phenylene bridged mesoporous silsesquioxanes with spherical morphology in ammonia solution. *Chem. Lett.* **33,** 88–89 (2004).
105. Rebbin, V., Jakubowski, M., Pötz, S. & Fröba, M. Synthesis and characterisation of spherical periodic mesoporous organosilicas (sph-PMOs) with variable pore diameters. *Microporous Mesoporous Mater.* **72,** 99–104 (2004).
106. Stöber, W., Fink, A. & Bohn, E. Controlled growth of monodisperse silica spheres in the micron size range. *J. Colloid Interface Sci.* **26,** 62–69 (1968).
107. Ide, M., De Canck, E., Van Driessche, I., Lynen, F. & Van Der Voort, P. Developing a new and versatile ordered mesoporous organosilica as a pH and temperature stable chromatographic packing material. *RSC Adv.* **5,** 5546–5552 (2015).
108. Walcarius, A. & Mercier, L. Mesoporous organosilica adsorbents: nanoengineered materials for removal of organic and inorganic pollutants. *J. Mater. Chem.* **20,** 4478–4511 (2010).
109. López, M. I. *et al.* Evaluation of different bridged organosilicas as efficient adsorbents for the herbicide S-metolachlor. *RSC Adv.* **5,** 24158–24166 (2015).
110. Gao, Y., De Canck, E., Leermakers, M., Baeyens, W. & Van Der Voort, P. Synthesized mercaptopropyl nanoporous resins in DGT probes for determining dissolved mercury concentrations. *Talanta* **87,** 262–267 (2011).
111. De Canck, E., Ascoop, I., Sayari, A. & Van der Voort, P. Periodic mesoporous organosilicas functionalized with a wide variety of amines for CO2 adsorption. *Phys. Chem. Chem. Phys.* **15,** 9792–9799 (2013).
112. Fried, D. I., Brieler, F. J. & Fröba, M. Designing Inorganic Porous Materials for Enzyme Adsorption and Applications in Biocatalysis. *ChemCatChem* **5,** 862–884 (2013).
113. Zhu, L., Liu, X., Chen, T., Xu, Z., Yan, W., Zhang, H., Functionalized periodic mesoporous organosilicas for selective adsorption of proteins. *Appl. Surf. Sci.* **258,** 7126–7134 (2012).
114. Jung, J. H., Han, W.S., Rim, J.A., Lee, S.J., Cho, S.J., Kim, S.Y., Kang, J.K., Shinkai, S., Hydrogen Adsorption in Periodic Mesoporous Organic– and Inorganic–Silica Materials at Room Temperature. *Chem. Lett.* **35,** 32–33 (2006).
115. Kubo, M., Ishiyama, K., Shimojima, A. & Okubo, T. Effect of organic groups on hydrogen adsorption properties of periodic mesoporous organosilicas. *Microporous Mesoporous Mater.* **147,** 194–199 (2012).
116. Kalantzopoulos, G. N., Antoniou, M.K., Enotiadis, A., Dimos, K., Maccalini, E., Policicchio, A., Colavita, E;, Agostino, R.G., Enhanced hydrogen and methane storage of hybrid mesoporous organosilicas. *J. Mater. Chem. A* **4,** 9275–9285 (2016).
117. Maex, K., Baklanov, M.R., Shamiryan, D., Lacopi, F., Brongersma, S.H., Yanovitskaya, Z.S., Low dielectric constant materials for microelectronics. *J. Appl. Phys.* **93,** 8793–8841

(2003).
118. Volksen, W., Miller, R. & Dubois, G. Low dielectric constant materials. *Chem. Rev.* **110,** 56–110 (2010).
119. Goethals, F. *et al.* Ultra-low-k cyclic carbon-bridged PMO films with a high chemical resistance. *J. Mater. Chem.* **22,** 8281–8286 (2012).
120. Goethals, F., Ciofi, I., Madia, O., Vanstreeks, K., Baklanov, M.R., Detavernier, C., Van Der Voort, P., Van Driessche, I., A new procedure to seal the pores of mesoporous low-k films with precondensed organosilica oligomers. *Chem. Commun. (Camb).* **48,** 2797–2799 (2012).
121. Goethals, F., Levreau, E., Pollefeyt, G., Baklanov, M.R., Ciofi, I., Vanstreels, K., Detavernier, C., Van Driessche, I., Van Der Voort, P., Sealed ultra low-k organosilica films with improved electrical, mechanical and chemical properties. *J. Mater. Chem. C* **1,** 3961–3966 (2013).
122. Wang, X., Lu, D., Austin, R., Agarwal, A., Mueller, L.J., Liu, Z., Wu, J., Feng, P., Protein refolding assisted by periodic mesoporous organosilicas. *Langmuir* **23,** 5735–5739 (2007).
123. Parambadath, S., Rana, V.K., Moorthy, S., Chu, S-M., Park, S-K., Lee, D., Sung, G., Ha, C-S., Periodic mesoporous organosilicas with co-existence of diurea and sulfanilamide as an effective drug delivery carrier. *J. Solid State Chem.* **184,** 1208–1215 (2011).
124. Parambadath, S., Rana, V. K., Zhao, D. & Ha, C.-S. N,N'-diureylenepiperazine-bridged periodic mesoporous organosilica for controlled drug delivery. *Microporous Mesoporous Mater.* **141,** 94–101 (2011).
125. Munaweera, I., Hong, J., D'Souza, A. & Balkus, K. J. Novel wrinkled periodic mesoporous organosilica nanoparticles for hydrophobic anticancer drug delivery. *J. Porous Mater.* **22,** 1–10 (2014).
126. Moorthy, M. S., Kim, M.J., Bae, J-H., Park, S.S., Saravanan, N., Kim, S-H., Ha, C-S., Multifunctional periodic mesoporous organosilicas for biomolecule recognition, biomedical applications in cancer therapy, and metal adsorption. *Eur. J. Inorg. Chem.* 3028–3038 (2013). doi:10.1002/ejic.201300118
127. Chen, Y., Meng, Q., Wu, M., Wang, S., Xu, P., Chen, H., Li, Y., Zhang, L., Wang, L., Shi, J., Hollow mesoporous organosilica nanoparticles: A generic intelligent framework-hybridization approach for biomedicine. *J. Am. Chem. Soc.* **136,** 16326–16334 (2014).
128. Lee, M. H., Yang, Z., Lim, C.W., Lee, Y.H., Dongbang, S., Kang, C., Kim, J.S., Disulfide-Cleavage-Triggered Chemosensors and Their Biological Applications. *Chem. Rev.* 5071–5109 (2013). doi:10.1021/cr300358b
129. Lu, N. *et al.* Smart Cancer Cell Targeting Imaging and Drug Delivery System by Systematically Engineering Periodic Mesoporous Organosilica Nanoparticles. *ACS Appl. Mater. Interfaces* **8,** 2985–2993 (2016).
130. Alvaro, M., Ferrer, B., García, H. & Rey, F. Photochemical modification of the surface area and tortuosity of a trans-1,2-bis(4-pyridyl)ethylene periodic mesoporous MCM organosilica. *Chem. Commun.* 2012–2013 (2002). doi:10.1039/b205883a
131. Alvaro, M., Benitez, M., Das, D., Garcia, H. & Peris, E. Reversible porosity changes in photoresponsive azobenzene-containing periodic mesoporous silicas. *Chem. Mater.* **17,** 4958–4964 (2005).
132. Maegawa, Y., Mizoshita, N., Tani, T. & Inagaki, S. Transparent and visible-light harvesting acridone-bridged mesostructured organosilica film. *J. Mater. Chem.* **20,** 4399–4403 (2010).

133. Ikai, M., Maegawa, Y., Goto, Y., Tani, T. & Inagaki, S. Synthesis of visible-light-absorptive and hole-transporting periodic mesoporous organosilica thin films for organic solar cells. *J. Mater. Chem. A* 11857–11865 (2014). doi:10.1039/c4ta01136h
134. Grösch, L., Lee, Y. J., Hoffmann, F. & Fröba, M. Light-Harvesting Three-Chromophore Systems Based on Biphenyl-Bridged Periodic Mesoporous Organosilica. *Chem. - A Eur. J.* **21,** 331–346 (2015).
135. Takeda, H., Ohashi, M., Goto, Y., Ohsuna, T., Tani, T., Inagaki, S., Light-harvesting photocatalysis for water oxidation using mesoporous organosilica. *Chem. - A Eur. J.* **20,** 9130–9136 (2014).
136. Ueda, Y., Takeda, H., Yui, T., Koike, K., Goto, Y., Inagaki, S., Ishitani, O., A Visible-Light Harvesting System for CO2 Reduction Using a RuII-ReI Photocatalyst Adsorbed in Mesoporous Organosilica. *ChemSusChem* **8,** 439–442 (2015).
137. Baleizão, C., Gigante, B., Das, D., Alvaro, M., Garcia, H., Corma, A., Periodic mesoporous organosilica incorporating a catalytically active vanadyl Schiff base complex in the framework. *J. Catal.* **223,** 106–113 (2004).
138. Gu, E., Zhong, W. & Liu, X. Periodic mesoporous organosilicas functionalized with iron(iii) complexes: preparation, characterization and catalysis on direct hydroxylation of benzene to phenol. *RSC Adv.* **6,** 98406–98412 (2016).
139. Zheng, X., Wang, M., Sun, Z., Chen, C., Ma, J., Xu, J., Preparation of copper (II) ion-containing bisimidazolium ionic liquid bridged periodic mesoporous organosilica and the catalytic decomposition of cyclohexyl hydroperoxide. *Catal. Commun.* **29,** 149–152 (2012).
140. Maegawa, Y. & Inagaki, S. Iridium-bipyridine periodic mesoporous organosilica catalyzed direct C-H borylation using a pinacolborane. *Dalt. Trans.* **44,** 13007–13016 (2015).
141. Liu, X., Maegawa, Y., Goto, Y., Hara, K. & Inagaki, S. Heterogeneous Catalysis for Water Oxidation by an Iridium Complex Immobilized on Bipyridine-Periodic Mesoporous Organosilica. *Angew. Chemie - Int. Ed.* **55,** 7943–7947 (2016).
142. Clerick, S., De Canck, E., Hendrickx, K., Van Speybroeck, V. & Van Der Voort, P. Heterogeneous Ru(III) oxidation catalysts via 'click' bidentate ligands on a periodic mesoporous organosilica support. *Green Chem.* (2016). doi:10.1039/C6GC01494A
143. Bilal, M., Iqbal, H. M. N., Hu, H., Wang, W. & Zhang, X. Enhanced bio-catalytic performance and dye degradation potential of chitosan-encapsulated horseradish peroxidase in a packed bed reactor system. *Sci. Total Environ.* (2016). doi:10.1016/j.scitotenv.2016.09.215
144. Na, S. Y. & Lee, Y. Elimination of trace organic contaminants during enhanced wastewater treatment with horseradish peroxidase/hydrogen peroxide (HRP/H2O2) catalytic process. *Catal. Today* (2015). doi:10.1016/j.cattod.2016.03.049
145. Ghasempur, S., Torabi, S-F., Ranaei-Siadat, S-O., Jalali-Heravi, M., Ghaemi, N., Khajeh, K., Optimization of Peroxidase-Catalyzed Oxidative Coupling Process for Phenol Removal from Wastewater Using Response Surface Methodology. *Environ. Sci. Technol.* **41,** 7073–7079 (2007).
146. Lin, N., Gao, L., Chen, Z. & Zhu, J. H. Elevating enzyme activity through the immobilization of horseradish peroxidase onto periodic mesoporous organosilicas. *New J. Chem.* **35,** 1867 (2011).
147. Wan, M. M., Gao, L., Chen, Z., Wang, Y.K., Wang, Y., Zhu, J.H., Facile synthesis of new periodic mesoporous organosilica and its performance of immobilizing horseradish peroxidase. *Microporous Mesoporous Mater.* **155,** 24–33 (2012).

148. Guan, L., Di, B., Su, M. & Qian, J. Immobilization of β-glucosidase on bifunctional periodic mesoporous organosilicas. *Biotechnol. Lett.* **35,** 1323–1330 (2013).
149. Na, W., Wei, Q., Lan, J-N., Nie, Z-R., Sun, H., Li, Q-Y., Effective immobilization of enzyme in glycidoxypropyl-functionalized periodic mesoporous organosilicas (PMOs). *Microporous Mesoporous Mater.* **134,** 72–78 (2010).
150. Ghanem, A. Trends in lipase-catalyzed asymmetric access to enantiomerically pure/enriched compounds. *Tetrahedron* **63,** 1721–1754 (2007).
151. Kapoor, M. & Gupta, M. N. Lipase promiscuity and its biochemical applications. *Process Biochem.* **47,** 555–569 (2012).
152. Shakeri, M. & Kawakami, K. Effect of the structural chemical composition of mesoporous materials on the adsorption and activation of the Rhizopus oryzae lipase-catalyzed trans-esterification reaction in organic solvent. *Catal. Commun.* **10,** 165–168 (2008).
153. Serra, E., Díez, E., Díaz, I. & Blanco, R. M. A comparative study of periodic mesoporous organosilica and different hydrophobic mesoporous silicas for lipase immobilization. *Microporous Mesoporous Mater.* **132,** 487–493 (2010).
154. Jiang, Y., Liu, X;, Chen, Y., Zhou, L., He, Y., Ma, L., Gao, J., Pickering emulsion stabilized by lipase-containing periodic mesoporous organosilica particles: A robust biocatalyst system for biodiesel production. *Bioresour. Technol.* **153,** 278–283 (2014).
155. MacLean, M. W. A., Reid, L. M., Wu, X. & Crudden, C. M. Chirality in ordered porous organosilica hybrid materials. *Chem. - An Asian J.* **10,** 70–82 (2015).
156. MacQuarrie, S., Thompson, M.P., Blanc, A., Mosey, N.J., Lemieux, R.P., Crudden, C.M., Chiral periodic mesoporous organosilicates based on axially chiral monomers: Transmission of chirality in the solid state. *J. Am. Chem. Soc.* **130,** 14099–14101 (2008).
157. Van der Voort, P., Esquivel, D., De Cankc, E., Goethals, F., Van Driessche, I., Romero-Salgero, F.J., Periodic Mesoporous Organosilicas: from simple to complex bridges; a comprehensive overview of functions, morphologies and applications. *Chem. Soc. Rev.* **42,** 3913–3955 (2013).
158. Polarz, S. & Kuschel, A. Preparation of a Periodically Ordered Mesoporous Organosilica Material Using Chiral Building Blocks. *Adv. Mater.* **18,** 1206–1209 (2006).
159. Inagaki, S., Guan, S., Yang, Q., Kapoor, M. P. & Shimada, T. Direct synthesis of porous organosilicas containing chiral organic groups within their framework and a new analytical method for enantiomeric purity of organosilicas. *Chem. Commun.* 202–204 (2008). doi:10.1039/b714163g
160. Morell, J., Chatterjee, S., Klar, P.J., Mauder, D., Shenderovich, I., Hoffmann, F., Fröba, M., Synthesis and characterization of chiral benzylic ether-bridged periodic mesoporous organosilicas. *Chem. - A Eur. J.* **14,** 5935–5940 (2008).
161. Kuschel, A. & Polarz, S. Effects of primary and secondary surface groups in enantioselective catalysis using nanoporous materials with chiral walls. *J. Am. Chem. Soc.* **132,** 6558–6565 (2010).
162. Kumobayashi, H. Industrial application of asymmetric reactions catalyzed by BINAP-metal complexes. *Recl. Trav. Chim. Pays-bas* **115,** 201–210 (1996).
163. Morales, V., Villajos, J. A. & García, R. A. Simultaneous synthesis of modified Binol-periodic mesoporous organosilica SBA-15 type material. Application as catalysts in asymmetric sulfoxidation reactions. *J. Mater. Sci.* **48,** 5990–6000 (2013).
164. Wu, X., Blackburn, T., Webb, J. D., Garcia-Bennett, A. E. & Crudden, C. M. The synthesis of Chiral periodic organosilica materials with ultrasmall mesopores. *Angew. Chemie - Int. Ed.* **50,** 8095–8099 (2011).

165. Liu, X., Wang, P., Yang, Y., Wang, P. & Yang, Q. (R)-(+)-binol-functionalized mesoporous organosilica as a highly efficient pre-chiral catalyst for asymmetric catalysis. *Chem. - An Asian J.* **5,** 1232–1239 (2010).
166. Wang, P., Liu, X;, Yang, J., Yang, Y., Zhang, L., Yang, Q., Li, C., Chirally functionalized mesoporous organosilicas with built-in BINAP ligand for asymmetric catalysis. *J. Mater. Chem.* **19,** 8009 (2009).
167. Yang, Q., Kapoor, M.P., Inagaki, S., Shirokura, N., Kondo, J.N., Domen, K., Catalytic application of sulfonic acid functionalized mesoporous benzene–silica with crystal-like pore wall structure in esterification. *J. Mol. Catal. A Chem.* **230,** 85–89 (2005).
168. López, M. I., Esquivel, D., Jiménez-Sanchidrián, C., Romero-Salguero, F. J. & Van Der Voort, P. A 'one-step' sulfonic acid PMO as a recyclable acid catalyst. *J. Catal.* **326,** 139–148 (2015).
169. López, M. I., Esquivel, D., Jiménez-Sanchidrián, C. & Romero-Salguero, F. J. Application of Sulfonic Acid Functionalised Hybrid Silicas Obtained by Oxidative Cleavage of Tetrasulfide Bridges as Catalysts in Esterification Reactions. *ChemCatChem* **5,** 1002–1010 (2013).
170. Bispo, C., Ferreira, P., Trouve, A., Batonneau-Gener, I., Liu, F., Jerome, F., Bion, N., Role of acidity and hydrophobicity in the remarkable catalytic activity in water of sulfonic acid-functionalized phenyl-PMO materials. *Catal. Today* **218–219,** 85–92 (2013).
171. Morales, G., Athens, G., Chmelka, B. F., van Grieken, R. & Melero, J. A. Aqueous-sensitive reaction sites in sulfonic acid-functionalized mesoporous silicas. *J. Catal.* **254,** 205–217 (2008).
172. An, S., Sun, Y., Song, D., Zhang, Q., Guo, Y., Shang, Q., Arenesulfonic acid-functionalized alkyl-bridged organosilica hollow nanospheres for selective esterification of glycerol with lauric acid to glycerol mono- and dilaurate. *J. Catal.* **342,** 40–54 (2016).
173. Kapoor, M. P., Kasama, Y., Yokoyama, T., Yanagi, M., Inagaki, S., Nanbu, H., Juneja, L.R., Functionalized mesoporous dendritic silica hybrids as base catalysts with volatile organic compound elimination ability. *J. Mater. Chem.* **16,** 4714 (2006).
174. Ohashi, M., Kapoor, M. P. & Inagaki, S. Chemical modification of crystal-like mesoporous phenylene-silica with amino group. *Chem. Commun.* 841–843 (2008). doi:10.1039/b716141g
175. El Hankari, S., Motos-Pérez, B., Hesemann, P., Bouhaouss, A. & Moreau, J. J. E. Pore size control and organocatalytic properties of nanostructured silica hybrid materials containing amino and ammonium groups. *J. Mater. Chem.* **21,** 6948 (2011).
176. Zhu, F., Yang, D., Zhang, F. & Li, H. Amine-bridged periodic mesoporous organosilica nanospheres as an active and reusable solid base-catalyst for water-medium and solvent-free organic reactions. *J. Mol. Catal. A Chem.* **363–364,** 387–397 (2012).
177. Zhang, L., Liu, J., Yang, J., Yang, Q. & Li, C. Direct synthesis of highly ordered amine-functionalized mesoporous ethane-silicas. *Microporous Mesoporous Mater.* **109,** 172–183 (2008).
178. Liu, M., Lu, X., Shi, L., Wang, F. & Sun, J. Periodic Mesoporous Organosilica with a Basic Urea-Derived Framework for Enhanced Carbon Dioxide Capture and Conversion Under Mild Conditions. *ChemSusChem* **18,** 1–11 (2016).
179. Shylesh, S., Zhou, Z., Meng, Q., Wagener, A., Seifert, A., Ernst, S., Thiel, W.R., Sustainable, green protocols for heterogenized organocatalysts: N-Phenylthiazolium salts heterogenized on organic–inorganic hybrid mesoporous supports. *J. Mol. Catal. A Chem.* **332,** 65–69 (2010).

180. Mouawia, R., Mehdi, A., Reyé, C. & Corriu, R. J. P. Bifunctional ordered mesoporous materials: direct synthesis and study of the distribution of two distinct functional groups in the pore channels. *J. Mater. Chem.* **18,** 4193 (2008).
181. Kuschel, A., Drescher, M., Kuschel, T. & Polarz, S. Bifunctional Mesoporous Organosilica Materials and Their Application in Catalysis: Cooperative Effects or Not? *Chem. Mater.* **22,** 1472–1482 (2010).
182. Sasidharan, M., Fujita, S., Ohashi, M., Goto, Y., Nakashima, K., Inagaki, S., Novel synthesis of bifunctional catalysts with different microenvironments. *Chem. Commun. (Camb).* **47,** 10422–10424 (2011).
183. Gianotti, E., Diaz, U., Velty, A. & Corma, A. Designing bifunctional acid–base mesoporous hybrid catalysts for cascade reactions. *Catal. Sci. Technol.* **3,** 2677–2688 (2013).
184. Song, D., An, S., Sun, Y. & Guo, Y. Efficient conversion of levulinic acid or furfuryl alcohol into alkyl levulinates catalyzed by heteropoly acid and ZrO2 bifunctionalized organosilica nanotubes. *J. Catal.* **333,** 184–199 (2016).
185. Li, W., Yang, Y., Huang, X;, Wang, Q., Liu, L., Wang, M., Tan, X., Luo, T., Patil, A.J., Compressed CO2 mediated synthesis of bifunctional periodic mesoporous organosilicas with tunable porosity. *Chem. Commun.* **52,** 9668–9671 (2016).
186. *Ullmann's Encyclopedia of Industrial Chemistry*. *Ullmann's Encyclopedia of Industrial Chemistry* (Wiley-VCH Verlag GmbH & Co. KGaA, Weinheim, 2008). doi:10.1002/14356007.a01
187. Chapuis, C. & Jacoby, D. Catalysis in the preparation of fragrances and flavours. *Appl. Catal. A Gen.* **221,** 93–117 (2001).
188. Wolfson, A., Litvak, G., Dlugy, C., Shotland, Y. & Tavor, D. Employing crude glycerol from biodiesel production as an alternative green reaction medium. *Ind. Crops Prod.* **30,** 78–81 (2009).
189. Kong, P. S., Aroua, M. K. & Daud, W. M. A. W. Conversion of crude and pure glycerol into derivatives: A feasibility evaluation. *Renew. Sustain. Energy Rev.* **63,** 533–555 (2016).
190. Chheda, J. N., Huber, G. W. & Dumesic, J. A. Liquid-phase catalytic processing of biomass-derived oxygenated hydrocarbons to fuels and chemicals. *Angew. Chemie - Int. Ed.* **46,** 7164–7183 (2007).
191. Huber, G. W., Chheda, J. N., Barrett, C. J. & Dumesic, J. A. Production of liquid alkanes by aqueous-phase processing of biomass-derived carbohydrates. *Science (80-.).* **308,** 1446–1450 (2005).
192. Stueben, K. C. & Deem, M. L. Surfactant-promoted Aldol Reactions. (1976). doi:Jan, 28, 1997
193. Lauwaert, J., De Canck, E., Esquivel, D., Van Der Voort, P., Thybaut, J.W., Marin, G.B., Effects of amine structure and base strength on acid–base cooperative aldol condensation. *Catal. Today* **246,** 35–45 (2015).
194. Werner Bonrath, Yann Pressel, Jan Schutz, Erich Ferfecki, K.-D. T. Aldol Condensations Catalyzed by Basic Anion-Exchange Resins. *ChemCatChem* 3584–3591 (2016). doi:10.1002/cctc.201600867
195. Lauwaert, J. *et al.* Spatial arrangement and acid strength effects on acid–base cooperatively catalyzed aldol condensation on aminosilica materials. *J. Catal.* **325,** 19–25 (2015).
196. Lauwaert, J., De Canck, E., Esquivel, D., Thyabaut, J.W., Van Der Voort, P., Marin, G.B., Silanol-Assisted Aldol Condensation on Aminated Silica: Understanding the Arrangement of Functional Groups. *ChemCatChem* **6,** 255–264 (2013).

197. Brunelli, N. A. & Jones, C. W. Tuning acid-base cooperativity to create next generation silica-supported organocatalysts. *J. Catal.* **308,** 60–72 (2013).
198. Brunelli, N. A., Venkatasubbaiah, K. & Jones, C. W. Cooperative catalysis with acid-base bifunctional mesoporous silica: Impact of grafting and Co-condensation synthesis methods on material structure and catalytic properties. *Chem. Mater.* **24,** 2433–2442 (2012).
199. Beretta, M., Morell, J., Sozzani, P. & Fröba, M. Towards peptide formation inside the channels of a new divinylaniline-bridged periodic mesoporous organosilica. *Chem. Commun.* **46,** 2495–2497 (2010).

Chapter 2

Towards a stable functionalized PMO

The results in paragraph 2.3 are published in:

W. Huybrechts, G. Mali, P. Kustrowski, T. Willhammar, M. Mertens, S. Bals, P. Van Der Voort and P. Cool, Microporous and Mesoporous Materials, 2016, 236, 244-249

The synthesis of the BTEVA precursor (paragraph 2.2) was performed at the ORSY group (Universiteit Antwerpen), in collaboration with P. Mampuys, under the supervision of Prof. B. U. W. Maes.

2.1 Introduction

This chapter discusses the results of the experiments that were undertaken in order to create a high potential PMO material. As synthesizing a PMO with a new precursor is a very difficult and time-consuming process, our strategy was based on a recent article by Fröba et al.[1]. In this work, the synthesis of a new 2,5-bis((*E*)-2-(triethoxysilyl)vinyl)aniline (BTEVA) precursor was described (Figure 14). This precursor was then used as the building block for the production of a highly ordered PMO material with crystalline like pore walls.

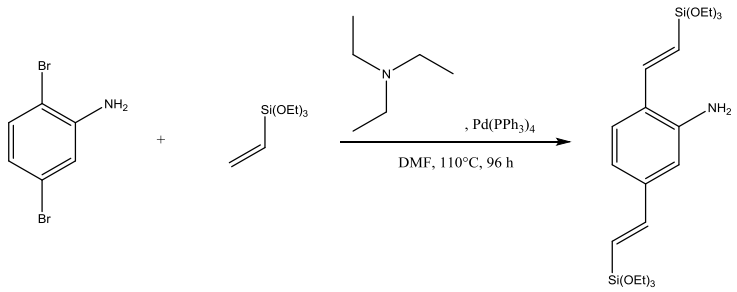

Figure 14. Synthesis of BTEVA precursor, according to Fröba et al.[1]

Due to the presence of both an aromatic amine functionality, as well as two vinyl bonds which are an inherent part of the structure and pore walls, this PMO can offer us an ideal starting position for post-synthetic modifications on two different reactive sites.

Organic synthesis on PMOs is, however, not so straightforward. As described in literature by Smeulders et al., structural changes may occur due to unwanted side reactions[2]. Bromobenzene bridged PMOs are susceptible for further chemical modification, because of the halogen carbon bond. It is well-known that bromine is a very good leaving group in substitution reactions and plays a vital role in organometallic chemistry[3–7]. Consequently, further substitution of the bromine creates new synthetic opportunities towards functionalization of PMOs in a variety of different fields. In their article, three different strategies for bromination of benzene bridged PMO are investigated: 1) Br_2 with $AlCl_3$ as catalyst, 2) N-bromosuccinimide (NBS) with azobisisobutyronitrile (AIBN) as radical initiator, and 3) $NaBrO_3$ in combination with

H_2SO_4 in order to create in situ generation of bromine. Although these reactions proved successful in liquid phase organic chemistry[8–14], they proved ineffective as a post-synthetic modification method on the PMO material. Moreover, it was difficult to prove the direct bonding site of the bromine on the PMO. Nonetheless, in said article, an important topic is touched upon which is summarized by its title "*Is there potential for post-synthetic brominating reactions on benzene bridged PMOs?".* The authors conclude that, at that time, only pre-synthesized precursors can result in the desired brominated benzene bridged PMOs[2].

Therefore, we focused our efforts on these two approaches simultaneously. On one hand, we started with aniline bridged PMO, which can be made in a reproducible way[15], and developed a post-synthetic strategy to convert the amine group with bromine. On the other hand, we attempted to reproduce and enhance the synthesis of BTEVA bridged PMO. Combining the two in the end, should lead us to the development of divinylbromobenzene bridged PMO. This material can then be modified using a variety of different organic reactions.

2.2 2,5-bis((*E*)-2-(triethoxysilyl)vinyl)aniline

2.2.1 Double Heck coupling reaction

The desired molecule was successfully synthesized by Fröba in his 2010 article[1]. Using a double Heck coupling, with tetrakis(triphenylphosphine)palladium as a catalyst, BTEVA could be obtained. Figure 15 shows the reaction mechanism of a single Heck coupling, yielding (*E*)-2-bromo-5-(2-(triethoxysilyl)vinyl)aniline. This compound then undergoes another Heck reaction, resulting in the end product: BTEVA.

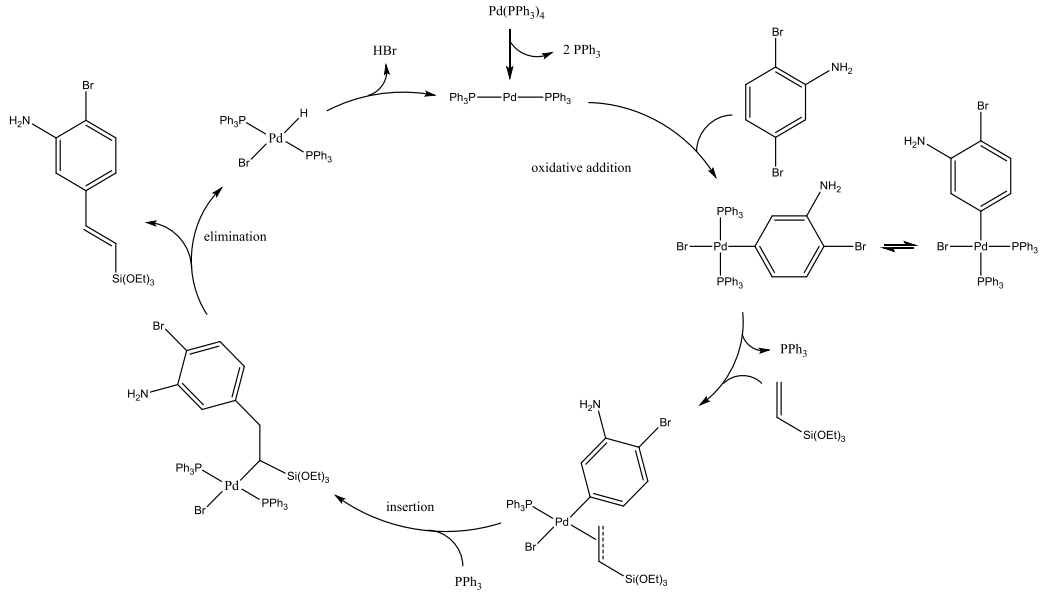

Figure 15. Reaction mechanism of a single Heck coupling, with formation of (E)-2-bromo-5-(2-(triethoxysilyl)vinyl)aniline

The recipe of Fröba et al., however, could be optimized and we therefore set about improving several reaction parameters. The molar ratio of both reagents is self-evident; 2,5-dibromoaniline:triethoxysiylsilane is 1:2. A catalytic amount of tetrakis(triphenylphosphine)palladium of 0.33 mol% was used in combination with triethylamine (4:1) as a base for neutralizing the formed HBr acid after the β hydride elimination. In contrast to the original recipe, we used an inert atmosphere of argon instead of nitrogen during preparation, as well as during the reaction which lasted for 4 days at 383 K. The solvent used was *N,N'*-dimethylformamide (DMF), which was evaporated under reduced pressure together with the excessive triethylamine. In the next section, we will discuss the improvements that we made to the synthesis, giving rise to a more pure end product.

2.2.2 Synthesis optimization and purification

Firstly, triethylamine was dried with CaH_2 and stirred overnight. Subsequently, fractional distillation was carried out under an atmosphere of argon and the dry triethylamine was stored over molecular sieves. The removal of every trace of water was important in order not to deactivate the palladium catalyst.

Secondly, the amount of (dry) DMF used, was reduced drastically by 65%. Not only is DMF a toxic product, it is also impossible to remove completely using only evaporation under reduced pressure. Before optimization, we obtained the following ^{1}H NMR spectrum (Figure 16), after 36 h of lyophilization.

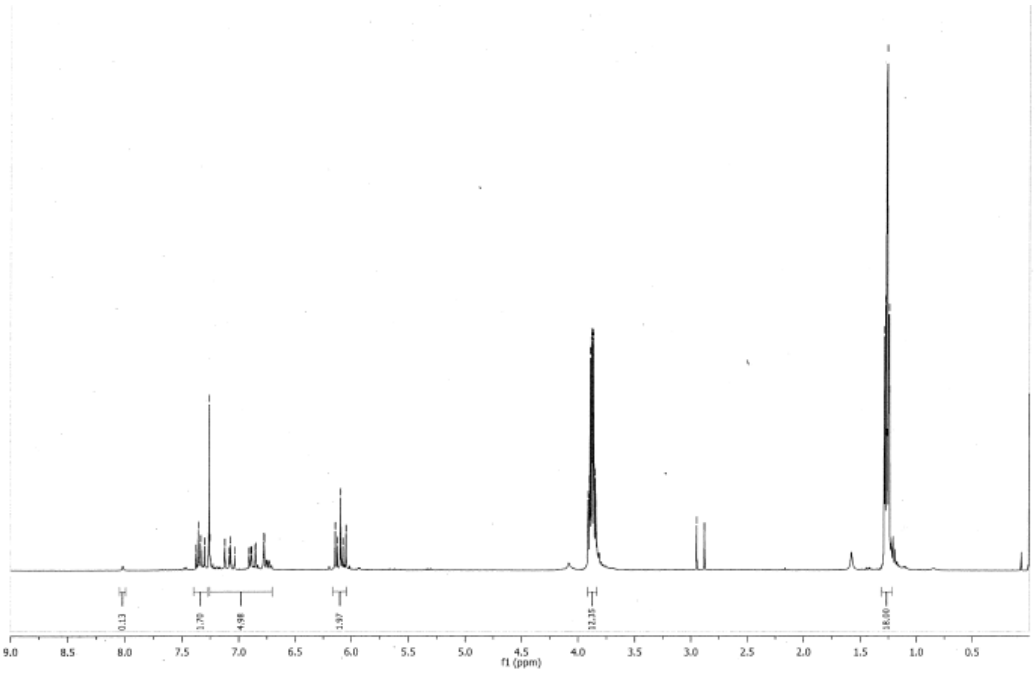

Figure 16. ^{1}H NMR spectrum of the end product, synthesized according to Fröba et al., after 36 h of lyophilization.

It is clear that the two singlets around δ = 2.9 ppm and the singlet at δ = 8.0 ppm can be assigned to a residual amount of DMF in the product, even after 36 h of lyophilization. However, this compound would most probably not interfere during the PMO synthesis.

On the other hand, it is apparent that optimizations can still lead to a more pure end product.

Furthermore, using high performance liquid chromatography (HPLC), we were able to distinguish different compounds in our end product. These products could be separated and several fractions were characterized using liquid chromatography-mass spectrometry (LC-MS), depicted in Figure 17.

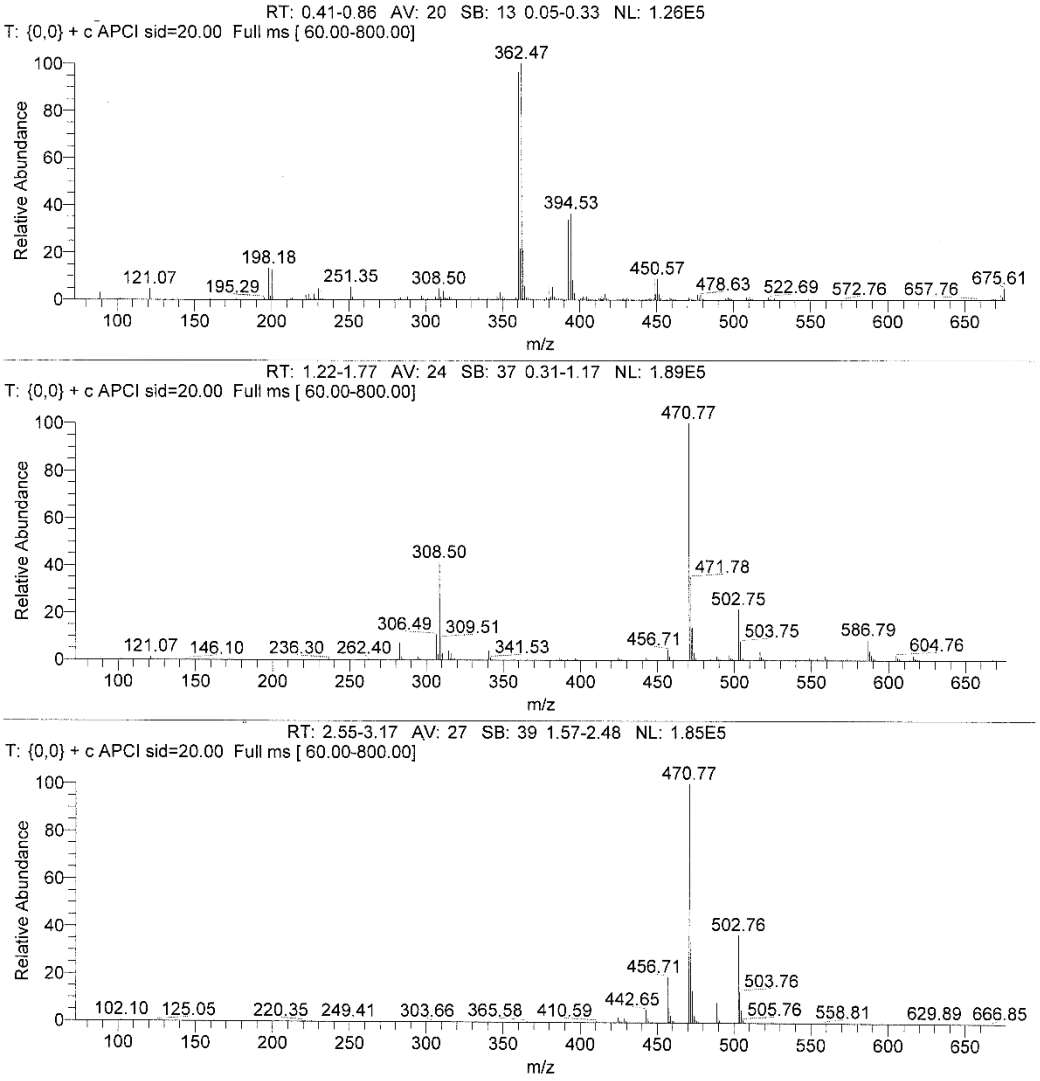

Figure 17. LC-MS of HPLC fractions, showing the presence of different compounds.

Despite the fact that no more starting material (2,5-dibromoaniline) is present, we still observe the m/z signal of the mono-Heck coupled intermediate (*E*)-5-bromo-2-(2-(triethoxysilyl)vinyl)aniline in the first fraction at m/z = 362 and m/z = 394 (+ MeOH). This makes the synthesis of a highly ordered and porous PMO impossible.

The signal at m/z = 470 and m/z = 502 (+ MeOH) can be attributed to the double Heck coupled product BTEVA. When concentrating the fractions containing only the right end product, another ^{1}H NMR spectrum was taken, see Figure 18.

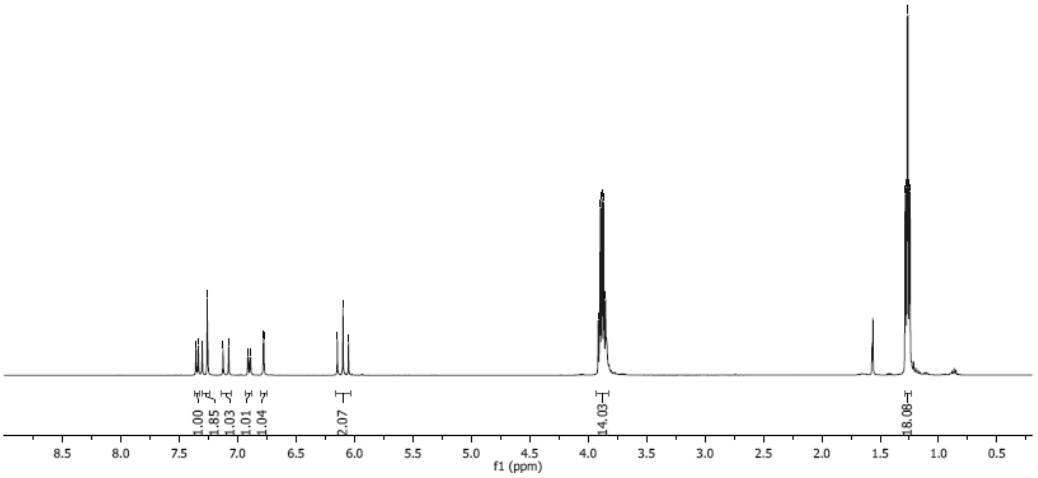

Figure 18. ^{1}H NMR spectrum after purification with HPLC.

First of all, DMF could no longer be observed. The singlet at δ = 1.6 ppm can be assigned H_2O, which itself originates from the deuterated chloroform used for the NMR measurement. The $CHCl_3$ hydrogen is responsible for the peak at δ = 7.26 ppm. Except for these artefacts, this spectrum shows only the signals that can be attributed to the pure end product. The comparison with the unpurified mixture of products, (as can be seen in Figure 16), is striking.

2.2.3 BTEVA PMO

Evidently, the attempts to synthesize a PMO material with the unpurified product were not successful. In the presence of the mono-coupled Heck product, (*E*)-5-bromo-2-(2-

(triethoxysilyl)vinyl)aniline, a controlled synthesis of a periodically ordered material cannot be obtained. After purification however, one would expect to be able to synthesize a PMO. Unfortunately, we did not succeed in producing a structured material. Several parameters were varied, such as pH, concentration of precursor and template, co-condensations, pressure during the aging process, different templates, ultrasonic treatments, amongst others. A solid material with some porosity, although far from uniform, was attained with a surface area up to 260 m^2g^{-1} using OTAC as a template (Figure 19) . In contrast, Fröba achieved a PMO with a very high surface area of 1350 $m^2\ g^{-1}$ and a very narrow pore size distribution. It did not fit in the timeframe of this PhD to examine whether the synthesis of this PMO is altogether possible.

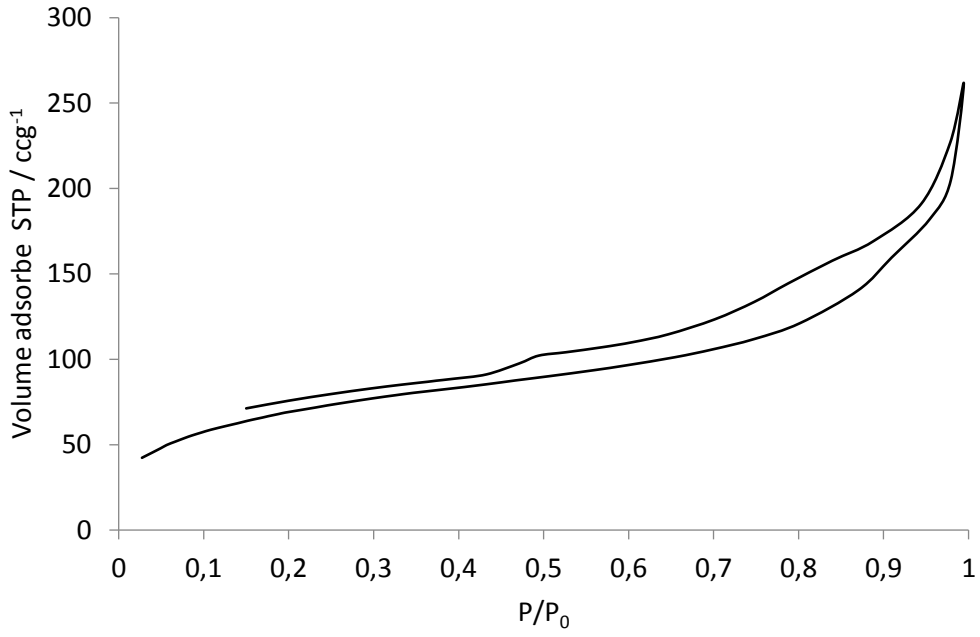

Figure 19. N_2 sorption isotherm of BTEVA PMO.

At the time of writing, no other research group has so far published a work describing the successful production of Fröba's BTEVA PMO since its first publication in 2010.

2.3 Bromination of benzene bridged PMO[16]

As mentioned before, bromination of PMOs can lead to materials which are susceptible to a variety of different possible modification reactions. If one is possible to halogenate a PMO, in this case the aromatic ring of benzene bridged PMO, a hybrid material is created with a reactive site known to exhibit excellent leaving group properties. However, it has been shown in the past that bromination of a benzene bridged PMO is not as straight-forward, especially when compared with the ease of bromination in the liquid phase[2]. Several strategies were pursued, as can be seen in Figure 20, although without success. The radical reaction led to no conversion whatsoever, both the other two reactions caused the C-Si bond to break, giving rise to the destruction of the porous material.

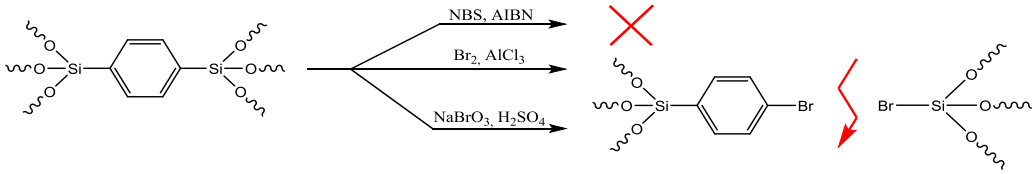

Figure 20. Bromination reactions attempted by Smeulders et al[2].: radical reaction with N-bromosuccinimide and azobisisobutyronitrile, $Br_2/AlCl_3$ and sodium bromate with sulfuric acid for in-situ generation of bromine.

In the next section we report a successful way to brominate a benzene bridged PMO whilst maintaining the structural integrity of the material. By first performing a nitration, followed by the reduction of the nitro group we obtained an aniline bridged PMO[15]. Secondly, we executed the bromination using a synthesis described by Baik et al.[17]. In this article, the authors were able to use a homogeneous one-step procedure for converting amino arenes to haloarenes. At the same time they were able to avoid the environmental pollutants resulting from the traditional Sandmeyer reaction using copper halides. Using this synthesis strategy, we were able to employ the amino function as a leaving group, thus creating a C-Br bond and avoiding the chance of Si-C cleavage. Thorough characterization of the brominated material with X-ray

photoelectron spectroscopy (XPS) and solid state nuclear magnetic resonance (SS NMR) confirms this.

2.3.1 Experimental

Benzene bridged PMO was synthesized using the following procedure. 10 g cetyltrimethylammonium bromide (CTAB, 99+%, Acros) was dissolved in 300 mL 0.35 M NaOH (NaOH pellets, 98.5%, Acros) solution and stirred for 1 h at 313 K. After cooling to room temperature, 10 mL 1,4-bis(triethoxysilyl)benzene (BTEB, 96%, Sigma-Aldrich) was added dropwise followed by ultrasonic treatment for 30 min. Subsequently, the solution was stirred for 20 h at room temperature. Following this step was the hydrothermal treatment in Teflon lined stainless steel autoclaves during 24 h at 373 K. The autoclaves were quenched and the solid was filtered and washed with water. Afterwards the organic template was removed by two consecutive extractions for 2 h in a 10 vol% HCl/EtOH mixture (HCl, 37%, Acros; ethanol, p.a., VWR).

In order to synthesize the aniline bridged PMO, the recipe according to Inagaki et al.[15] was slightly adjusted. A mixture of 5 mL HNO_3 (65%, Acros) and 16 mL H_2SO_4 (96%, Acros) was added to 1 g of benzene bridged PMO and stirred at 300 K for 72 h. Afterwards, the solution was added to 600 mL cold water, followed by washing with a copious amount of water. After drying in open air at ambient temperature, the yellow solid was added to a solution containing 31 mL HCl and 3.3 g $SnCl_2$ (98%, Sigma-Aldrich). This solution was stirred at 300 K for 72 h, followed by the addition of 600 mL water and filtration of the solid product. The obtained material was again washed with a copious amount of water, followed by washing with 25 mL sec-butylamine (>99%, Merck) and 200 mL EtOH. The resulting aniline bridged PMO was vacuum dried at 373 K for 24 h before further modifications were performed.

The procedure used to brominate aniline bridged PMO is based on the article of Baik et al.[17], in which they describe the bromination of p-nitroaniline, with the exception that we used $NaNO_2$ (≥97.0%, Sigma-Aldrich) instead of KNO_2. When performing a standard

synthesis we added 180 mL HBr (p.a., Acros) to 10 mL dimethylsulfoxide (DMSO, 99.7%, Acros). This solution was added dropwise to a flask containing aniline bridged PMO (corresponding to 0.4 mmol N), 0.11 g $NaNO_2$ and 10 mL DMSO whilst stirring at 308 K. This results in an aniline-PMO:HBr:NO_2^- molar ratio of 1:4:4. The mixture was stirred at 308 K for 15 min to 1 h after which it was added to 2 g K_2CO_3 (p.a., Acros) in 40 mL ice water. The obtained solid was filtered, washed with a large amount of water and vacuum dried at 373 K for 24 h.

2.3.2 Results, analysis and characterization

Our approach comprises a multi-step post-synthetical modification of benzene bridged PMO (Figure 21). By first introducing a nitro functionality, which can then be reduced to an amino functionality, we can create a reactive site on the benzene ring for further modification[15]. Moreover, by then performing a diazotation reaction followed by bromination[17], with the loss of N_2 gas, the bromobenzene bridged PMO product is obtained. The latter step involves the in-situ generation of the bromodimethylsulfonium bromide nucleophile whilst forming the diazonium salt which acts as a leaving group, hence forming the bromobenzene bridged PMO. This PMO allows for further functionalization through simple nucleophilic aromatic substitution reactions.

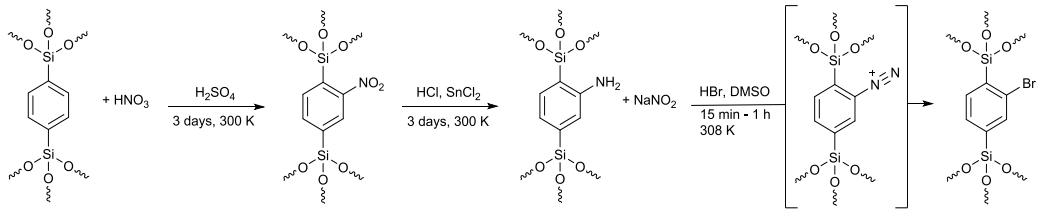

Figure 21. Modification pathway

Porosity information is obtained through nitrogen sorption and is summarized in Table 2. Converting the benzene bridged PMO into aniline bridged PMO, translates into a drop in specific surface area. This is to be expected as a combination of a mass increase of the sample originating from the additional amino group and a slight pore volume

reduction. The average pore diameter decreases as well and can be attributed to the presence of the amino groups which are faced towards the inside of the pores. The same observations can be made after bromination, thus confirming a successful substitution.

Table 2. Porosity data obtained through N_2 sorption at 77 K.

Sample name	S_{BET}/m^2g^{-1}	V_P/cm^3g^{-1}	d/nm[a]
Benzene PMO	750	0.52	2.78
NH_2 PMO	678	0.43	2.54
Br PMO	648	0.40	2.47

[a] By the BJH method of the adsorption branch

Nitrogen sorption isotherms of the three materials and their pore size distribution are displayed in Figure 22. The isotherms are all type IV(b), typical for adsorbents having mesopores < 4 nm[18].

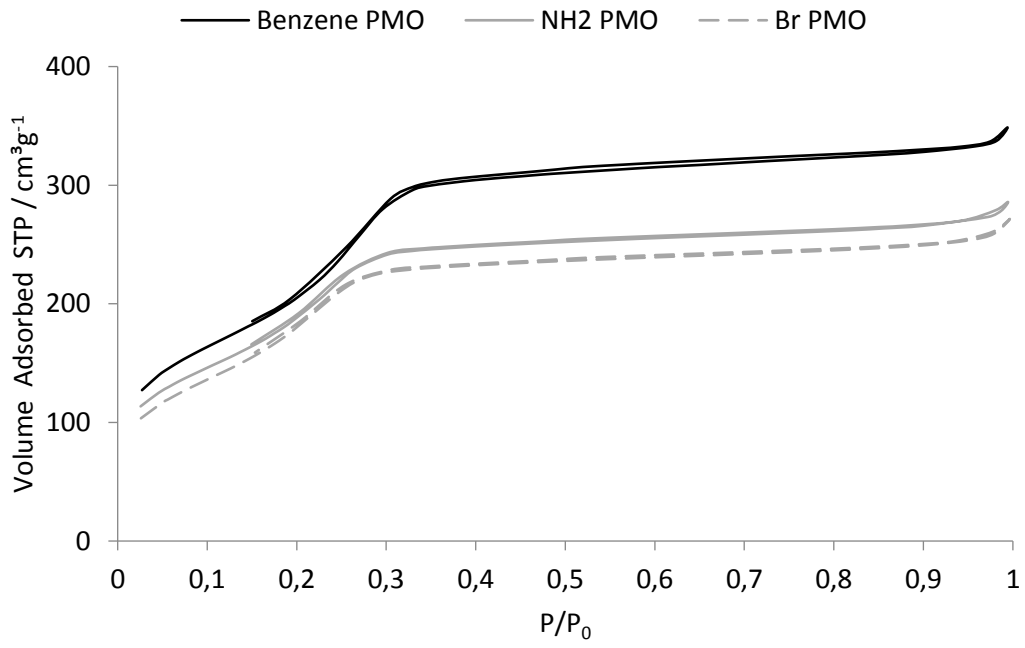

Figure 22. N_2 sorption isotherms

Figure 23 shows the XRD patterns of both the benzene bridged PMO, as well as the brominated PMO. It is apparent that the molecular scale periodicity is retained after the modification steps. Three sharp diffractions can be observed and using Bragg's law one can calculate the d spacing at d = 7.6 Å (2θ = 11.66°), 3.8 Å (2θ = 23.46°) and 2.5 Å (2θ = 35.62°). This shows the preservation of the crystal-like periodicity at the molecular scale within the pore walls and is consistent with the literature[19]. This once more proves the chemical stability of the PMO structure in harsh conditions. The small angle spectra reveal the first order [1 0 0] signal which shifts towards higher angles, attributable to a smaller unit cell, due to further condensation of the silica catalyzed by the acidic modification reactions.

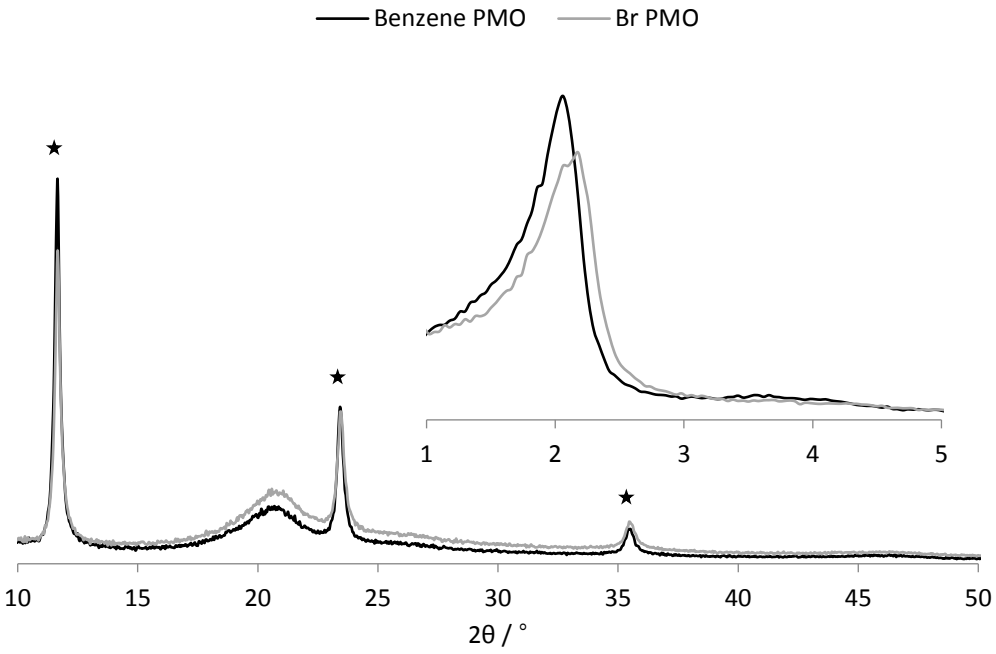

Figure 23. Wide angle and small angle (insets) powder X-ray diffraction patterns of the PMOs before and after the modifications.

Figure 24 (left) shows the annular dark-field scanning transmission electron microscopy (ADF-STEM) image of the brominated PMO where one can see the mesoporous structure with straight channels at a distance of approximately 4 nm. An ADF-STEM image at a higher magnification is displayed in Figure 24 (right), showing the layered

structure formed by alternating silicate and benzene layers running perpendicular to the mesoporous channels with a periodicity of approximately 7.8 Å. These results confirm the preservation of the mesostructure after the different modifications.

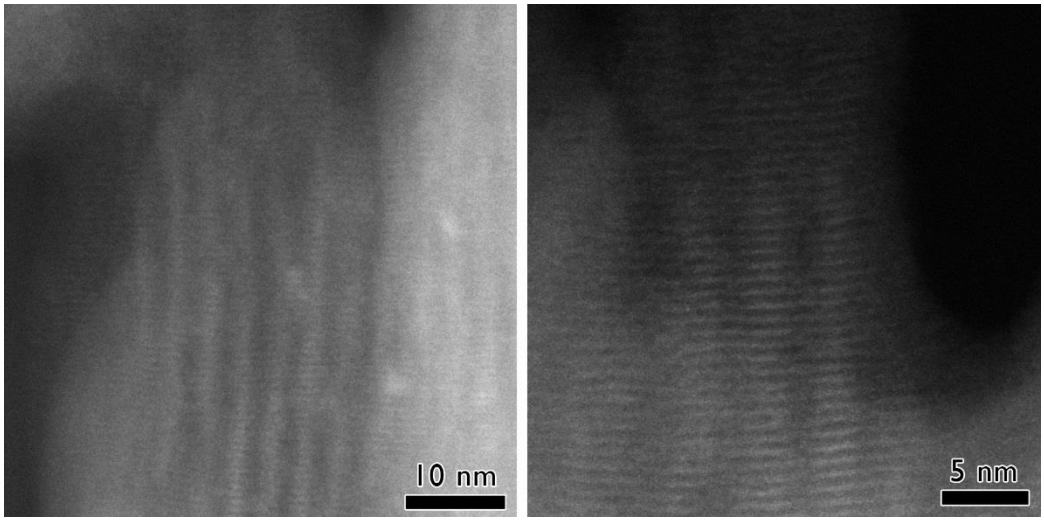

Figure 24. Annular dark-field STEM images of brominated PMO.

In order to assess the success of each reaction step, elemental analysis of the respective material was performed (Table 3). Only the results for N and C are shown here.

Table 3. Elemental analysis

Sample name	N/mmol g^{-1}	C/mmol g^{-1}
NH_2 PMO	2.0210	28.053
Br PMO	0.72892	27.155

Considering the C signals can only originate from the benzene rings in the pore walls and the N signals solely from the NH_2 group, one can calculate the conversion of each step. The complete removal of CTAB by our procedure is clear from the absence of the corresponding aliphatic peaks between 10 and 70 ppm in the ^{1}H-^{13}C CPMAS NMR spectrum (Figure 25). After the first reaction step, this results in 43% conversion of all benzene moieties to aniline. Taking into account that the benzene rings are also an

inherent part of the PMO's structure, the actual conversion of accessible benzene rings is much higher. Remarkably, this is a much higher yield compared to that achieved by Inagaki et al.[15]. After the bromination step 63% of the converted benzene rings lose their NH_2 group, leaving only 16% of all benzene rings aminated.

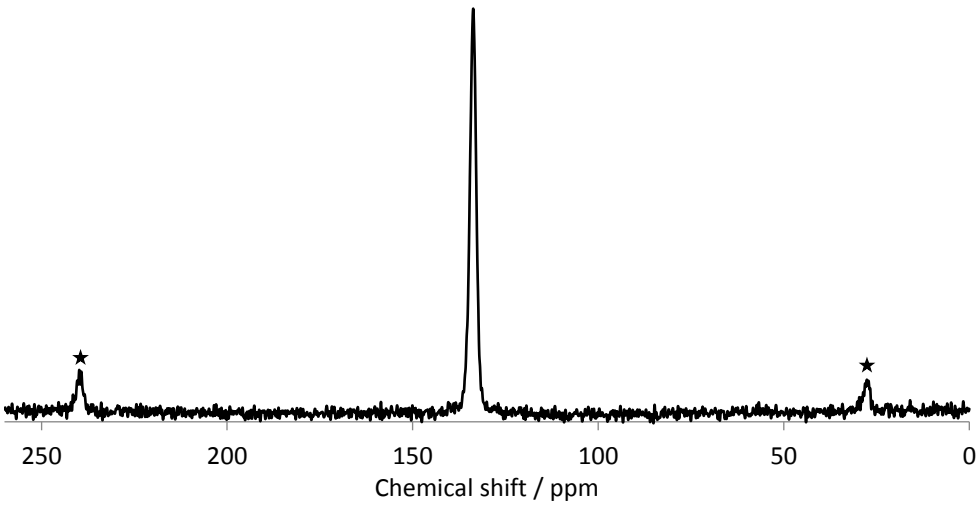

Figure 25. ^{1}H-^{13}C CPMAS NMR spectrum of benzene bridged PMO, the spinning side bands are denoted with a symbol.

Figure 26 displays the DRIFT spectra of the benzene bridged and aniline bridged PMO materials, measured under vacuum at 393 K in order to remove any physisorbed water. The spectra are in compliance with the expectations, showing the typical absorption bands of isolated OH (3725 cm^{-1}) and aromatic C-H stretching (3000-3100 cm^{-1}) at higher wavelength. The 1,4-disubstituted benzene fingerprint, originating from the C-H deformation over- tones between 1650 cm^{-1} and 2000 cm^{-1}, is clearly visible in the benzene PMO sample. After modification the distinctive signals which can be attributed to aromatic C-NH_2 formation, are apparent. The absorbance at 1300 cm^{-1} can be assigned to the stretching mode of C-N, proving the covalent linkage. New bands also appear at 1595 cm^{-1}, 1624 cm^{-1} and 3390-3473 cm^{-1} attributable to N-H deformation, bending and stretching, respectively. The N-O stretching modes at 1350 cm^{-1} and 1550 cm^{-1} disappeared completely.

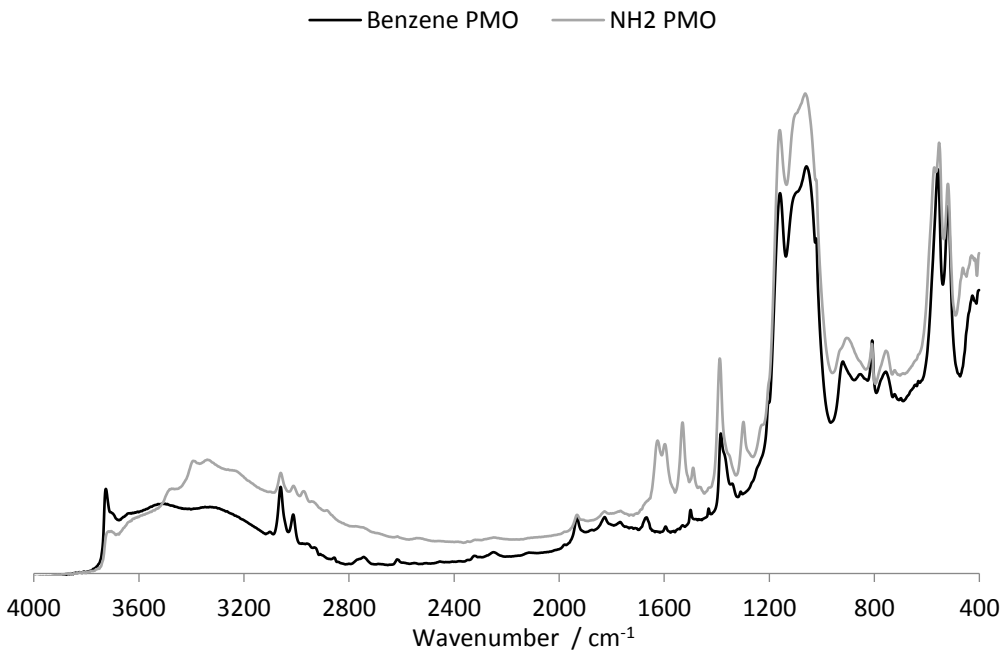

Figure 26. DRIFT spectra measured under vacuum at 393 K.

Since the C-Br bond is not IR active, the DRIFT spectrum of the bromobenzene bridged PMO is not displayed. In order to prove the existence of the latter bond, X-ray photoelectron spectroscopy (XPS) was performed. Figure 27 shows the XPS spectrum with the Br $3d_{3/2}$ and Br $3d_{5/2}$ spin double recorded for the brominated PMO. The chemical state of Br $3d_{5/2}$ positioned at 70.0 eV is attributed to a C-Br bond, proving the modification is successful[20]. To our knowledge this is the first time a post-synthetic bromination has successfully taken place on a PMO.

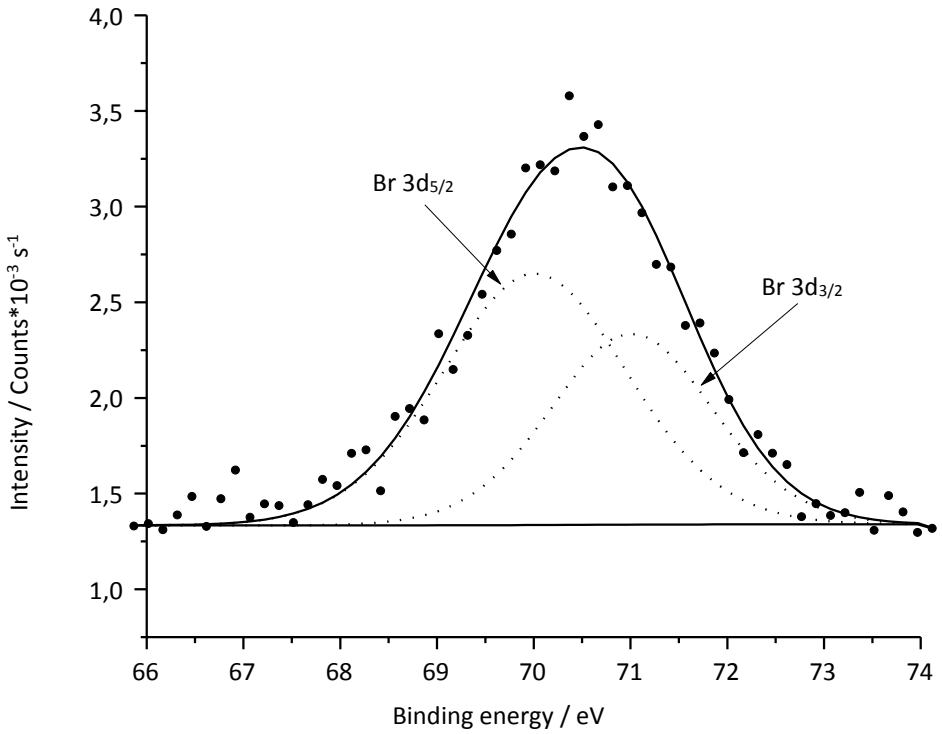

Figure 27. Br 3d XPS spectrum of brominated PMO.

In order to exclude the possibility of structural decay during the modification reactions, our synthesis strategy comprises a multi-step approach with the formation of a good leaving group. As could be seen in Figure 22, the porosity of the material was maintained which suggests that no deterioration of the pore structure occurred. Moreover, by performing NMR analysis of the final product one can provide an in-depth view of the chemical stability before and after modification. As described by Smeulders et al.[2], assessment of the chemical linkages between the organic bridging units is of pivotal importance. Figure 28 shows the ^{1}H-^{29}Si CPMAS NMR spectra of benzene bridged and bromobenzene bridged PMO.

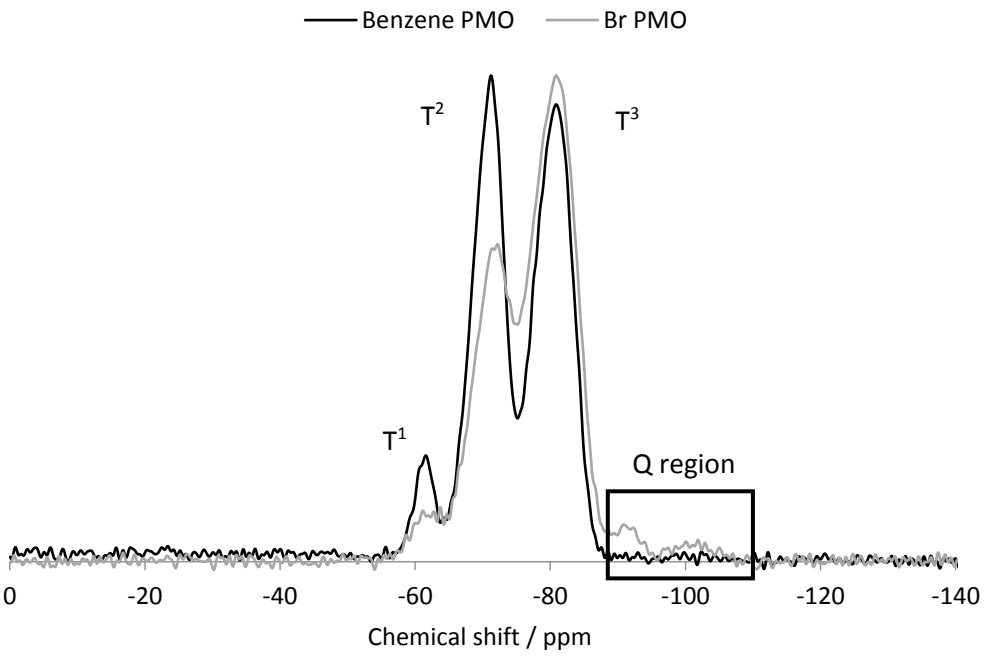

Figure 28. ^{1}H-^{29}Si CPMAS NMR spectra of benzene bridged and bromobenzene bridged PMO.

As can be seen in the ^{1}H-^{29}Si CPMAS NMR spectra, only small differences exist between the starting material and the end product. The T signals vary, evolving to a more condensed structure with the modification as could also be seen in the XRD spectrum (See appendix for explanation of the T and Q signals). The Q signals are of greater importance, as these are correlated to Si-C breakage and are therefore a measure of structural deterioration. An important observation is that the Q signals in the bromobenzene bridged spectrum each represent less than 1% of the total intensity, confirmed by the analysis of the deconvoluted ^{29}Si MAS NMR spectrum (Figure 29), meaning that our synthesis strategy is the right approach to create a halogenated PMO material whilst maintaining its structural integrity.

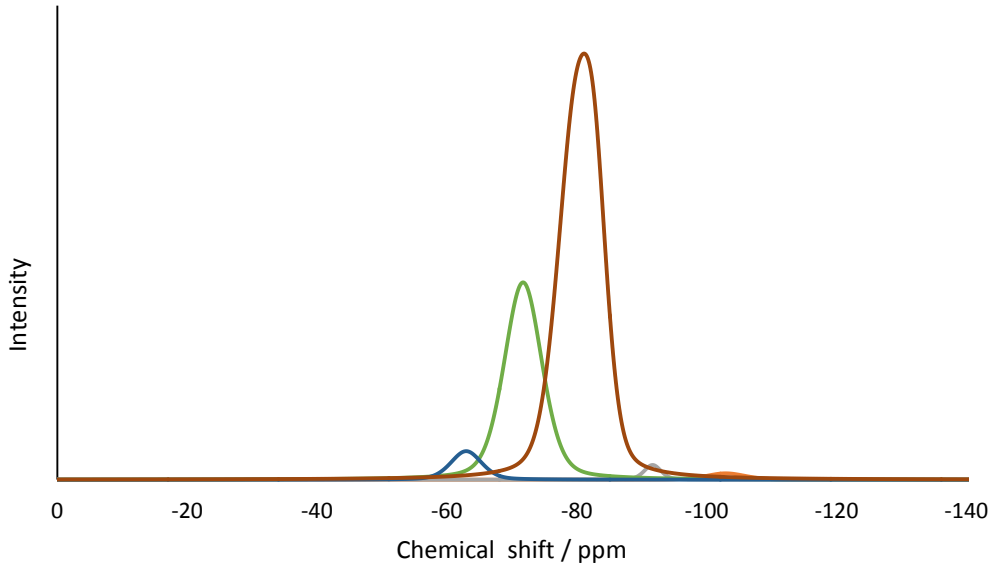

Figure 29. Deconvoluted ^{29}Si MAS NMR spectrum of the brominated PMO.

We also recorded the ^{1}H-^{13}C CPMAS NMR spectrum (Figure 30), it shows that several new signals arise after modification. It is clear that the shoulder of the intense peak at 133 ppm, represented by point B, can be attributed to the carbon atoms of the modified benzene rings. The signal at 150 ppm can be attributed to the C-N carbon, and clearly disappears after bromination. The signals represented by point C and D can originate from the carbon atoms of bromobenzene, or alternatively from the carbon atoms of a phenol ring. A small contribution of phenol rings is confirmed by the signal at 160 ppm (point A in the spectrum), which can be assigned to the ipso carbon of phenol. This contribution suggests that water, present in the reaction mixture, is also able to act as a nucleophile, creating a minor fraction of phenol bridges.

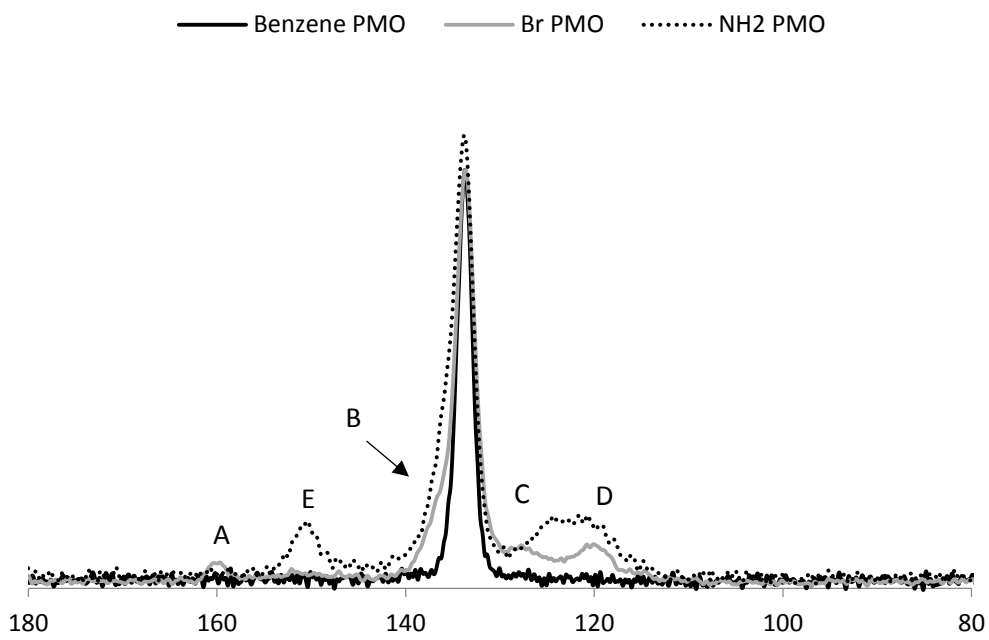

Figure 30. ^{1}H-^{13}C CPMAS NMR spectra of benzene bridged and bromobenzene bridged PMO.

This means that, although we have obtained bromobenzene bridged PMO material, this is not the only product formed. Considering the synthetic approach used here (Figure 21), the last reaction step where de-diazotation takes place allows for side reactions to arise. When the diazonium salt is formed, any molecule or atom with sufficient nucleophilic character can substitute this leaving group. Except for the bromodimethylsulfonium bromide, molecular water can also be present in the reaction mixture as a potential nucleophile forming agent thus creating phenol bridged PMO.

2.4 Conclusion

In an attempt to synthesize divinylbromobenzene bridged PMO, we synthesized the 2,5-bis((*E*)-2-(triethoxysilyl)vinyl)aniline (BTEVA) precursor as described by Fröba's group. This, however, led to a mixture of products in which the intermediate was still present. Therefore, an optimization of the synthesis procedure is suggested in this work which resulted in the pure end product: BTEVA. Nonetheless, the production of a structured,

highly-porous PMO material using this pure precursor was not viable. More research is needed in order to successfully synthesize a BTEVA PMO material.

Simultaneously, we investigated the bromination of aniline bridged PMO. By performing a single step diazotation and bromo-de-diazotation, we were able to achieve bromination of the benzene ring. By thoroughly characterizing the material using solid state NMR, we concluded that the structural integrity is retained after the modification steps. Additionally, this technique also showed the existence of side reactions resulting in phenol bridged PMO due to water being present in the reaction mixture.

2.5 References

1. Beretta, M., Morell, J., Sozzani, P. & Fröba, M. Towards peptide formation inside the channels of a new divinylaniline-bridged periodic mesoporous organosilica. *Chem. Commun.* **46,** 2495–2497 (2010).
2. Smeulders, G., Meynen, V., Houthoofd, K., Mullens, S., Martens, J.A., Maes, B.U.W., Cool, P., Is their potential for post-synthetic brominating reactions on benzene bridged PMOs? *Microporous Mesoporous Mater.* **164,** 49–55 (2012).
3. Bruice, P. Y. *Organic Chemistry*. (Pearson Prentice Hall, 2007).
4. Kuschel, A. & Polarz, S. Organosilica Materials with Bridging Phenyl Derivatives Incorporated into the Surfaces of Mesoporous Solids. *Adv. Funct. Mater.* **18,** 1272–1280 (2008).
5. Corral, J., Lopez, M.I., Esquivel, D., Mora, M., Jimenez-Sanchidrian, C., Romero-Salguero, F.J., Preparation of Palladium-Supported Periodic Mesoporous Organosilicas and their Use as Catalysts in the Suzuki Cross-Coupling Reaction. *Materials (Basel).* **6,** 1554–1565 (2013).
6. De Canck, E., Dosuna-Rodríguez, I., Gaigneaux, E. & Van der Voort, P. Periodic Mesoporous Organosilica Functionalized with Sulfonic Acid Groups as Acid Catalyst for Glycerol Acetylation. *Materials (Basel).* **6,** 3556–3570 (2013).
7. Nakai, K., Oumi, Y., Horie, H., Sano, T. & Yoshitake, H. Bromine addition and successive amine substitution of mesoporous ethylenesilica: Reaction, characterizations and arsenate adsorption. *Microporous Mesoporous Mater.* **100,** 328–339 (2007).
8. Mehta, G., Likhite, N. S. & Ananda Kumar, C. S. A concise synthesis of the bioactive meroterpenoid natural product (+/-)-liphagal, a potent PI3K inhibitor. *Tetrahedron Lett.* **50,** 5260–5262 (2009).
9. Ameriks, M. K. Bembenek, S.D., Burdett, M.T., Choong, I.C., Edwards, J.P., Begauer, D., Gu, Y., Karlsson, L., Purkey, H.E., Staker, B.L., Sun, S., Thuermond, R.L., Zhu, J., Diazinones as P2 replacements for pyrazole-based cathepsin S inhibitors. *Bioorganic Med. Chem. Lett.* **20,** 4060–4064 (2010).
10. Gedrich, K., Heitbaum, M., Notzon, A., Senkovska, I., Fröhlich, R., Getzschmann, J., Mueller, U., Glorius, F., Kaskel, S., A family of chiral metal-organic frameworks. *Chem. - A Eur. J.* **17,** 2099–2106 (2011).
11. Senthilmnrugan, A. & Aidhen, I. S. Synthesis of (+)-varitriol analogues via novel and versatile building blocks based on julia olefination. *European J. Org. Chem.* 555–564 (2010). doi:10.1002/ejoc.200901012
12. Zhou, Q. & Snider, B. B. Synthesis of hexacyclic parnafungin A and C models. *J. Org. Chem.* **75,** 8224–8233 (2010).
13. Bodzioch, A., Owsianik, K., Skalik, J., Kowalska, E., Stasiak, A., Rozycka-Sokolowska, E., Marciniak, B., Balczewski, P., Efficient Synthesis of Bis(dibromomethyl)arenes as Important Precursors of Synthetically Useful Dialdehydes. *Synth.* 1–6 (2016). doi:10.1055/s-0035-1561651
14. Groweiss, A. Use of Sodium Bromate for Aromatic Bromination : Research and Development. *Org. Process Res. Dev.* **4,** 30–33 (2000).
15. Ohashi, M., Kapoor, M. P. & Inagaki, S. Chemical modification of crystal-like mesoporous phenylene-silica with amino group. *Chem. Commun.* 841–843 (2008). doi:10.1039/b716141g
16. Huybrechts, W., Mali, G., Kustrowski, P., Willhammar, T., Mertens, M., Bals, S., Van Der

Voort, Cool, P., Post-synthesis bromination of benzene bridged PMO as a way to create a high potential hybrid material. *Microporous Mesoporous Mater.* **236,** 244–249 (2016).

17. Baik, W., Luan, W., Lee, H.J., Yoon, C.H., Koo, S., Kim, B.H., Efficient one-pot transformation of aminoarenes to haloarenes using halodimethylisulfonium halides generated in situ. *Can. J. Chem.* **83,** 213–219 (2005).
18. Thommes, M. *et al.* Physisorption of gases, with special reference to the evaluation of surface area and pore size distribution (IUPAC Technical Report). *Pure Appl. Chem.* **87,** 1051–1069 (2015).
19. Inagaki, S., Guan, S., Ohsuna, T. & Terasaki, O. An ordered mesoporous organosilica hybrid material with a crystal-like wall structure. *Nature* **416,** 304–307 (2002).
20. Zhang, Y. P., He, J. H., Xu, G. Q. & Tok, E. S. Architecturing covalently bonded organic bilayers on the Si(111)-(7 × 7) surface via in situ photoinduced reaction. *J. Phys. Chem. C* **116,** 8943–8949 (2012).

Chapter 3

L-serine modified PMO as a bifunctional aldol catalyst

The results of this chapter are published in:

W. Huybrechts, J. Lauwaert, A. De Vylder, M. Mertens, G. Mali, J. W. Thybaut, P. Van Der Voort, P. Cool, Microporous and Mesopororous Materials, 2017, 251, 1-8

3.1 Introduction

In this chapter, the development of a novel aldol condensation catalyst based on modified benzene bridged PMO is reported. More specifically, an L-serine modified benzene bridged PMO was synthesized in pursuit of a bifunctional catalyst. This *bifunctionality* concerns the presence of two functional groups, an amine and an alcohol, that work together in catalyzing the aforementioned aldol condensation reaction. Aldol condensations are carbon-carbon forming reactions between two carbonyl compounds of either an aldehyde or ketone. The resulting β-hydroxycarbonyl adduct can then undergo dehydration with formation of an α,β-unsaturated aldehyde or an α,β-unsaturated ketone. In this way, biomass derived carbohydrates can first be dehydrated, then formed into large organic compounds by the aldol condensation which can subsequently be turned into alkanes by dehydration/hydrogenation (Figure 31)[1]. Finally, these resulting liquid alkanes can be applied as biodiesel fuel[1,2].

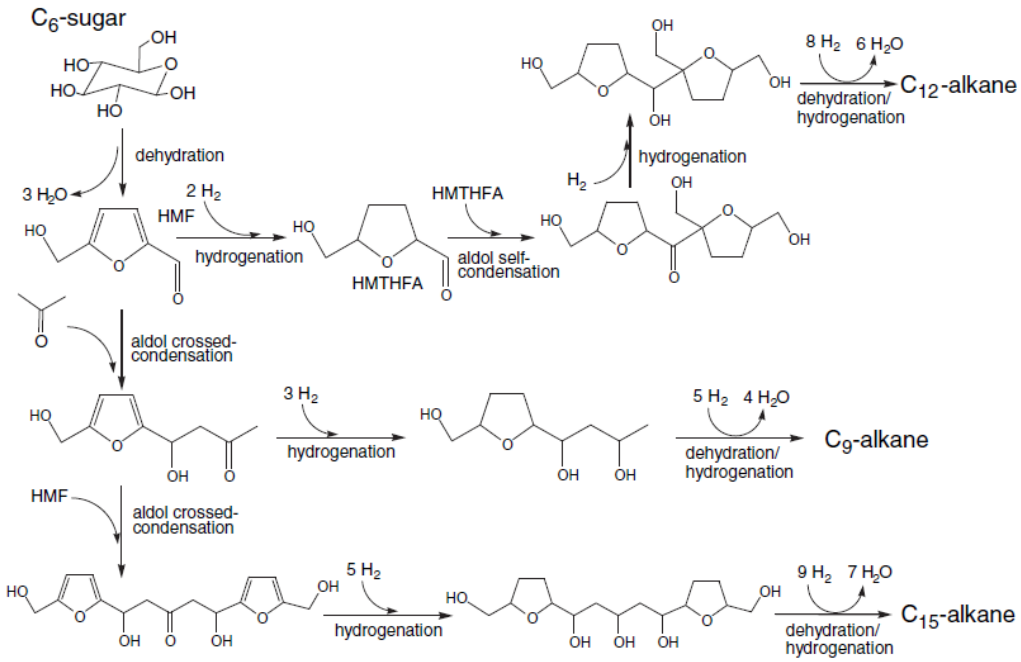

Figure 31. Conversion of biomass derived glucose to liquid alkanes for biodiesel (from Dumesic et al.[1])

Although nowadays aldol condensations are mostly catalyzed by strong homogeneous Brønsted bases such as NaOH[3–6], the group of Thybaut concluded that amines were promoted by the presence of silanol groups for the catalysis of the aldol condensation of acetone and 4-nitrobenzaldehyde[7]. In 2015, they then specified that primary and secondary amines were preferred over tertiary amines[5] and that a secondary amine with an alcohol function on the β-carbon, anchored on silica supports, enhanced its catalytic activity[8]. The reason for this promoting effect was hydrogen bonding between the alcohol and the carbonyl moiety of the reactant[9]. Altering the alcohol function to a more strongly acidic carboxylic acid, for example, had a detrimental effect. The same conclusion was drawn by Van Der Voort et al. when they clicked cysteine and cysteamine on an ethylene bridged PMO[10].

So far, the catalytic evaluation of the materials mentioned above took place with *n*-hexane as the solvent. However, one has to take into account that silica materials are susceptible for hydrolysis in the presence of water[11]. Since the latter is an important side product in the aldol condensation, PMOs can offer significant advantages. Moreover, compared to the homogeneous bases that are used nowadays, a heterogeneous catalyst offers the advantage of easy separation and avoids waste streams and corrosion to industrial equipment. In this chapter, we discuss the synthesis of L-serine modified PMO and its catalytic evaluation in an aqueous environment.

3.2 Post-synthetic L-serine modification

We focused our efforts on the post-synthetic modification of benzene bridged PMO with L-serine because this amino acid bears one amine function, an alcohol function on the β-carbon and a carboxylic acid. As mentioned earlier, the carboxylic acid is of no interest for our goal of creating an aldol condensation catalyst, hence our proposed reaction pathway which is shown in Figure 32. By attaching the amino acid on the PMO via its carbonyl carbon, the presence of a carboxylic acid is avoided. This then results into the (*S*)-2-amino-3-hydroxy-*N*-phenylpropanamide bridged PMO, or L-serine

modified PMO. In this way, we introduce a promoting alcohol function for each base catalyst site. Moreover, using our approach, the alcohol function is situated on the β-carbon of the amine. This ensures a good promoting effect in aldol condensations[8].

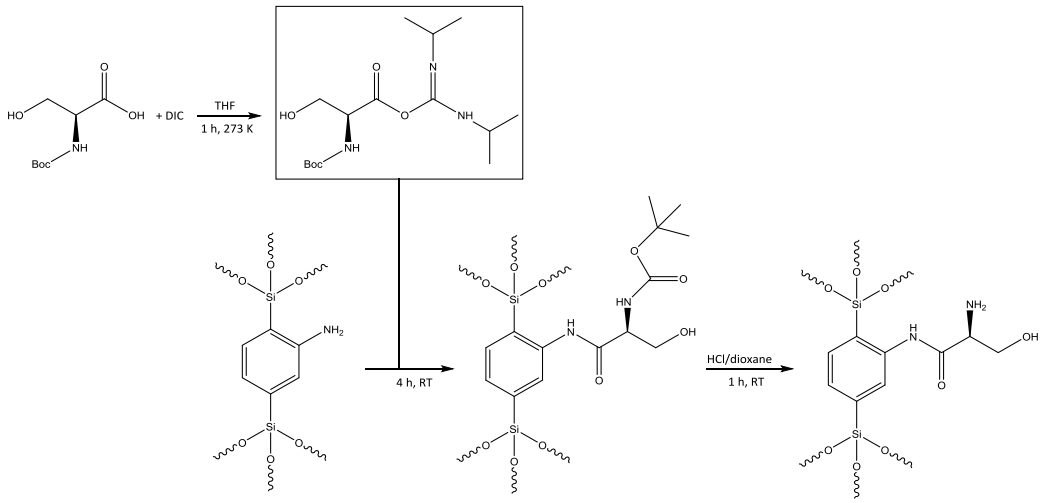

Figure 32. Reaction pathway for the synthesis of L-serine modified PMO.

3.2.1 Experimental

Benzene bridged PMO and its subsequent amination to aniline bridged PMO was synthesized according to the procedure described in the previous chapter.

Aniline bridged PMO was then used for further modification with L-serine as follows (Figure 32): Activation of the serine carbonyl carbon was done by adding 965 µL *N,N'*-diisopropylcarbodiimide (DIC, 99%, Sigma-Aldrich) to a solution of 1.29 g *N*-(*tert*-butoxycarbonyl)-L-serine (Boc-L-serine, ≥99.0%, Sigma-Aldrich) in 25 mL tetrahydrofuran (THF, anhydrous, ≥99.9%, Sigma-Aldrich). This solution was stirred for 1 h at 273 K. Afterwards, 0.933 g aniline bridged PMO (corresponding to 1.56 mmol N) was added to the solution and the mixture was brought to room temperature to stir for 4 h. After filtration of the boc-protected L-serine modified PMO, it was washed with

THF, water and ethanol. Subsequently, the residue was vacuum dried overnight at 333 K.

The boc group was removed by stirring the PMO in 126 mL 4M HCl/dioxane (1,4-dioxane, ≥99%, Sigma-Aldrich) during 1 h at room temperature[12,13]. After filtration the obtained L-serine modified PMO was washed with a large amount of water and vacuum dried at 373 K for 24 h.

The considered benchmark reaction is the aldol condensation reaction of acetone (99.6%, Acros Organics) with 4-nitrobenzaldehyde (99%, Acros Organics), resulting in 4-hydroxy-4-(4-nitrophenyl)butan-2-one as primary aldol product and 4-(4-nitrophenyl)-3-buten-2-one as secondary ketone product (Figure 39). Assessment of the catalytic activity was done using a Parr 4560 mini batch type reactor. 55 g Water was used as a solvent, together with 45 g acetone and 0.45 g 4-nitrobenzaldehyde. Methyl 4-nitrobenzoate was used as the internal standard. The operating temperature was 328 K and the amount of catalyst was 0.3032 g with a catalyst active site loading of 0.55 mmol N/g. 15 Samples of 0.3 mL were taken during 360 minutes of monitoring the reaction. These samples were then analyzed using reversed-phase high-performance liquid chromatography (RP-HPLC). The RP-HPLC contains a XDB-C18 column (Zorbax) which is operated at a temperature of 30 °C, using a gradient method with water (0.1 v% trifluoroacetic acid, Acros) and acetonitrile (HPLC grade, Acros) as solvents. In this method, the percentage acetonitrile is varied between 30 v% and 62 v% over a period of 14 min. The components are identified using a UV-detector with a variable wavelength, programmed for an optimal absorption for each component. Quantification of the different components in the reaction mixture is performed by relating the peak surface areas to the amount of internal standard.. The catalytic activity has been determined by calculating the turnover frequency (TOF) from the slope of the linear part of the conversion of 4-nitrobenzaldehyde as a function of time, the concentration of active sites and the initial concentration of 4-nitrobenzaldehyde.

3.2.2 Results, analysis and characterization

In order to obtain L-serine PMO from aniline bridged PMO, we devised a modification strategy that is shown in Figure 32. The first step comprised the activation of the serine carbonyl carbon using DIC, thus attaching a good leaving group to the aforementioned carbon[14]. This method converts the carboxyl group into an imidate, which is then immediately added to aniline bridged PMO for the subsequent reaction to take place. The resulting boc-L-serine PMO was then deprotected, giving rise to the final product.

N_2 sorption analysis of the materials was performed to determine their porosity. Figure 33 shows the corresponding isotherms and pore size distributions of the aniline bridged PMO (NH_2 PMO) and the L-serine modified PMO (L-Ser-PMO), the porosity data are summarized in Table 4. The isotherms are characteristic of type IV(b) with mesopores < 4 nm[15]. After modification the specific surface area, as well as the total pore volume and average pore diameter, decrease due to the addition of a larger and heavier functional serine group.

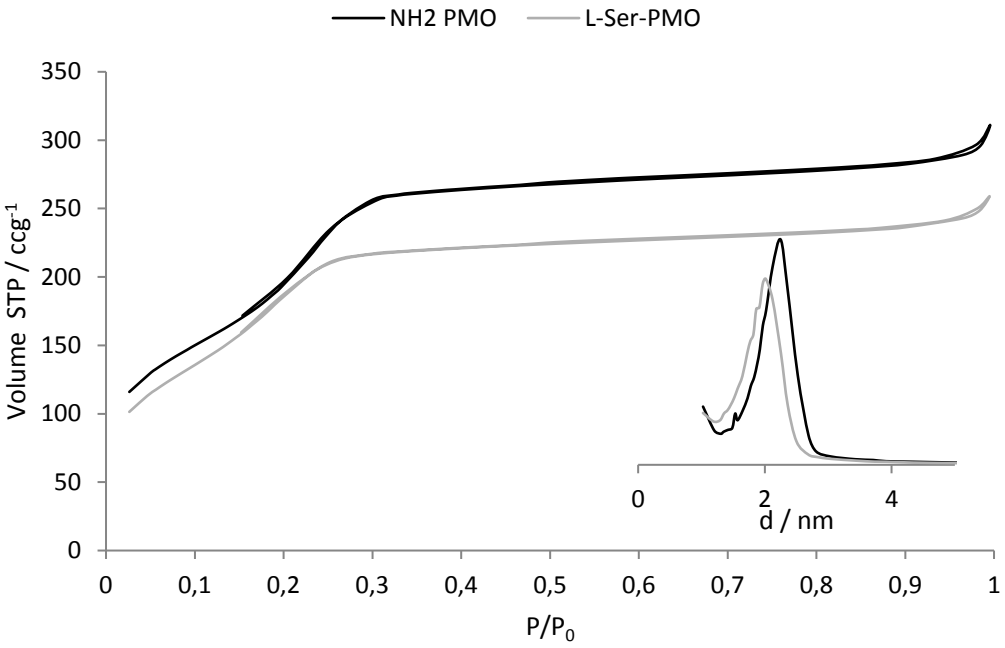

Figure 33. N_2 sorption isotherms at 77 K and the adsorption pore size distribution (BJH).

Table 4. Porosity data obtained through N_2 sorption at 77 K.

Sample name	S_{BET}/m^2g^{-1}	V_P/cm^3g^{-1}	d/nm[a]
NH_2 PMO	682	0.46	2.68
L-Ser-PMO	624	0.38	2.46

[a] By the BJH method of the adsorption branch

For the sake of completeness, an interesting comparison can also be made with the intermediate boc-L-serine-PMO. The N_2 sorption isotherms of these samples can be found in Figure 34 which clearly show a slight decrease in S_{Bet}, V_p and average pore diameter after the first modification step. After the deprotection step, all these values increase again, resulting from the loss of a heavy and bulky boc group.

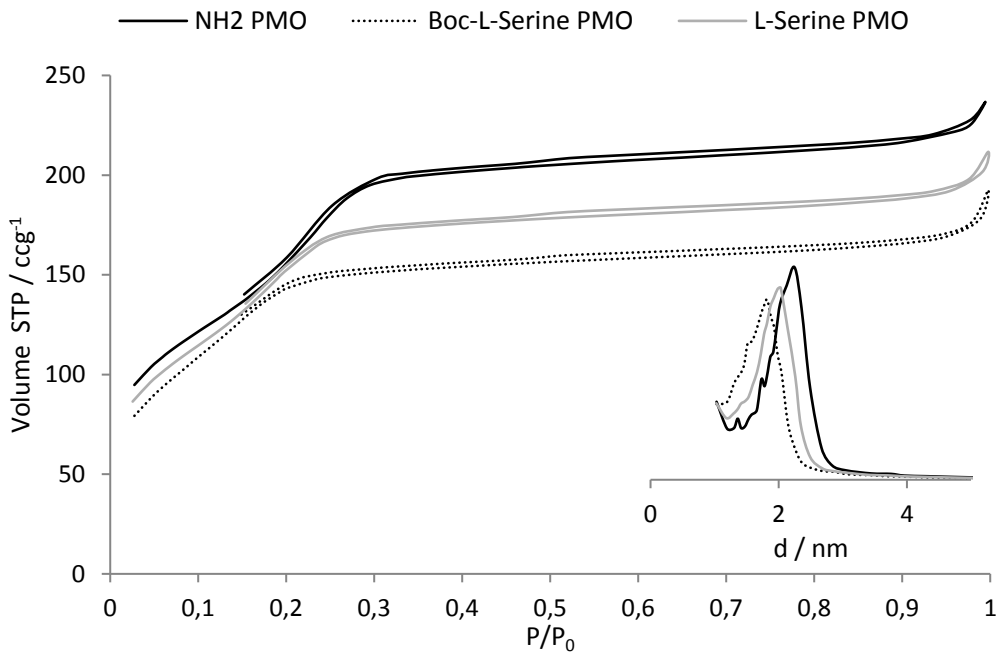

Figure 34. N_2 sorption isotherms at 77 K and the adsorption pore size distribution (BJH) showing the comparison with the intermediate boc-L-serine PMO.

XRD analysis of the L-serine PMO is shown in Figure 35, clearly showing the molecular scale periodicity as well as the signal of amorphous silica at 2θ = 21°. Using Bragg's law one can calculate the *d* spacing of the three sharp and distinct diffractions at *d* = 7.6 Å (2θ = 11.66°), *d* = 3.8 Å (2θ = 23.46°) and *d* = 2.5 Å (2θ = 35.58°). These values are in accordance with previously reported *d* spacing values[16], confirming that the crystal-like periodic structure on the molecular scale is retained after the modification steps. The small angle XRD spectrum shows the first order [1 0 0] signal, characteristic for the mesoscale periodicity (inset Figure 35).

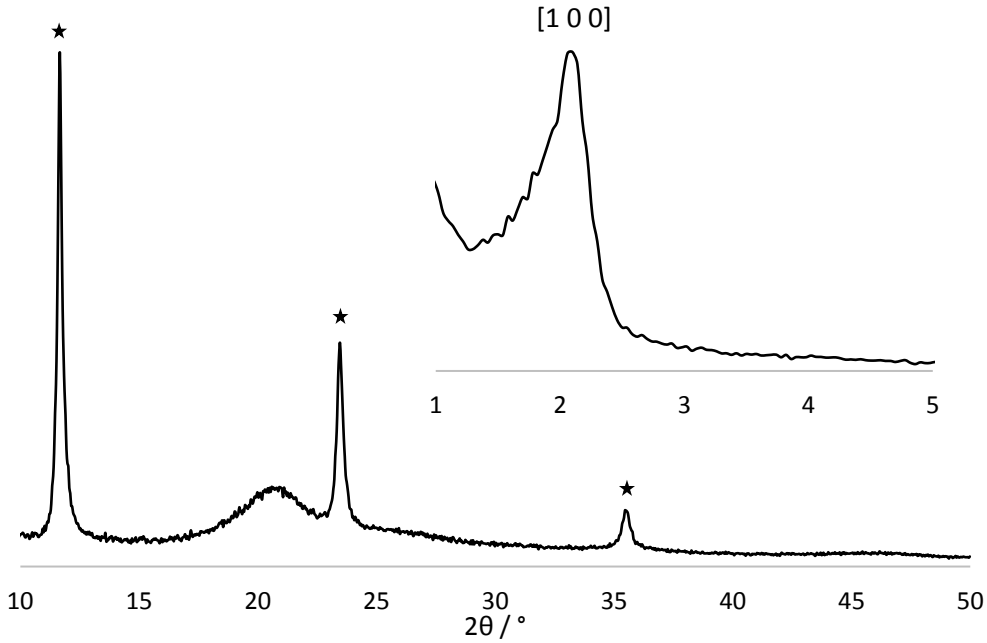

Figure 35. Wide angle and small angle (inset) XRD pattern of L-serine modified PMO.

In order to prove the presence of the serine functionality, the results of the elemental analysis are provided in Table 5. An increased amount of N and C can be observed when comparing the starting aniline bridged PMO to the final L-serine modified PMO material. The amount of N increases with 0.55 mmol g^{-1}, indicating a 33% conversion of all anilines to the end product. Amines that were not converted, can participate in the aldol catalysis. However, because they are not promoted by the alcohol function on a β-carbon, this will be a minor effect. The amount of C increases with a C:N ratio of about 4:1. However, the introduction of a serine moiety should lead to an increase of three carbons for every one nitrogen. Vacuum drying avoids the possibility that solvent is still present and our NMR study, which is presented below, shows the absence of boc groups or residual surfactant. The reason for this higher amount of C can therefore be found in physisorbed CO_2 from the ambient air. In order to confirm the presence of the serine moiety, DRIFT measurements were performed.

Table 5. Elemental analysis

Sample name	N / mmol g^{-1}	C / mmol g^{-1}
NH_2 PMO	1.67	23.23
L-Ser-PMO	2.22	25.49

Figure 36 displays the DRIFT spectra of the aniline bridged-, boc-L-serine and L-serine modified PMO materials, measured under vacuum at 373 K in order to remove any physisorbed water. A complete description of the DRIFT spectrum of the former material has already been provided in the previous chapter. The boc-L-serine PMO spectrum presents two distinct new signals at 2985 cm^{-1} and 1683 cm^{-1}. These signals can be attributed to the $–CH_3$ asymmetric stretch and the secondary amide C=O stretching vibration, respectively. As the boc group disappears after the deprotection step, with formation of the L-serine-PMO, the $–CH_3$ asymmetric stretch can no longer be observed. This is also endorsed by the diminished secondary amide C=O stretching vibration, due to the loss of one out of two secondary amides, with the removal of the boc group.

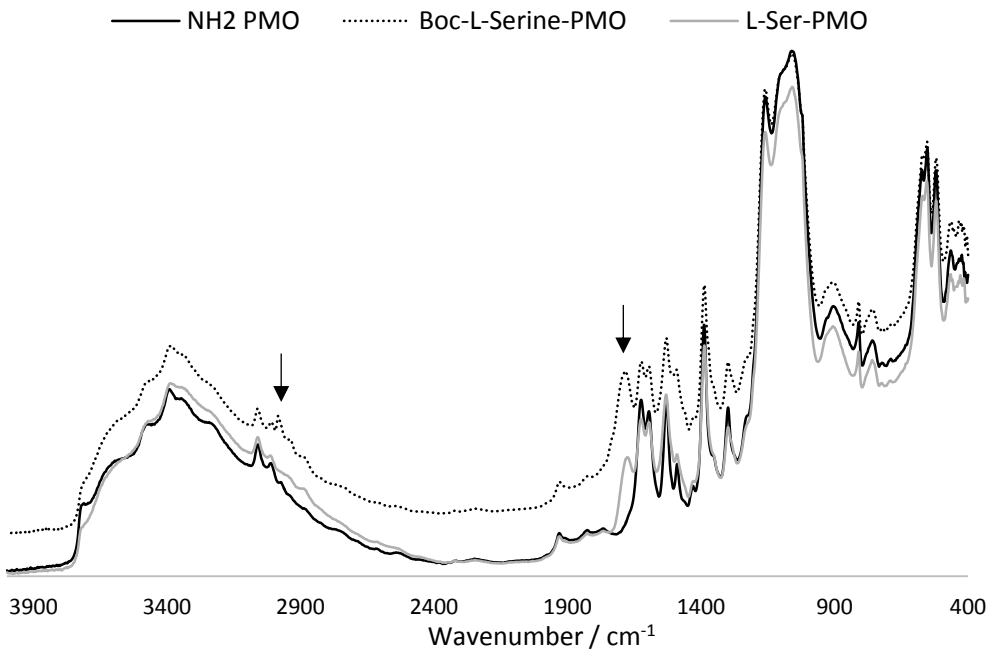

Figure 36. DRIFT spectra measured under vacuum at 373 K.

The complete removal of the protecting boc group, resulting in the formation of the desired L-serine modified PMO, can also be confirmed using solid state NMR. The ^{1}H-^{13}C CPMAS NMR spectra are presented in Figure 37, together with the assignment of the peaks. The signal at 133 ppm and around 120 ppm can be attributed to the aromatic carbons of the pristine PMO benzene ring and the modified PMO benzene ring, respectively. The peaks numbered 1 to 4, present in both spectra, can be assigned to the L-serine carbons and the *ipso* aromatic carbon. Carbons belonging to the boc protecting group are only observed in the boc-L-serine-PMO spectrum, as expected. The signals at 25 ppm, 80 ppm and 155 ppm are absent in the spectrum of the desired end product, proving our successful post-synthetic modification approach for synthesizing bifunctional PMOs.

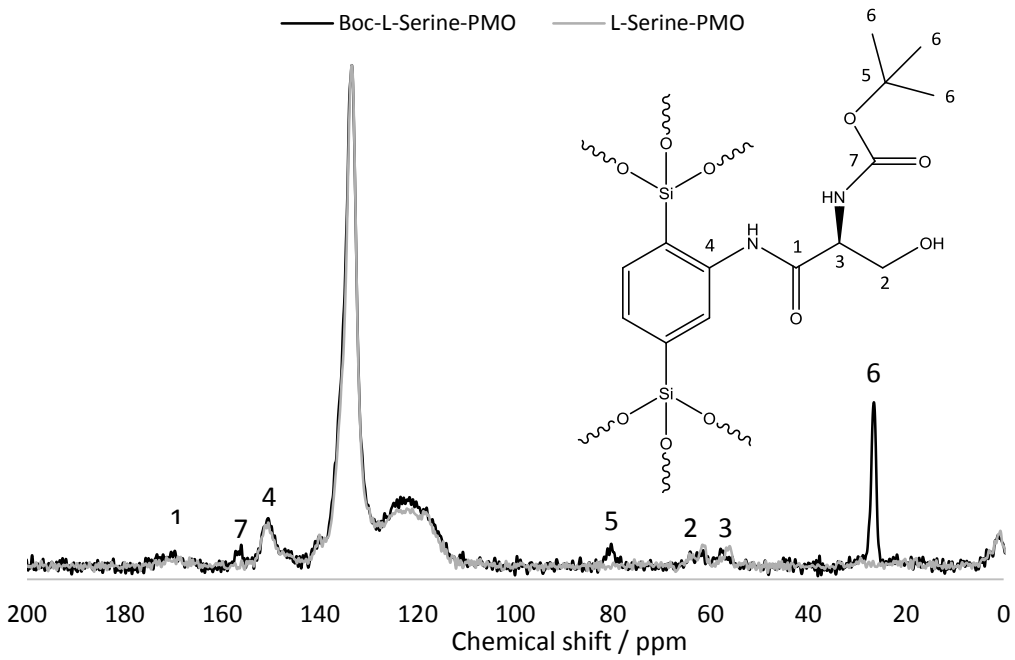

Figure 37. ^{1}H-^{13}C CPMAS NMR spectra of the boc protected and L-serine modified PMO.

However, as there is a possibility for structural decay of the PMO during post-synthetic modifications[17], also a ^{29}Si MAS NMR spectrum was recorded (Figure 38). This technique allows us to quantitatively measure the signals in the Q region, which are correlated to the Si-C breakage. The spectrum shows that the Q signal only represented 7% of the total intensity of the NMR spectrum, which is relatively low[18]. We can therefore conclude that there is only a very minor degradation of the PMO material upon the modification reactions. The pristine PMO and aniline bridged PMO did not show any Q signal.

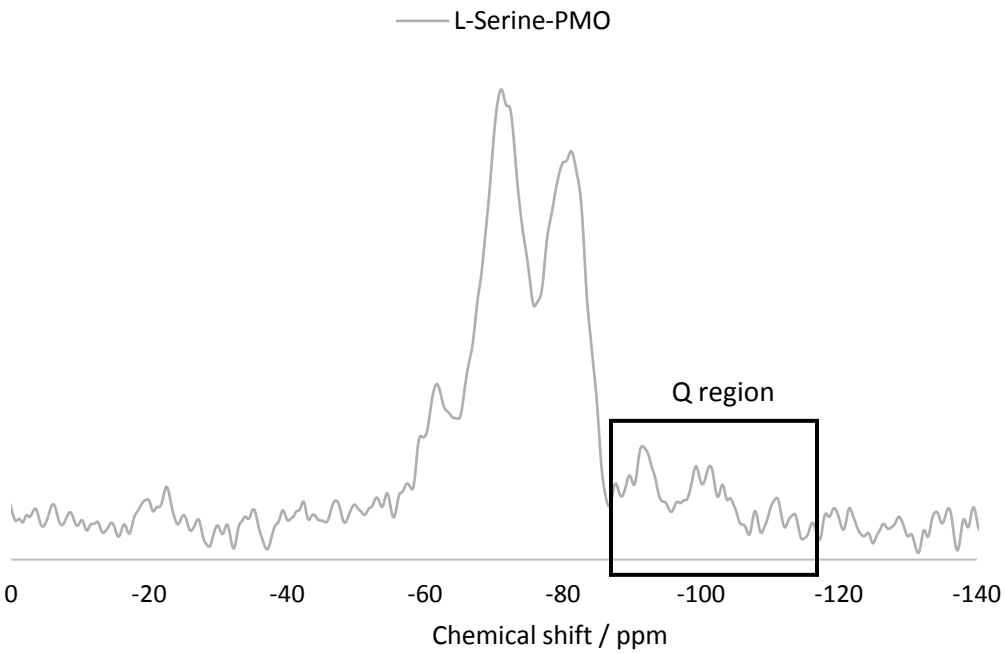

Figure 38. ^{29}Si MAS NMR of L-serine modified PMO.

Finally, the L-serine modified PMO was tested as a bifunctional catalyst in the aldol condensation of acetone and 4-nitrobenzaldehyde (Figure 39). Because of the electron withdrawing nitro group, this reaction allows for less active catalysts to be tested without having to apply more severe reaction conditions. The alcohol function of the catalyst exhibits a promoting effect by a hydrogen-bridge interaction with the carbonyl moiety of acetone. Consequently, the carbonyl carbon becomes more susceptible for nucleophilic attacks. Furthermore, this interaction will direct an acetone molecule in close proximity to the primary amine of the L-serine group. After the nucleophilic attack and dehydration, an enamine is formed. The production of water during the dehydration step again emphasizes the importance of a stable material. Next, a hydrogen bridge interaction occurs between the alcohol function and the carbonyl moiety of 4-nitrobenzaldehyde. Reaction between the enamine and 4-nitrobenzaldehyde then leads to the iminium ion, which subsequently desorbs in the presence of water yielding the aldol product[7].

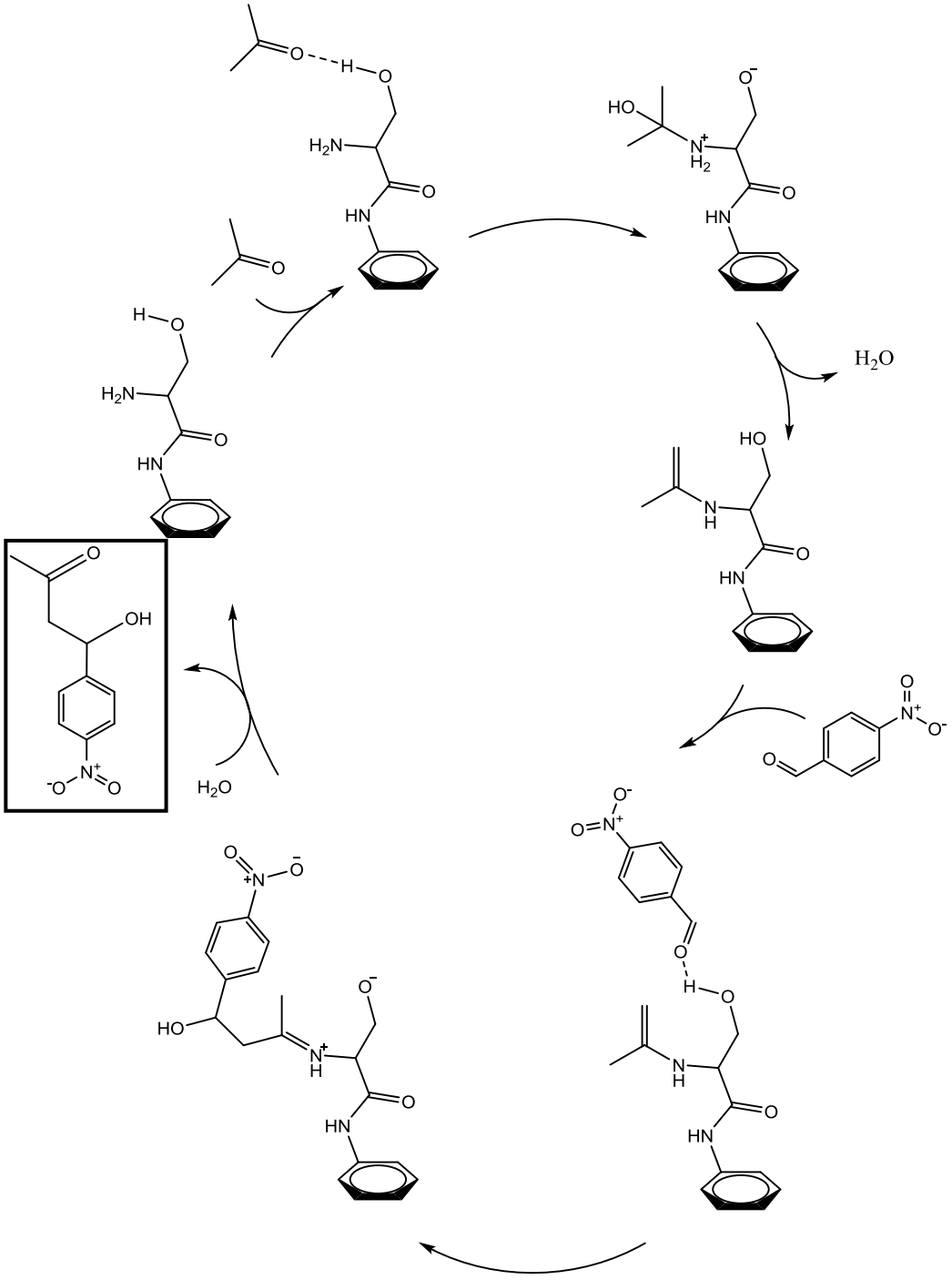

Figure 39. Reaction mechanism for the aldol condensation of acetone and 4-nitrobenzaldehyde by L-serine modified benzene bridged PMO. The dehydrated product is not shown here.

By plotting the obtained data points (Figure 40), the turnover frequency (TOF) was calculated to be 1.61 ± 0.08 x 10^{-4} s^{-1}. Moreover, under the applied conditions, the catalyst exhibited a very high selectivity towards the aldol product (> 96%), as can be seen from Table 6. This proves that L-serine modified PMO material is catalytically active in the aldol condensation reaction, with a high selectivity towards the aldol product. Figure 41 shows the reaction leading to the dehydrated ketone product. Furthermore, compared to the aminosilica materials synthesized previously by Lauwaert et al.[8], our TOF value is in the same order of magnitude as the TOF values of the ethylamine and ethanolamine modified SBA materials. However, because our material was successfully tested for the aldol condensation in an aqueous environment, as to *n*-hexane in Lauwaert's work, the prospects for using this PMO material in the conversion of biomass are promising. However, in order to check the reusability of the material several catalytic runs should be performed. If the iminium intermediate would not be allowed to desorb, after drying, it could dehydrate with the formation of a stable group attached to the catalytic surface. This should be checked in future work.

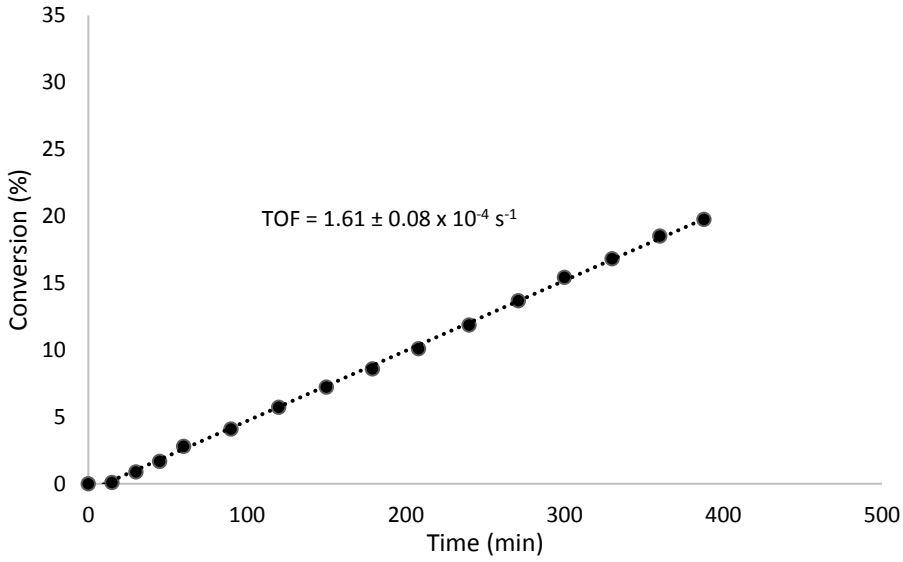

Figure 40. Plotted data points for calculating the TOF value.

Table 6. Catalytic data showing the high selectivity towards the aldol product.

Time (min)	Conversion (%)	Aldol product (%)	Ketone product (%)
0	0.00	0.00	0.00
15	0.11	100.00	0.00
30	0.89	100.00	0.00
45	1.67	100.00	0.00
60	2.81	97.21	2.79
90	4.10	97.07	2.93
120	5.71	96.48	3.52
150	7.23	96.24	3.76
179	8.60	96.12	3.88
208	10.09	96.01	3.99
240	11.88	96.25	3.75
271	13.70	96.07	3.93
300	15.44	96.20	3.80
330	16.82	96.64	3.36
360	18.51	96.38	3.62
388	19.77	96.36	3.64

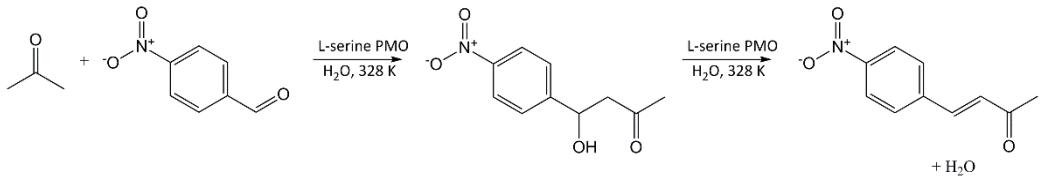

Figure 41. Aldol condensation catalyzed by L-serine modified benzene bridged PMO, showing the dehydrated ketone product.

3.3 Conclusion

In this chapter, we demonstrated a successful post-synthetic modification of benzene bridged PMO to L-serine modified PMO. The L-serine group bears a primary amine with

an alcohol group on the β-carbon, thus making it a bifunctional material with interesting catalytic properties towards the valorization of biomass-based resources. The material was characterized thoroughly, including a solid state NMR study, showing that the molecular and mesostructural order was retained. In order to test the catalytic performance of this material, an aldol condensation of acetone and 4-nitrobenzaldehyde was performed in an aqueous environment. This led to a TOF value of $1.61 \pm 0.08 \times 10^{-4}$ s^{-1} and a very high selectivity towards the aldol product under the applied conditions. Compared to previous work, our material is very promising due to its stability towards water based environments, in which the valorization of biomass-based resources are typically performed. In the future, it would be very interesting to perform a reusability study by using the material in several catalytic runs.

3.4 References

1. Huber, G. W., Chheda, J. N., Barrett, C. J. & Dumesic, J. A. Production of liquid alkanes by aqueous-phase processing of biomass-derived carbohydrates. *Science (80-.).* **308,** 1446–1450 (2005).
2. Chheda, J. N., Huber, G. W. & Dumesic, J. A. Liquid-phase catalytic processing of biomass-derived oxygenated hydrocarbons to fuels and chemicals. *Angew. Chemie - Int. Ed.* **46,** 7164–7183 (2007).
3. *Ullmann's Encyclopedia of Industrial Chemistry*. *Ullmann's Encyclopedia of Industrial Chemistry* (Wiley-VCH Verlag GmbH & Co. KGaA, Weinheim, 2008). doi:10.1002/14356007.a01
4. Stueben, K. C. & Deem, M. L. Surfactant-promoted Aldol Reactions. (1976).
5. Lauwaert, J., De Canck, E., Esquivel, D., Van Der Voort, P., Thybaut, J.W., Marin, G.B., Effects of amine structure and base strength on acid–base cooperative aldol condensation. *Catal. Today* **246,** 35–45 (2015).
6. Werner Bonrath, Yann Pressel, Jan Schutz, Erich Ferfecki, K.-D. T. Aldol Condensations Catalyzed by Basic Anion-Exchange Resins. *ChemCatChem* 3584–3591 (2016). doi:10.1002/cctc.201600867
7. Lauwaert, J. *et al.* Silanol-Assisted Aldol Condensation on Aminated Silica: Understanding the Arrangement of Functional Groups. *ChemCatChem* **6,** 255–264 (2013).
8. Lauwaert, J. *et al.* Spatial arrangement and acid strength effects on acid–base cooperatively catalyzed aldol condensation on aminosilica materials. *J. Catal.* **325,** 19–25 (2015).
9. Brunelli, N. A., Venkatasubbaiah, K. & Jones, C. W. Cooperative catalysis with acid-base bifunctional mesoporous silica: Impact of grafting and Co-condensation synthesis methods on material structure and catalytic properties. *Chem. Mater.* **24,** 2433–2442 (2012).
10. Ouwehand, J., Lauwaert, J., Esquivel, D., Hendrickx,, K., Van Speybroeck, V., Thybaut, J.W., Van Der Voort, P., Facile Synthesis of Cooperative Acid-Base Catalysts by Clicking Cysteine and Cysteamine on an Ethylene-Bridged Periodic Mesoporous Organosilica. *Eur. J. Inorg. Chem.* (2016). doi:10.1002/ejic.201501179
11. Smeulders, G., Meynen, V., Silvestre-Albero, A., Houthoofd, K., Mertens, M., Silvestre-Albero, J., Martens, J.A., Cool, P., The impact of framework organic functional groups on the hydrophobicity and overall stability of mesoporous silica materials. *Mater. Chem. Phys.* **132,** 1077–1088 (2012).
12. Wuts, P. G. M. & Greene, T. W. *Greene's protective groups in organic synthesis*. (John Wiley & Sons, Inc., 2007).
13. Han, G., Tamaki, M. & Hruby, V. J. Fast , efficient and selective deprotection of the tert-butoxycarbonyl (Boc) group using HCl / dioxane (4 M). *J. Pept. Res.* **58,** 338–341 (2001).
14. Bruice, P. Y. *Organic Chemistry*. (Pearson Prentice Hall, 2007).
15. Thommes, M. *et al.* Physisorption of gases, with special reference to the evaluation of surface area and pore size distribution (IUPAC Technical Report). *Pure Appl. Chem.* **87,** 1051–1069 (2015).
16. Inagaki, S., Guan, S., Ohsuna, T. & Terasaki, O. An ordered mesoporous organosilica hybrid material with a crystal-like wall structure. *Nature* **416,** 304–307 (2002).
17. Smeulders, G., Meynen, V., Houthoofd, K., Mullens, S., Martens, J.A., Maes, B.U.W., Cool, P., Is their potential for post-synthetic brominating reactions on benzene bridged PMOs?

Microporous Mesoporous Mater. **164,** 49–55 (2012).

18. Morell, J., Chatterjee, S., Klar, P.J., Mauder, D., Shenderovich, I., Hoffmann, F., Fröba, M., Synthesis and characterization of chiral benzylic ether-bridged periodic mesoporous organosilicas. *Chem. - A Eur. J.* **14,** 5935–5940 (2008).

Chapter 4

PMO as a host for "superbases"

4.1 Introduction

Periodic mesoporous organosilicas as catalysts might well be the most extensively studied application. The use of PMOs as a base catalyst is, however, rather restricted[1–5]. Nevertheless, such catalysts are of particular interest for carbon-carbon bond forming reactions such as the Henry (nitroaldol) condensation[6–10]. This is a coupling reaction between a carbonyl compound and a nitroalkyl compound bearing α hydrogens. In this way, β-nitroalcohols can be synthesized and used as versatile reagents in organic synthesis, for example, for the development of pharmaceuticals, as described in the recent review of Zlotin et al.[7].

In light of using PMOs as base catalysts, we investigated the ability to post-synthetically modify benzene bridged PMO with *N,N'*-diisopropylcarbodiimide (DIC), in order to obtain a hybrid mesoporous material functionalized with an organic "superbase" group: a guanidine[11,12]. The basicity of a guanidine is comparable to the hydroxyl ion[11,13], with a proton affinity of 235-236 kcal mol^{-1}, and can be attributed to the conjugation system of the guanidinium ion after protonation (Figure 42)[11].

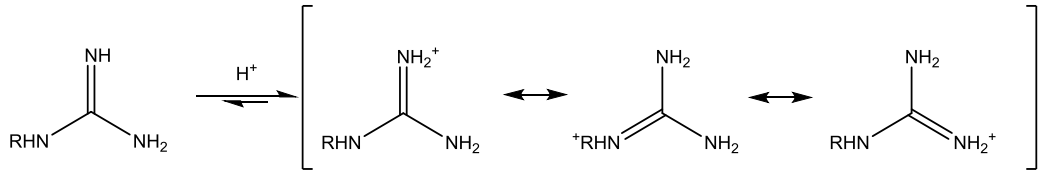

Figure 42. Conjugation of the guanidinium ion after protonation.

Nowadays, guanidines have been investigated as catalysts for CO_2 capture and utilization[14–16], as well as for catalyzing Michael-addition reactions[17,18], as drug carriers when loaded on mesoporous silica nanoparticles[19] and most extensively as a catalyst, loaded on a silica based support, towards the transesterification of vegetable oils[20–23]. The latter reaction is of particular interest in the production of biodiesel and is commonly catalyzed by homogeneous bases, leading to washing and purification steps which, evidently, adversely affect the quality and the costs[24]. Only very recently, silica nanoparticles were modified with guanidine and were successfully tested in the Henry

reaction of 4-nitrobenzaldehyde and nitromethane[25]. Therefore, in this chapter, we discuss the synthesis of a 1,2-diisopropyl-3-phenylguanidine bridged PMO (Figure 43) in order to combine the catalytic properties of the guanidine group with the advantages inherent to PMOs, as described earlier in this work. The material was thoroughly characterized and tested in the Henry reaction of benzaldehyde and nitromethane.

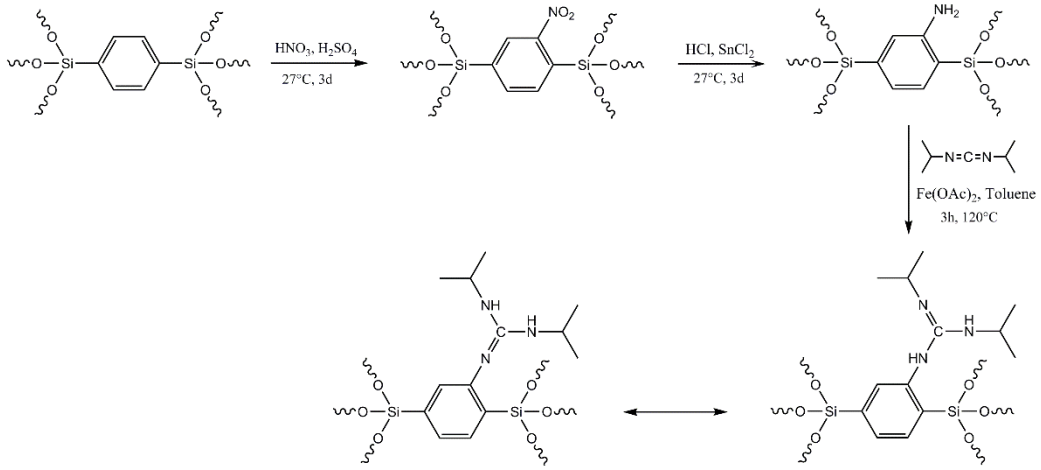

Figure 43. Reaction pathway for the synthesis of DIC PMO.

4.2 Experimental

Firstly, benzene bridged PMO was synthesized, followed by the conversion to aniline bridged PMO, according to the procedure reported earlier. Subsequently, based on the work of Pottabathula et al.[26], guanylation of the PMO was performed by using the following steps: To 0.80 g aniline bridged PMO was added 0.0057 g $Fe(OAc)_2$ (≥99.99%, trace metal basis, Sigma-Aldrich), 300 µL *N,N’*-diisopropylcarbodiimide (DIC, 99%, Sigma-Aldrich) and 16 mL toluene (99.8%, anhydrous, Sigma-Aldrich). The mixture was stirred for 3 h at 393 K. After filtration, the residue was washed with toluene and water. The guanylated PMO was then vacuum dried at 373 K for 24 h.

The catalytic activity was studied for the condensation reaction of nitromethane with benzaldehyde. The catalyst (0.095 mg) was pretreated at 120 °C overnight under vacuum and then added to a mixture of nitromethane (20 mmol) and benzaldehyde (5

mmol). The catalytic reaction occurred at 90 °C under nitrogen atmosphere for 12 h. Samples were analyzed by gas chromatography using a FID detector and a VF-5 m capillary column (30 m x 0,25 mm ID). Dodecane was used as the internal standard.

4.3 Results, analysis and characterization

The synthesized PMO materials were subjected to N_2 sorption in order to characterize their porosity (Figure 44, Table 7). Two batches were selected, based on their difference in specific surface area (S_{BET}), total pore volume (V_P) and average pore diameter (d). PMO 1 shows about 30% less surface area and V_P compared to PMO 2. Nonetheless, both PMOs have a similar average pore diameter. Table 7 shows the porosity data of both the modified PMOs as well as their parent PMO. Clearly, benzene PMO 1 was already a less porous parent material to start with compared to PMO 2. Interestingly, due to the difference in porosity, the post-synthetic modification reactions have a different impact on their surface area. Nitration and subsequent reduction to the amine results in a 19% decrease in specific surface area for PMO 2, while the less porous PMO 1 loses 33% of its specific surface area. Possibly, PMO 1 was less well condensed around the micellar template, resulting in a more amorphous material. The difference in modification rate could then be explained by the limited diffusion of reagents in the pores of PMO 2, while the external surface of PMO 1 is readily accessible for modification. The guanidine group is a very bulky functional group, supporting this hypothesis.

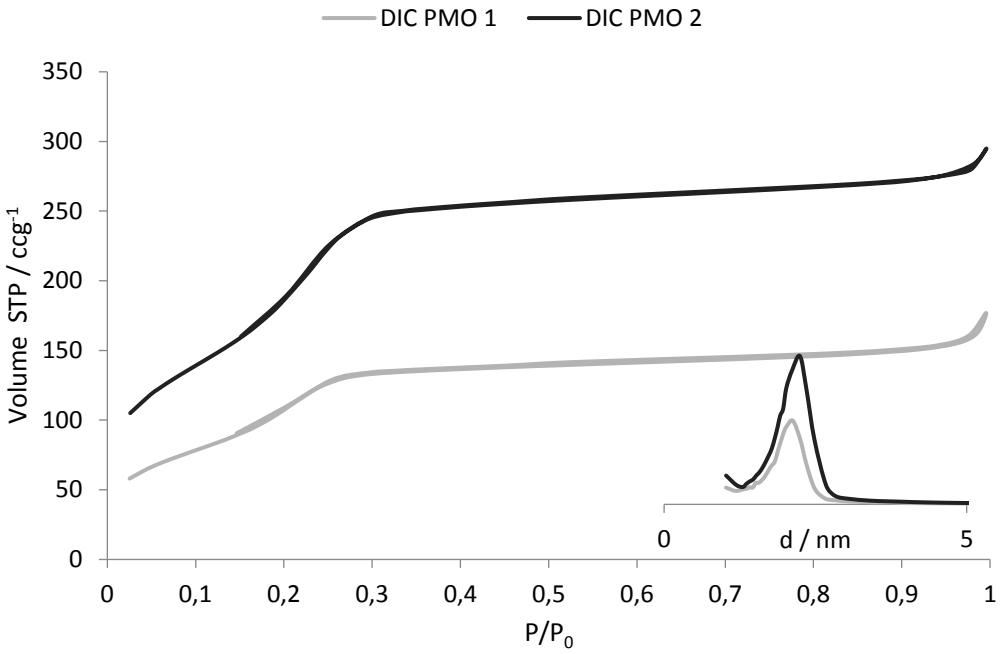

Figure 44. N_2 sorption isotherms at 77 K and the adsorption pore size distribution (BJH).

Table 7. Porosity data obtained through N2 sorption at 77K.

Sample name	S_{BET}/m^2g^{-1}	V_p/cm^3g^{-1}	d/nm[a]
Benzene PMO 1	583	0.39	2.67
NH_2 PMO 1	388	0.28	2.89
DIC PMO 1	375	0.25	2.69
Benzene PMO 2	801	0.57	2.86
NH_2 PMO 2	646	0.45	2.80
DIC PMO 2	643	0.43	2.70

[a] By the BJH method of the adsorption branch

This observation can also be seen in elemental analysis where amination occurs on 75% of the benzene moieties of PMO 1, in comparison to 54% of PMO 2 (Table 8). The higher modification degree of the former, therefore explains its higher decrease in surface area compared to PMO 2. Guanylation to the resulting DIC PMOs yields an increase in the amount of N for PMO 1, however no increase can be observed for PMO 2. Solid state

NMR measurements, later in this chapter, will show that guanylation does take place on both materials.

Table 8. Elemental analysis.

Sample name	N/mmol g^{-1}	C/mmol g^{-1}
NH_2 PMO 1	2.80	22.47
DIC PMO 1	3.17	24.75
NH_2 PMO 2	2.12	23.24
DIC PMO 2	2.12	25.39

In order to confirm the structural difference of (NH_2) PMO 1 in comparison to its peers, XRD analysis was performed and is depicted in Figure 45. Based on our previous observations the XRD measurements confirm that although NH_2 PMO 1 maintains its molecular scale periodicity, in comparison to what we're used to, it shows less distinct ordering. This originates from either less well stacked benzene rings (π-π interaction), causing the rings to not form a homogeneously structured surface on which further post-synthetic modifications can take place, or because of the less well condensed structure of PMO 1 compared to PMO 2 as mentioned earlier. The first hypothesis is based on the way in which the benzene rings are oriented on the pore wall surface, and therefore their availability as a substrate in a chemical reaction, will affect the degree of post-synthetic modification. The second hypothesis, on the other hand, can be supported by the fact that the small angle XRD of PMO 1 shows a less distinct signal than PMO 2 proving that the former is more amorphous.

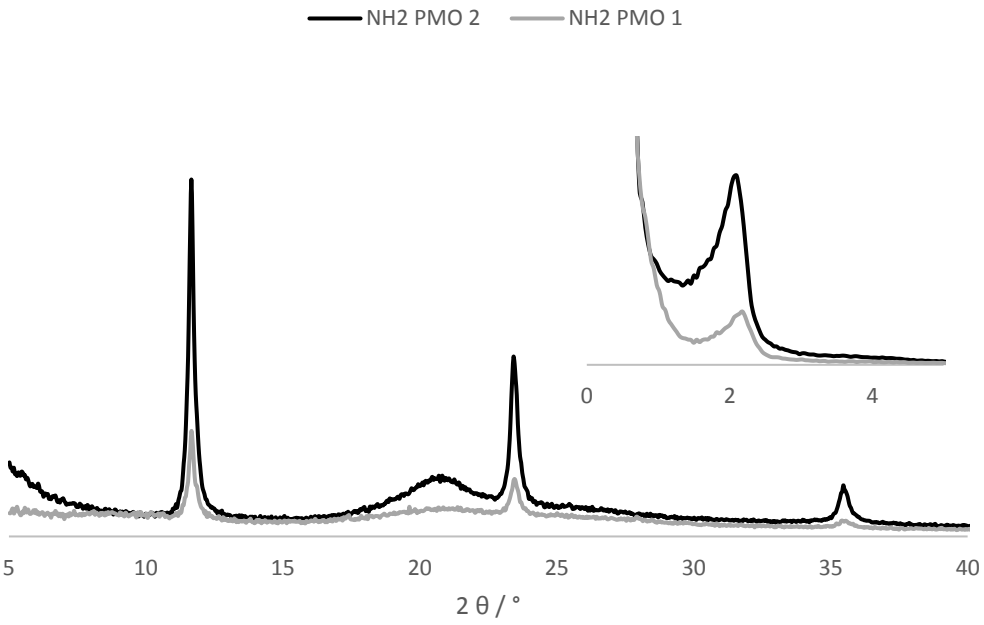

Figure 45. Wide angle and small angle (inset) XRD pattern of NH2 PMO 1 compared to a standard NH2 PMO pattern.

Although elemental analysis suggests that no modification took place on PMO 2, solid-state NMR measurements (Figure 46) distinctly show the presence of isopropyl carbons (**1** and **2**), as well as the central guanidine carbon (**3**) and the carbon attached to the ring structure (**4**) for both PMO materials. The signals at 133 ppm and 120 ppm can be attributed to the aromatic carbons of the pristine PMO benzene ring and the modified PMO benzene ring, respectively.

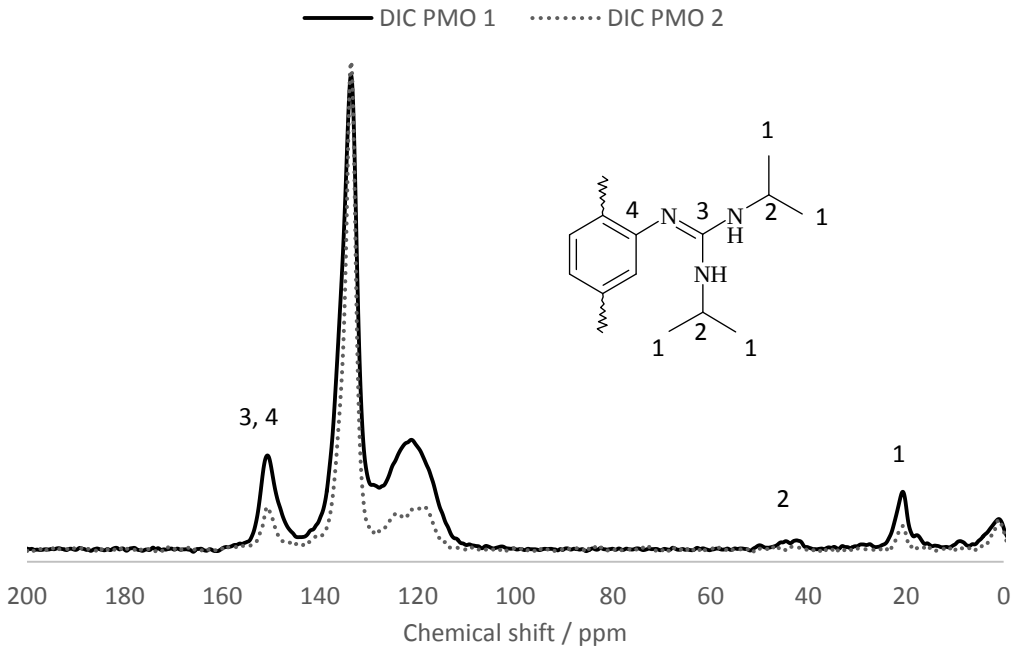

Figure 46. ^{1}H-^{13}C CPMAS NMR spectra of the guanylated PMOs.

The catalytic performance of both DIC PMOs were tested in the Henry reaction of nitromethane and benzaldehyde as depicted in Figure 47. Nitromethane is deprotonated, followed by alkylation with benzaldehyde and protonation of the alkoxide.

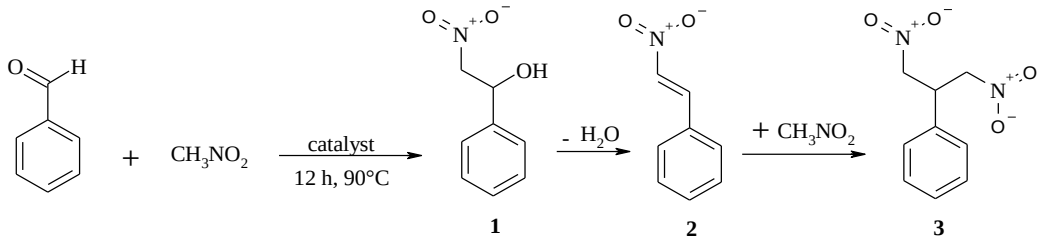

Figure 47. Henry reaction catalyzed by DIC PMO.

As shown in Table 9 , the guanylated PMOs were active in the Henry reaction, reaching 50% and 58% conversion, respectively, and 100% selectivity towards product **2** after 12 h of reaction. No formation of byproducts **1** or **3** was observed in the reaction mixture. In absence of the catalyst, no conversion was obtained. Compared to guanylated silica nanoparticles in the work of Feng *et al.*[25], who achieved a conversion of nearly 90%, after 10h at 298K, our conversion is rather limited. However, in contrast to that work, we used a lower amount of catalyst.

Table 9. Catalytic data obtained from the Henry reaction after the first run.

Sample name	Conversion (%)	Selectivity **1** (%)	Selectivity **2** (%)	Selectivity **3** (%)
DIC PMO 1	50	0	100	0
DIC PMO 2	58	0	100	0

The guanylated PMO was recycled after the first run and reused for a second and third run in order to study its reusability. After reaction, the catalyst was filtered off and washed with CH_2Cl_2 at room temperature. During the second run, the conversion of DIC PMO 1 dropped from 50% to 25%. The third run resulted in a conversion of 22%. The conversion of DIC PMO 2 dropped to 23% after two runs and to 13% after three runs. The drop in activity, especially after the first run, could be explained by deactivation of the basic sites due to adsorption of the reactants or reaction intermediates on the surface of the catalyst. In order to confirm this hypothesis, ^{13}C CPMAS NMR was performed on the DIC-PMO 1 material after its third run.

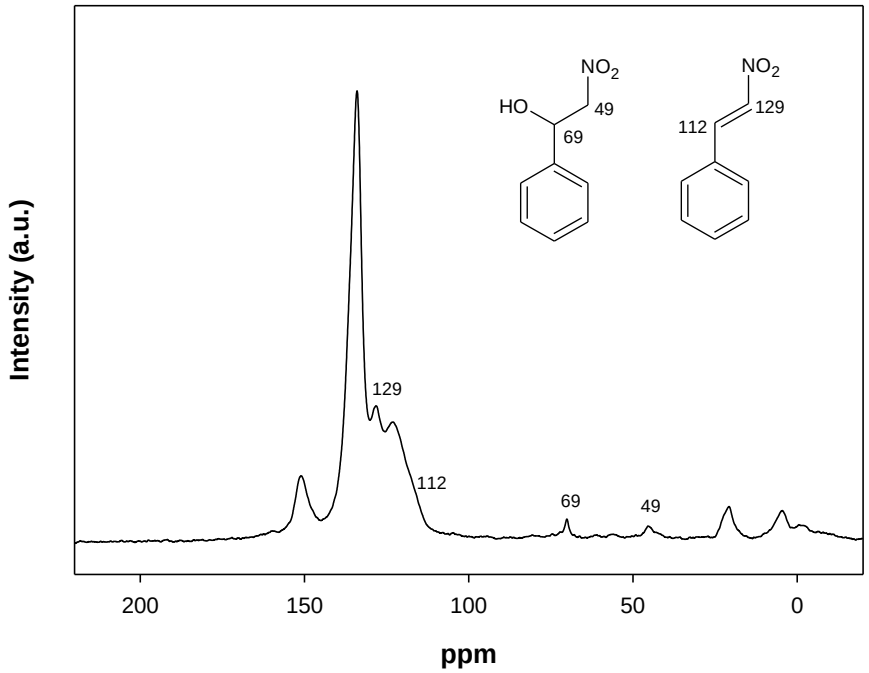

Figure 48. ^{13}C CPMAS NMR of DIC PMO 1 after 3 catalytic runs.

Figure 48 clearly shows two distinct peaks at 69 ppm and 49 ppm that can be attributed to the reaction intermediate (**1**). Additionally, evidence of the reaction product (**2**) was also found at 129 ppm and 112 ppm. No presence of the bis-nitro compound (**3**) could be found in the NMR spectrum. Although the materials were thoroughly washed after each catalytic run, it would still be possible that the aromatic reagents and reaction products are not washed away due to π-π interactions with the aromatic building blocks of the PMO.

The stability of DIC PMO 1 after three catalytic cycles was tested by performing XRD analysis. Figure 49 shows the diffractograms of the DIC-PMO 1 material before and after the catalytic runs and shows the preservation of the 2-D hexagonal ordered mesostructure, thus proving its stability.

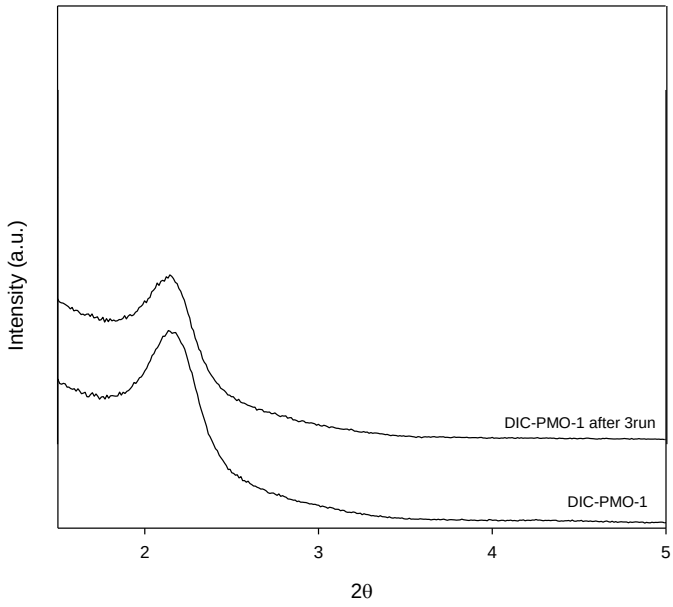

Figure 49. Low angle XRD spectra of DIC PMO 1 before and after three catalytic runs.

4.4 Conclusion and outlook

This chapter discusses the guanylation of benzene bridged PMOs and their potential use as a base catalyst for Henry reactions. We have shown that modifying PMOs using our synthesis strategy can lead to successful guanylation of the materials. It was shown that less ordered PMOs led to a higher modification degree in comparison to a very well ordered material. That said, due to limited time, the reproducibility should be checked and a further optimization of the guanylation reaction should be performed. The first preliminary catalytic test, on the other hand, already shows promising results towards the use of guanylated PMOs as base catalysts in Henry reactions. Conversions up to 58% were obtained for guanylated PMO, with 100% selectivity towards 1 reaction product. The materials proved to be structurally stable after 3 catalytic runs. However, their performance decreased during the 2nd run, probably due to adsorption of aromatics on the PMO surface, thus deactivating the basic catalytic sites. A further optimization of the catalytic evaluation should also be performed in the future.

4.5 References

1. Ohashi, M., Kapoor, M. P. & Inagaki, S. Chemical modification of crystal-like mesoporous phenylene-silica with amino group. *Chem. Commun.* 841–843 (2008). doi:10.1039/b716141g
2. Liu, M., Lu, X., Shi, L., Wang, F. & Sun, J. Periodic Mesoporous Organosilica with a Basic Urea-Derived Framework for Enhanced Carbon Dioxide Capture and Conversion Under Mild Conditions. *ChemSusChem* **18,** 1–11 (2016).
3. Zhu, F., Yang, D., Zhang, F. & Li, H. Amine-bridged periodic mesoporous organosilica nanospheres as an active and reusable solid base-catalyst for water-medium and solvent-free organic reactions. *J. Mol. Catal. A Chem.* **363–364,** 387–397 (2012).
4. Borah, P., Mondal, J. & Zhao, Y. Urea-pyridine bridged periodic mesoporous organosilica: An efficient hydrogen-bond donating heterogeneous organocatalyst for Henry reaction. *J. Catal.* **330,** 129–134 (2015).
5. Elhamifar, D. & Kazempoor, S. Synthesis and characterization of ionic liquid based bifunctional periodic mesoporous organosilica supported potassium carbonate as very efficient nanocatalyst for the Knoevenagel condensation. *J. Mol. Catal. A Chem.* **415,** 74–81 (2016).
6. Luzzio, F. A. The Henry reaction: recent examples. *Tetrahedron* **57,** 915–945 (2001).
7. Sukhorukov, A. Y., Sukhanova, A. A. & Zlotin, S. G. Stereoselective reactions of nitro compounds in the synthesis of natural compound analogs and active pharmaceutical ingredients. *Tetrahedron* **72,** 6191–6281 (2016).
8. Murugavel, G., Sadhu, P. & Punniyamurthy, T. Copper(II)-Catalyzed Nitroaldol (Henry) Reactions: Recent Developments. *Chem. Rec.* 1906–1917 (2016). doi:10.1002/tcr.201500268
9. Ashokkumar, V., Duraimurugan, K. & Siva, A. A new series of bipyridine based chiral organocatalysts for enantioselective Henry reaction. *New J. Chem.* **40,** 7148–7156 (2016).
10. Surneni, N., Barua, N. C. & Saikia, B. Application of natural feedstock extract: The Henry reaction. *Tetrahedron Lett.* **57,** 2814–2817 (2016).
11. Ishikawa, T. *Superbases for organic synthesis: Guanidines, amidines, phosphazenes and related organocatalysts*. (John Wiley & Sons, Inc., 2009). doi:10.1351/pac198860111627
12. Caubère, P. Unimetal Super Bases. *Chem. Rev.* **93,** 2317–2334 (1993).
13. Raczynska, E. D., Maria, P. C., Gal, J.-F. & Decouzon, M. Superbases in the gas phase. part II. Further extension of the basicity scale using acycling and cycling guanidines. *J. Phys. Org. Chem.* **7,** 725–733 (1994).
14. Barbarini, A. *et al.* Cycloaddition of CO2 to epoxides over both homogeneous and silica-supported guanidine catalysts. *Tetrahedron Lett.* **44,** 2931–2934 (2003).
15. Zhang, S. & He, L. N. Capture and fixation of CO2 promoted by guanidine derivatives. *Aust. J. Chem.* **67,** 980–988 (2014).
16. Adam, F. & Batagarawa, M. S. Tetramethylguanidine-silica nanoparticles as an efficient and reusable catalyst for the synthesis of cyclic propylene carbonate from carbon dioxide and propylene oxide. *Appl. Catal. A Gen.* **454,** 164–171 (2013).
17. Kalita, P. & Kumar, R. Immobilization of 1,5,7-triazabicyclo [4.4.0] dec-5-ene over mesoporous materials: An efficient catalyst for Michael-addition reactions under solvent-free condition. *Appl. Catal. A Gen.* **397,** 250–258 (2011).
18. Alizadeh, A., Khodaei, M. M., Kordestani, D., Fallah, A. H. & Beygzadeh, M. The successful

synthesis of biguanide-functionalized mesoporous silica catalysts: Excellent reactivity combined with facile catalyst recyclability. *Microporous Mesoporous Mater.* **159,** 9–16 (2012).

19. Ma’Mani, L., Nikzad, S., Kheiri-Manjili, H., Al-Musawi, S., Saeedi, M., Askerlou, S., Foroumadi, A., Shafiee, A., Curcumin-loaded guanidine functionalized PEGylated I3ad mesoporous silica nanoparticles KIT-6: Practical strategy for the breast cancer therapy. *Eur. J. Med. Chem.* **83,** 646–654 (2014).
20. Xie, W. & Fan, M. Immobilization of tetramethylguanidine on mesoporous SBA-15 silica: A heterogeneous basic catalyst for transesterification of soybean oil. *Bioresour. Technol.* **139,** 388–392 (2013).
21. Xie, W., Yang, X. & Fan, M. Novel solid base catalyst for biodiesel production: Mesoporous SBA-15 silica immobilized with 1,3-dicyclohexyl-2-octylguanidine. *Renew. Energy* **80,** 230–237 (2015).
22. de Lima, A. L., Mbengue, A., San Gil, R. A. S., Ronconi, C. M. & Mota, C. J. A. Synthesis of amine-functionalized mesoporous silica basic catalysts for biodiesel production. *Catal. Today* **226,** 210–216 (2014).
23. Xie, W. & Hu, L. Biguanide-functionalized mesoporous SBA-15 silica as an efficient solid catalyst for interesterification of vegetable oils. *Food Chem.* **197,** 92–99 (2016).
24. Semwal, S., Arora, A. K., Badoni, R. P. & Tuli, D. K. Biodiesel production using heterogeneous catalysts. *Bioresour. Technol.* **102,** 2151–2161 (2011).
25. Feng, G., Guan, M., Lai, Q., Mi, H., Li, G., Ma, Q., Fei, Q., Huan, Y., Song, Z., One-pot Synthesis and application of novel amino-functionalized silica nanoparticles using guanidine as amino group. *New J. Chem.* **40,** 8444–8450 (2016).
26. Pottabathula, S. & Royo, B. First iron-catalyzed guanylation of amines: a simple and highly efficient protocol to guanidines. *Tetrahedron Lett.* **53,** 5156–5158 (2012).

General summary

Periodic mesoporous organosilicas have been standing in the center of attention of many scientists working on hybrid materials since they first appeared in 1999. Due to their both inorganic and organic nature, they offer the best of both worlds. The inorganic network provides a highly porous framework in which the organic entity acts as a bridge inbetween two silica atoms. The precursors, or building blocks of the material, therefore carry one organic unit each. In contrast to the co-condensation or grafting technique with organosilanes, this thus results in a homogeneous distribution of the organic bridges throughout the entire PMO material. Moreover, the strong anchoring of these hydrophobic moieties makes PMOs hydrothermally, chemically and mechanically more stable than their purely siliceous counterpart.

Over the last 18 years, many of these precursors have been commercialized and many more have their synthesis described in literature. The choice of precursor leads to materials that considerably differentiate from one another. Depending on the application one has in mind, precursors can be used that are larger or smaller; are more or less hydrophobic; result in crystalline-like materials or are completely disordered; carry an active metal in its center or have dangling organic groups in its pores; bear a certain functional group that can be post-synthetically modified or have a simple aliphatic organic bridge. Because of this versatility, PMOs have found their way to a variety of applications, often in comparison to their siliceous analogues.

Certain applications however, require the presence of very specific functional groups that are not always directly attainable by utilizing a certain precursor. Furthermore, modifying the precursors with the desired functionality before PMO synthesis can lead to bulky building blocks that no longer offer the desired ordering or pore characteristics in the final material. It is therefore crucial that research is performed on post-synthetical modification reactions.

Nevertheless, transferring known organic modification reactions to the world of PMOs is hardly straightforward. Besides the reactions having to occur in a confined space, the substrate molecule is built in to the solid framework as well. Hence, the substrate molecule cannot arrange itself towards the reagents, nor can the anchoring carbon-silicon bonds be cleaved because of the reaction conditions.

The second chapter of this dissertation handles these difficulties by discussing the synthesis of a precursor with a divinylaniline bridge which was a challenge, although described in an article published by a renowned research group. It can be concluded that the recipe was lacking crucial purification steps and that there was also room for optimization of the double Heck coupling reaction itself. Firstly, reagents were purified before utilization. Secondly, the amount of solvent (DMF) could be drastically reduced by 65%. Final purification of the reaction product was deemed necessary since there was still intermediate mono Heck coupled product in the obtained solution. After HPLC purification the residual amounts of DMF and the intermediate product could be removed from the desired product, giving rise to the pure 2,5-bis((*E*)-2-(triethoxysilyl)vinyl)aniline (BTEVA) precursor. Unfortunately, within the designated timeframe of this PhD, we did not succeed in producing a structured highly-porous material with the BTEVA precursor.

The second part of the second chapter concerns the development of a post-synthetic modification strategy in order to brominate benzene bridged PMO, without affecting its structural integrity. By first performing a post-synthetic nitration reaction on benzene bridged PMO, followed by the reduction to the aniline moiety, we create a reactive site on the benzene ring for the bromination reaction. By then performing a one-step diazotation-de-diazotation-bromination reaction, with the loss of N_2 gas, the bromobenzene bridged PMO product is obtained. Using this synthesis strategy, we were able to employ the amino function as a leaving group, thus creating a C-Br bond and avoiding the chance of Si-C cleavage which was a major issue established by us in a previous PhD. Thorough characterization of the brominated material with X-ray

photoelectron spectroscopy (XPS) and solid state nuclear magnetic resonance (SS NMR) confirms this. It is well known that bromine is a very good leaving group in substitution reactions, thus creating new opportunities towards functionalization of PMOs in a variety of different fields.

The third chapter in this dissertation discusses the development of L-serine modified benzene bridged PMO. Subsequently, this material was catalytically tested in the aldol condensation of acetone and 4-nitrobenzaldehyde. The aldol condensation is an important carbon-carbon forming reaction often used in the pharmaceutical industry and during the process of biomass conversion into biodiesel. Since water is an important side product in the latter process, PMOs can offer significant advantages compared to siliceous materials which are easily hydrolysable. Moreover, the L-serine moiety that we successfully attached to the benzene bridged PMO carries both a primary amine, acting as the base catalyst, and an alcohol function on the β-carbon that has a promoting effect during the catalytic reaction. The catalytic performance test gave rise to a TOF value of $1.61 \pm 0.08 \times 10^{-4}$ s^{-1} and is the same order of magnitude as the TOF values of modified siliceous materials. However, because our material was tested in an aqueous environment, as to *n*-hexane in other works, the prospects for using this PMO material in the conversion of biomass are very promising.

The final chapter discusses the guanylation of benzene bridged PMO as means to create a PMO for base catalysis. Again, the application of interest is catalyzing the formation of carbon-carbon bonds for biodiesel purposes. First of all, we observe a substantial difference in using a well ordered PMO or a less ordered one. This impacts the degree of modification, due to either the orientation of the benzene moieties in the PMO structure or the diffusion limited modification reaction. Although there is still need for an optimization of the guanylation reaction, the first catalytic tests showed promising results. The Henry reaction of nitromethane and benzaldehyde was studied with a guanylated PMO as the base catalyst. After three runs a conversion of 13-22% was observed, depending on the ordering of the PMO, dropping from 50-58% in the first run.

The reason for this drop in activity can be attributed to the adsorption of the reaction product and intermediate on the surface of the PMO material. Further research is therefore needed, in order to maintain the high catalytic activity after several runs.

Algemene samenvatting

Periodisch mesoporeuze organosilica's genieten, sinds hun ontdekking in 1999, van veel aandacht bij de vele wetenschappers actief in het gebied van hybride materialen. Dankzij de combinatie van anorganische en organische eigenschappen, bieden deze materialen veel voordelen. Het anorganische netwerk leidt tot een hoog poreuze structuur waarbij de organische component een soort brug vormt tussen twee silicium atomen. De precursoren, of bouwstenen van het materiaal, bevatten met andere woorden één organische component. In tegenstelling tot co-condensatie of *graften* met organosilanen, zorgt dit ervoor dat er een homogene verdeling is van de organische entiteiten doorheen het PMO materiaal. Bovendien zorgen deze sterk verankerde hydrofobe componenten voor een hydrothermale, chemische en mechanische superioriteit ten aanzien van hun silica gebaseerde tegenhangers.

Gedurende de laatste 18 jaar werden vele van deze precursoren gecommercialiseerd en veel meer nog zijn beschreven in de literatuur. De keuze van precursor leidt tot materialen die sterk verschillen van elkaar. Afhankelijk van de toepassing die men voor ogen heeft, kunnen precursoren groter of kleiner zijn; meer of minder hydrofoob; resulteren in kristallijn-achtige materialen of ongeordend zijn; een actief metaal centrum of hangende organische groepen bevatten in de poriën; een bepaalde functionele groep hebben die post-synthetisch gemodificeerd kan worden of slechts een eenvoudige alifatische verbinding. Omwille van deze verscheidenheid, worden PMOs in verschillende toepassingen gebruikt, vaak in tegenstelling tot hun silica gebaseerde tegenhangers.

Echter, bepaalde toepassingen vereisen zeer specifieke functionele groepen die niet altijd ter beschikking zijn in een zekere precursor. Bovendien kan het chemisch modificeren van precursoren met een specifieke functionaliteit, voorafgaand aan de PMO synthese, ervoor zorgen dat deze bouwstenen té sterisch gehinderd worden. Dit kan leiden tot een materiaal dat niet meer de gewenste orde of porositeitseigenschappen bevat.

Bovendien is het toepassen van gekende organische reacties naar de wereld van PMOs niet vanzelfsprekend. Niet alleen moeten de reacties plaatsvinden in een beperkte ruimte, maar is de substraat molecule ook nog eens ingebouwd in de vaste structuur. Dit wil zeggen dat de substraat molecule zich niet kan richten naar de reagentia, noch mag de koolstof-silicium verbinding gebroken worden.

Het tweede hoofdstuk van deze thesis brengt deze moeilijkheden aan het licht. Er werd getracht een precursor te synthetiseren met een divinylaniline component aan de hand van een artikel gepubliceerd door een befaamde onderzoeksgroep. Er kon geconcludeerd worden dat dit recept nood had aan een cruciale zuiveringsstap, alsook aan een optimalisatie van de dubbele Heck koppelingsreactie. Ten eerste, werden de reagentia gezuiverd voor gebruik. Ten tweede, werd de hoeveelheid solvent (DMF) drastisch gereduceerd met 65%. De opzuivering van het reactieproduct werd tenslotte noodzakelijk geacht gezien de aanwezigheid van het mono gekoppelde Heck intermediair. Na HPLC zuivering werden de overige resten DMF en intermediair verwijderd en verkregen we de zuivere 2,5-bis((*E*)-2-(triethoxy)vinyl)aniline (BTEVA) precursor. Nochtans kon er binnen de tijdspanne van dit doctoraat niet in geslaagd worden om met deze precursor een goed gestructureerde PMO te bekomen.

In het tweede deel van het tweede hoofdstuk werd een post-synthetische modificatie strategie ontwikkeld om benzeen gebrugd PMO te bromeren, zonder de structurele integriteit aan te tasten. Door eerst een post-synthetische nitreringsreactie uit te voeren op benzeen gebrugd PMO, gevolgd door reductie tot het aniline, wordt er op de benzeen ring een reactieve site gecreëerd voor de bromering. Vervolgens werd er een éénstaps diazotatie-de-diazotatie-bromerings-reactie uitgevoerd, met verlies van stikfstof gas. Hierdoor werd bromobenzeen gebrugd PMO als product bekomen. Door gebruik te maken van deze synthese strategie konden we de amine functie gebruiken als *leaving* groep, waarbij er een C-Br binding gemaakt wordt. Op deze manier kon bovendien vermeden worden dat de Si-C binding gebroken werd, wat in het verleden reeds aangetoond werd als een probleem. Diepgaande karakterisatie met X-stralen foto

elektron spectroscopie (XPS) en vaste stof nucleaire magnetische resonantie (SS NMR) van het gebromeerd materiaal bevestigt dit.

Het derde hoofdstuk van dit doctoraat beschrijft de ontwikkeling van L-serine gemodificeerd benzeen gebrugd PMO. Dit materiaal werd vervolgens katalytisch getest in de aldol condensatie van aceton en 4-nitrobenzaldehyde. De aldol condensatie is een belangrijke koolstof-koolstof vormende reactie die vaak toegepast wordt in de farmaceutische industrie en om biomassa om te zetten in biodiesel. Aangezien water een belangrijk nevenproduct is in dit laatste proces, kunnen PMOs aanzienlijke voordelen bieden ten opzichte van hun silicium gebaseerde tegenhangers die gemakkelijk te hydrolyseren zijn. Daarenboven bevat de L-serine functionaliteit die we succesvol inbouwden op benzeen gebrugd PMO zowel een primair amine, dat dienst doet als base katalysator, en een alcohol functie op de β-koolstof, dat een promoverend effect heeft tijdens de katalyse reactie. De katalytische test gaf een TOF waarde van 1.61 ± 0.08 x 10^{-4} s^{-1} en is in dezelfde grootteorde als de TOF waarden van silica gebaseerde materialen. Echter, aangezien ons materiaal getest werd in een waterige omgeving, in tegenstelling *n*-hexaan in andere werken, is de mogelijke toepassing van dit PMO materiaal voor de omzetting van biomassa zeer beloftevol.

Het laatste hoofdstuk beschrijft de guanylering van benzeen gebrugd PMO met als doel een PMO te synthetiseren als base katalysator. Wederom zou dit een interessant materiaal zijn voor de koolstof-koolstof vorming voor biodiesel toepassingen. Ten eerste, werd er een aanzienlijk verschil opgemerkt in het gebruik van een goed geordende PMO en een minder geordend materiaal. Dit had een impact op de modificatiegraad, omwille van de ruimtelijke oriëntatie van de benzeen ringen in de PMO structuur of ten gevolge van diffusie limitaties tijdens de modificatie reactie. Hoewel er nog nood is aan optimalisering van de guanyleringsreactie, toonden de eerste katalytische testen reeds goede resultaten. De Henry reactie tussen nitromethaan en benzaldehyde werd bestudeerd met guanidine PMO als base katalysator. Na drie katalytische *runs* werd er een conversie van 13-22% vastgesteld, afhankelijk van de orde

van het materiaal, komende van 50-58% na de eerste *run*. De reden voor de daling in activiteit is waarschijnlijk toe te schrijven aan de adsorptie van het reactieproduct en intermediair op het oppervlak van het PMO materiaal. Daarom is er nog verder onderzoek nodig om de hoge katalytische activiteit van het materiaal te behouden na meerdere katalytische *runs*.

Appendix: Characterization techniques

N_2 sorption measurements at 77 K

Porosity characterization was performed on a Quantachrome Quadrasorb *SI* automated gas adsorption system. The measurements were preceded by outgassing the samples on a Quantachrome Autosorb Degasser at 373 K for 16 h. Nitrogen sorption was carried out at liquid nitrogen temperature, 77 K. The specific surface area was calculated using the Brunauer-Emmet-Teller (BET) method, between a relative pressure of 0.05 and 0.35. Using the Barret-Joyner-Halenda (BJH) method, applied on the adsorption isotherm, the pore size distribution was calculated. The total pore volume was obtained by determining the total amount of nitrogen adsorbed at $P/P_0 = 0.95$.

X-ray diffraction (XRD)

XRD analysis was performed in collaboration with VITO NV (M. Mertens) on a PANalytical X'Pert Pro with CuK_α radiation and a proportional detector, using variable slits and a monochromator. Continuous scanning was used with a scanning speed of 0.04°/4 s. The generator voltage and tube current were 40 kV and 40 mA, respectively. The *d* spacing was calculated using Bragg's law: $n\lambda = 2d\sin(\theta)$.

Elemental analysis

Elemental analysis was performed in collaboration with prof. Van Der Voort's research group at UGent on a Thermo Flash 2000 CHNS/O analyzer, using V_2O_5 as a catalyst.

In-situ diffuse reflectance infrared spectroscopy (DRIFT)

In-situ DRIFT spectra were measured using a Nicolet 6700 Fourier Transform IR spectrometer and a DTGS detector. The samples were diluted to 2% with KBr and 200 scans were performed with a resolution of 4 cm^{-1}. All samples were measured under vacuum at the given temperature.

Solid state nuclear magnetic resonance (SS NMR)

SS NMR measurements were performed in collaboration with prof. Mali at the National Institute of Chemistry in Ljubljana, Slovenia. ^{1}H-^{13}C CPMAS, ^{1}H-^{29}Si CPMAS (cross-polarization magic-angle spinning) and ^{29}Si MAS NMR spectra were recorded on a 600 MHz Varian NMR system operating at ^{1}H, ^{13}C and ^{29}Si Larmor frequencies of 599.54, 150.76 and 119.11 MHz, respectively. The system is equipped with a 3.2 mm Varian HX MAS probe. For chapter 2 sample rotation frequency was 16 kHz for ^{1}H-^{13}C CPMAS measurements and 10 kHz for (^{1}H-)^{29}Si (CP)MAS measurements. For chapter 3 sample rotation was 20 kHz. All measurements employed RAMP[1] on proton channel during CP block and high-power XiX[2] proton decoupling during acquisition. Contact time was 5 ms and repetition delay was 3 s. 2000-4000 Scans were accumulated for ^{1}H-^{13}C CPMAS measurements and 10 000 for ^{1}H-^{29}Si CPMAS measurements. In ^{29}Si MAS measurement repetition delay was 60 s and 4000 scans were accumulated. Chemical shifts of ^{13}C and ^{29}Si signals were referenced to the corresponding signals of tetramethylsilane, which was used as an external reference. Figure 50 shows the condensation states of silica and their accompanying signals in ^{29}Si NMR.

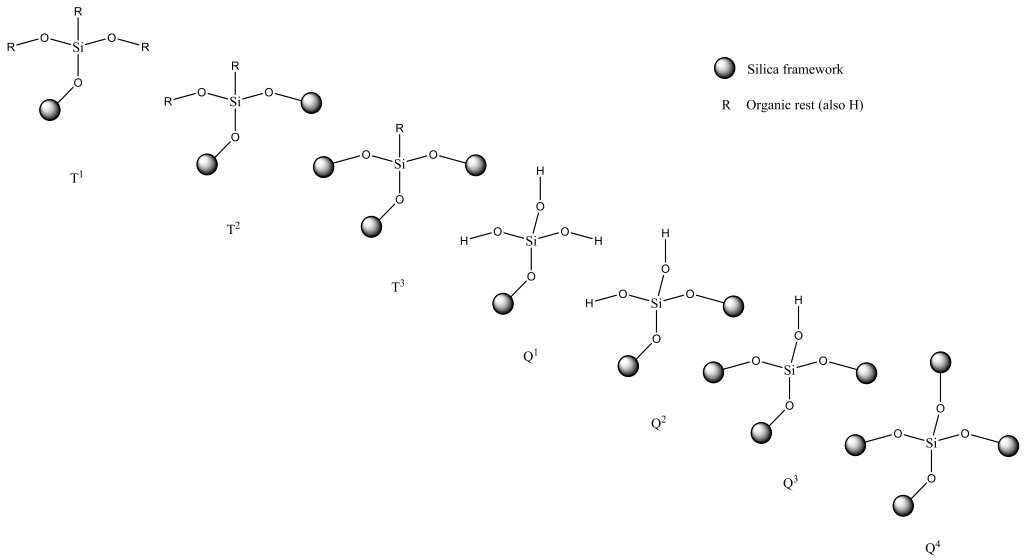

Figure 50. ^{29}Si MAS NMR signals

X-ray photoelectron spectroscopy (XPS)

XPS was carried out in collaboration with prof. Kuśtrowski at the Jagiellonian University in Krakow, Poland. The X-ray photoelectron spectra were acquired using a Prevac photoelectron spectrometer equipped with a hemispherical VG SCIENTA R3000 analyzer. The spectra were taken using a monochromatized aluminum source AlKα (E = 1486.6 eV) and a low-energy electron flood gun (FS40A-PS) to compensate for the charge accumulation on the surface of nonconductive samples. The spectra were processed and deconvoluted using the CasaXPS software. The binding energy values of measured regions were referenced to the C-C peak at 284.7 eV in the C 1s core level. The surface composition was studied based on the areas and binding energies of C 1s, N 1s, O 1s, Cl 2p, Br 3d, Sn 3d and Si 2p core levels.

Annular dark-field scanning transmission electron microscopy (ADF-STEM)

TEM measurements were performed at EMAT, University of Antwerp, in collaboration with prof. Bals. ADF-STEM images were acquired using a cubed FEI Titan operated at 300 kV. The sample was prepared for TEM analysis by crushing in an agate mortar, dispersing it in ethanol and attaching it to a copper grid covered with a holey carbon film.

References

1. Metz, G., Wu, X. & Smith, S. O. Ramped-Amplitude Cross Polarization in Magic-Angle-Spinning NMR. *J. Magn. Reson. A* **110,** 219–227 (1994).
2. Detken, A., Hardy, E. H., Ernst, M. & Meier, B. H. Simple and efficient decoupling in magic-angle spinning solid-state NMR: The XiX scheme. *Chem. Phys. Lett.* **356,** 298–304 (2002).

List of publications

Articles

W. Huybrechts, G. Mali, P. Kuśtrowski, T. Willhammar, M. Mertens, S. Bals, P. Van Der Voort and P. Cool

Post-synthesis bromination of benzene bridged PMO as a way to create a high potential hybrid material

Microporous and Mesoporous Materials, 2016, 236, 244-249

W. Huybrechts, J. Lauwaert, A. De Vylder, M. Mertens, G. Mali, J.W. Thybaut, P. Van Der Voort and P. Cool

Synthesis of L-serine modified benzene bridged periodic mesoporous organosilica and its catalytic performance towards aldol condensations

Microporous and Mesoporous Materials, 2017, 251, 1-8

Presentations

W. Huybrechts, G. Mali, P. Kuśtrowski, P. Van Der Voort and P. Cool

Synthesis of bromobenzene bridged periodic mesoporous organosilica

Netherlands' Catalysis and Chemistry Conference, 09/03/2016, Noordwijkerhout, the Netherlands

W. Huybrechts, G. Mali, P. Kuśtrowski, P. Van Der Voort and P. Cool

Synthesis of bromobenzene bridged periodic mesoporous organosilica

Balard Conference – Prospects in porous materials, 04/04/2016, Montpellier, France

Poster presentations

W. Huybrechts, P. Mampuys, B.U.W. Maes and P. Cool

Synthesis of periodic mesoporous organosilica (PMO) as bifunctional acid/base catalysts

Netherlands' Catalysis and Chemistry Conference, 11/03/2014, Noordwijkerhout, the Netherlands

W. Huybrechts, P. Mampuys, B.U.W. Maes and P. Cool

Synthesis of periodic mesoporous organosilica (PMO) as bifunctional acid/base catalysts

Dutch Zeolite Association 2014, 07/10/2014, Ghent, Belgium